

INVESTIGATION OF UNIFORM BIOMATERIAL-BASED MICROSPHERES
WITH PRECISELY CONTROLLED SIZE AND SIZE DISTRIBUTION FOR
DEVELOPMENT OF ADVANCED DRUG DELIVERY SYSTEMS

BY

YOUNG BIN CHOY

B.S., Seoul National University, 1999
M.S., University of Wisconsin–Madison, 2000

DISSERTATION

Submitted in partial fulfillment of the requirements
for the degree of Doctor of Philosophy in Electrical and Computer Engineering
in the Graduate College of the
University of Illinois at Urbana-Champaign, 2006

Urbana, Illinois

UMI Number: 3242824

INFORMATION TO USERS

The quality of this reproduction is dependent upon the quality of the copy submitted. Broken or indistinct print, colored or poor quality illustrations and photographs, print bleed-through, substandard margins, and improper alignment can adversely affect reproduction.

In the unlikely event that the author did not send a complete manuscript and there are missing pages, these will be noted. Also, if unauthorized copyright material had to be removed, a note will indicate the deletion.

UMI[®]

UMI Microform 3242824

Copyright 2007 by ProQuest Information and Learning Company.

All rights reserved. This microform edition is protected against unauthorized copying under Title 17, United States Code.

ProQuest Information and Learning Company
300 North Zeeb Road
P.O. Box 1346
Ann Arbor, MI 48106-1346

© 2006 by Young Bin Choy. All rights reserved.

CERTIFICATE OF COMMITTEE APPROVAL

*University of Illinois at Urbana-Champaign
Graduate College*

May 23, 2006

We hereby recommend that the thesis by:

YOUNG BIN CHOY


Entitled:

**INVESTIGATION ON UNIFORM BIOMATERIAL-BASED
MICROSPHERES WITH PRECISELY CONTROLLED SIZE AND SIZE
DISTRIBUTION FOR DEVELOPMENT OF
ADVANCED DRUG DELIVERY SYSTEMS**

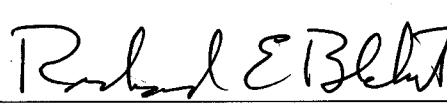
Be accepted in partial fulfillment of the requirements for the degree of:

Doctor of Philosophy


Signatures:



Director of Research -



Head of Department -




Chairperson -


Committee on Final Examination*



Committee Member -

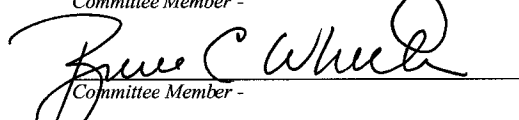


Committee Member -



Committee Member -

Committee Member -



Committee Member -

* Required for doctoral degree but not for master's degree

ABSTRACT

Uniform microspheres (MS) of biocompatible polymers were investigated for use as advanced drug delivery vehicles. Novel methods of fabricating the precision particles (i.e., precision particle fabrication (PPF) techniques) of biomaterials were developed utilizing mechanical, hydrodynamic and electric forces. A number of biodegradable/biocompatible polymers, such as ethyl cellulose (EC), chitosan, starch, and gelatin, were employed to investigate their characteristics and suitability as drug carriers. Because the MS size determines the drug diffusion and/or the degree of polymer degradation, the drug release kinetics could be accurately controlled without uncertainties resulting from uncontrolled size distribution.

Monodisperse MS of EC with two different polymer viscosities (4- and 45-cp) were fabricated by the PPF method. With use of a surfactant, uniformly generated EC solution drops could be successfully separated until dry EC MS were obtained by solvent evaporation at room temperature. The drugs encapsulated in the EC MS tended to concentrate near the surface depending on their hydrophilicity. The more hydrophilic the drug, the more concentration near the surface. The 30- and 35- μm MS exhibited more even distribution of the drug than the larger ones, possibly due to their fast hardening. The 30- and 35- μm MS of 4 cp EC showed almost linear release during the first 24 hrs for both hydrophilic and hydrophobic drugs.

To fabricate uniform MS of a hydrophilic polymer (hydrogel) such as chitosan, starch, and gelatin, an electric force was utilized to separate the uniformly generated drops. Both direct and indirect drop charging were incorporated, resulting in coulombic repulsion among the drops. Because no surfactant was involved, the method became nontoxic. For chitosan and starch, the dry MS were

obtained by solvent evaporation at a high temperature (140 ~ 160 °C). However, due to their degradation at such high temperature, the gelatin solution drops were gelled at a low temperature (0 ~ 4 °C). The solvent was extracted afterwards utilizing acetone. Uniform hydrogel MS with three different sizes were successfully fabricated regardless of the kinds of hydrogels used.

Gelatin MS (GMS), 60- μ m in diameter, were crosslinked using glutaraldehyde solutions with different concentrations. An acidic drug was introduced to form polyion complex with GMS, thereby prolonging the drug release. More sustained drug release was obtained with higher glutaraldehyde concentrations. As a result of glutaraldehyde concentration gradient in the MS, heterogeneous crosslinking seemed to exist. The amount of complexed drug near the surface decreased as the glutaraldehyde concentration increased. In situ study of the degradation profiles of the GMS with higher glutaraldehyde concentrations revealed faster erosion at the center than near the surface.

Uniform chitosan MS (CMS) were employed for precisely controlled delivery of acidic drug, where colon-specific delivery could be realized without any additive polymers or toxic process. For strong acidic drug with multiple anionic functional groups, the smaller the CMS, the more drugs could be contained until the colonic site hence the better candidate for colon-specific delivery. Weak acidic drug preferred the larger CMS due to the smaller amount of release at the gastric fluid.

ACKNOWLEDGMENTS

Thanks be to God for His love and blessing beyond description throughout my whole life.

I wish to thank my adviser, Professor Kyekyoon Kim, for his continuous support, encouragement, and help in this research, and Professor Hyungsoo Choi, for her guidance and special advice on chemistry throughout this work. Their support and love like good parents set an excellent example for me. I would also like to thank my PhD committee members, Professors Russell Jamison, Bruce Wheeler, and Brian Cunningham, for their guidance and help. I am also grateful to Dr. Cory Berkland, who patiently taught me the recipes for material preparation and in-vitro drug release study.

I would like to thank all members of the Thin Film and Charged Particle Research Laboratory for their help and support. Their kindness and friendship will never be forgotten. I am particularly thankful to Hee Kyung and Felice Cheng for their assistance with the particle fabrication and characterization. I will not forget the brotherhood with Seung Jae Hong, Changwook Kim, Huichan Seo, Sangho Lim, and Jinkeun Park. The discussion with Ravindra Singh, Anil Kumar, and Phil Heil will also be in my pleasant memory.

I am thankful to Professor Russell Jamison and his group members for their useful suggestions. Many thanks go to Abby Morgan and Aylin Sendemir-Urkmez for their masterful work on tissue engineering with our gelatin microspheres. I would like to thank Professor Jamison for providing us the gelatin and allowing us to use the optical microscope. Thanks also go to Professor Daniel Pack for allowing us to use the spectrophotometer in his lab and to Summer Rhodes and Professor Jennifer Lewis for helping me with the measurement of zeta-potential.

I would like to thank Pastor Rick Bloom and his wife, Denise Bloom, for their continuous prayer for the life of our family in Christ. I thank my wife, Young Mi Kim, son, Tobias Tae-Hwan Choy, and all other family members for their love and help. Thanks also go to my parents-in-law for their continuous support. I wish to thank my mother for guiding me with her unconditional love. I especially thank my father, Professor Jin-Ho Choy, for introducing me to science and engineering and for continuously maintaining interest in my work.

This work was financially supported by the University of Illinois.

TABLE OF CONTENTS

CHAPTER 1	INTRODUCTION.....	1
CHAPTER 2	PRECISION PARTICLE FABRICATION METHOD FOR BIOCOMPATIBLE POLYMERS.....	5
2.1	Generation of Uniform Polymer Solution Drops.....	5
2.2	Prevention of Drop Agglomeration.....	6
2.3	Particle Hardening.....	8
2.4	Apparatus for Precision Particle Fabrication.....	9
2.5	Figures.....	10
CHAPTER 3	UNIFORM ETHYL CELLULOSE MICROSPHERES OF CONTROLLED SIZES AND POLYMER VISCOSITIES AND THEIR DRUG RELEASE PROFILES.....	15
3.1	Purpose.....	15
3.2	Materials and Experimental Methods.....	17
3.2.1	Materials.....	17
3.2.2	Microsphere preparation.....	17
3.2.3	Particle size distribution.....	17
3.2.4	Scanning electron microscopy (SEM).....	18
3.2.5	Confocal microscopy.....	18
3.2.6	In vitro drug release.....	18
3.3	Results.....	19
3.3.1	Preparation of drug-loaded microspheres.....	19
3.3.2	Drug distribution in the microspheres.....	20
3.3.4	In vitro drug release study.....	21
3.4	Discussion.....	22
3.5	Conclusion.....	24
3.6	Figures and Table.....	25
CHAPTER 4	A NOVEL ELECTRIC FIELD ASSISTED METHOD FOR FABRICATION OF UNIFORM BIODEGRADABLE HYDROGEL MICROSPHERES.....	30
4.1	Hydrogel Microspheres for Controlled Drug Release.....	30
4.2	Conventional Fabrication Methods and Their Problems.....	32
4.3	Fabrication and Characterization of Uniform Hydrogel Microspheres.....	33
4.3.1	Materials.....	34
4.3.2	Preparation of uniform hydrogel microspheres.....	34
4.3.3	Characterization.....	36
4.4	Results and discussions.....	36
4.5	Conclusion.....	37
4.6	Figures.....	38

CHAPTER 5	DRUG RELEASE PROFILES OF UNIFORM GELATIN MICROSPHERES UNDER DIFFERENT CROSS-LINKING CONDITIONS.....	42
5.1	Crosslinked Gelatin Microspheres.....	42
5.2	Experimental.....	43
5.2.1	Cross-linking uniform gelatin microspheres...	43
5.2.2	Drug loading.....	44
5.2.3	In vitro drug release study.....	44
5.2.4	Observation of intraparticle drug distribution..	44
5.2.5	Zeta-potential measurement.....	45
5.2.6	In situ degradation study.....	45
5.3	Results and Discussion.....	45
5.4	Conclusion.....	50
5.5	Figures and Table.....	52
CHAPTER 6	UNIFORM CHITOSAN MICROSPHERES WITH DIFFERENT CROSSLINKING DENSITIES FOR ORAL DELIVERY.....	58
6.1	Chitosan Microspheres for Oral Delivery.....	58
6.2	Purpose.....	59
6.3	Materials and Experimental Methods.....	61
6.3.1	Materials.....	61
6.3.2	Preparation of uniform chitosan microspheres..	61
6.3.3	Drug loading in chitosan microspheres.....	62
6.3.4	Characterization.....	62
6.3.5	Drug distribution in the microspheres.....	62
6.3.6	In vitro drug release.....	63
6.4	Results.....	63
6.4.1	Differently crosslinked uniform chitosan microspheres.....	63
6.4.2	Drug distribution.....	64
6.4.3	In vitro drug release study.....	65
6.5	Discussion.....	67
6.6	Conclusion.....	69
6.7	Figures and Tables.....	70
CHAPTER 7	CONCLUSIONS.....	86
	REFERENCES.....	90
	AUTHOR'S BIOGRAPHY.....	103

CHAPTER 1

INTRODUCTION

With rapid advances in biotechnology, a variety of potent and specific drugs were discovered, many of which have become available in the market place or under regulatory review by the United States Food and Drug Administration [1, 2]. However, when the bolus drug is administered, due to its high potency and/or short half-life, frequent dosing is often needed to maintain therapeutic concentrations in a patient's body. To minimize such inconvenience and improve the patients' comfort and compliance, new devices employing biocompatible polymers as delivery vehicles have been widely investigated [3]. The drug encapsulated in a polymer could be protected from the severe body milieu and released in sustained and controlled manners minimizing unwanted side effects.

Microsphere (MS) of biocompatible polymers is one of the most common forms of drug delivery vehicle due to its ease of fabrication, simplicity of administration to various sites, and possible use in localized and targeted delivery [4]. Various polymers were utilized in those purposes. Poly (D,L-lactide-co-glycolide) (PLG) has been one of the good candidates of biocompatible and biodegradable polymers, widely used to formulate drug-loaded MS. The drugs, such as protein, vaccine, and antimicrobial agent, were encapsulated in PLG MS and exhibited sustained release for days or months by diffusion and PLG degradation [5-7]. Ethyl cellulose (EC) has been also widely investigated as a material for controlled drug release for various administration routes [8-12]. For example, indomethacin-loaded EC was studied as a rectal delivery vehicle and provided more than 5 h of prolonged release [9, 12]. EC MS loaded with potassium chloride, aspirin, fenoterol HBr, etc. were studied as oral delivery vehicles achieving 24 h of continuous release [8, 10, 13].

In addition to such synthetic polymers, natural hydrogels are known to be attractive polymers for encapsulation because of their excellent compatibility with tissue, ease of manipulation of their swelling level, and good control on their solute permeability [14]. For these reasons, the MS of such hydrogels as chitosan, starch, and gelatin have been widely investigated. Due to the cationic charge of chitosan, chitosan microspheres (CMS) are considered effective for the delivery of proteins and, especially, DNA [15, 16]. Positively charged CMS can form a polyion complex with a negatively charged protein/DNA thus prolonging their release [17, 18]. CMS were also used for site-specific delivery: due to their bioadhesiveness, the residence time of CMS in the lung and stomach increased, facilitating targeted drug delivery [19, 20]. Starch, another natural hydrogel, has been explored as a material for drug delivery because it is cheap, inert, biocompatible, and biodegradable [21]. MS of various starches were studied as adjuvant in oral immunization and as a protein delivery system [22, 23]. Gelatin microspheres (GMS) have been of great interest because of their excellent biocompatibility and degradation to non-toxic products [24]. Due to their good bioadhesive properties, GMS were suggested as a drug carrier for such administration routes as nasal, gastrointestinal, and rectal [25, 26]. GMS are well known as good protein delivery vehicles since they can be positively or negatively charged to form a polyion complex with an oppositely charged protein, prolonging the protein release [27, 28]. Due to these favorable properties, GMS have been widely used as a delivery vehicle for growth factors in tissue engineering [29, 30].

Drug release from MS-based delivery systems critically depends on the size and size distribution of the MS. The critical determinants in drug release, such as the rate of diffusion of the drug and degradation of the polymer matrix, were strongly influenced by the surface area-to-volume ratio of the particles. For site-specific delivery, the MS size was also known to be a critical factor. The MS less

than 10 μm were reported to be effective for the particle transportation via Peyer's patches [31]. The MS, 10–20 μm in diameter, have been used to specifically target the tortuous capillary bed of tumor tissues by chemo-embolization [32]. The MS size could also determine the porosity of a scaffold. When embedded in a scaffold, the MS were shown to function as both digestive porogen and drug delivery vehicle [30]. To fabricate the MS of biocompatible polymers, various methods such as coacervation [33, 34], aqueous precipitation [35, 36], classic emulsion [24, 30, 37, 38], and spray drying [39-42], were employed. However, due to a lack of control over agitation and an inability to prevent drop agglomeration, none of them produced uniform MS. In this study, we utilize the precision particle fabrication (PPF) method and fabricate uniform MS of various biocompatible polymers with precisely controlled size and size distribution. Concurrent use of mechanical and hydrodynamic forces allowed the method to be not so limited by the solution viscosity or the nozzle dimension, which provided flexibility in particle size control. With the use of electric force, originally introduced in this work, particle agglomeration was prevented without recourse to toxic surfactants, making the method suitable for biomedical application. Most of all, due to the excellent uniformity of the resulting MS, the detailed drug release study could be performed without uncertainties caused by wide particle size distribution.

In Chapter 2, we explain the theory and background of the PPF scheme to understand its significance and advantages. Chapter 3 describes uniform EC MS fabricated by the PPF method and the drug release profiles of the drug-containing MS. Chapter 4 outlines new improving features of the PPF apparatus that are particularly suited to fabrication of uniform hydrogel MS. In Chapters 5 and 6, we examine the drug release from thus-prepared uniform hydrogel MS. Chapter 5 describes the effect of crosslinking on uniform GMS and their drug release profiles. In Chapter 6, we investigate uniform CMS with different crosslinking densities for

oral delivery of the drugs with different ionic charges. Chapter 7 summarizes the present work and presents concluding remarks.

CHAPTER 2

PRECISION PARTICLE FABRICATION (PPF) METHOD FOR BIOCOMPATIBLE POLYMERS

The PPF scheme was evolved from the previous work by Kim and colleagues [43-49], in which precision microspheres (MS) and microcapsules comprising frozen hydrogen, silica aerogel, and other materials were fabricated. By combining mechanical, hydrodynamic, and electric forces, uniform particles with micro- or nanosizes were successfully fabricated relatively free from limitations imposed by the viscosity of the source solution, dimension of the drop-producing nozzle, and drop agglomeration.

In this chapter, we describe the PPF methodology specifically responsible for manufacturing uniform MS of biocompatible polymers and the apparatus built to practice the method. The PPF consists of three techniques: generation of uniform solution drops, prevention of agglomeration, and particle hardening.

2.1 Generation of Uniform Solution Drops

To fabricate uniform MS, one needs to first generate uniform polymer-solution drops. To achieve this, the polymer solution was pumped through a small nozzle forming a jet, which was subsequently broken into uniform droplets by precisely controlled mechanical (acoustic) force as shown in Figure 2.1(A). All figures and tables appear at the end of each chapter. The drop radius predicted by Lord Rayleigh [50, 51] is:

$$r_d = (3r_j^2 v_j / 4f)^{1/3} \quad (2.1)$$

where r_j is the radius of the undisturbed jet, v_j the linear velocity of the jet, and f the

frequency of the acoustic excitation. Thus, the size of the droplets produced by this method, can be accurately controlled by adjusting the jet velocity and the acoustic frequency.

However, with this scheme alone, the smallest drop size achievable is about twice the nozzle opening. To further reduce the drop size, therefore, the nozzle opening has to be accordingly further reduced, which is not applicable to high-viscosity solutions. To overcome this difficulty, a hydrodynamic force employing a carrier stream was utilized achieving further reduction in the jet thickness. As shown in Figure 2.1(B), the carrier stream, consisting of a solvent immiscible with an aqueous hydrogel solution, surrounded the jet and was adjusted to move faster than the jet. Consequently, the resulting frictional force accelerated the jet and made it thinner. This jet was then broken up into uniform drops much smaller than the nozzle opening.

Previously, we fabricated uniform MS of various polymers including PLG, polyanhydride, etc. [2, 52-54]. Because the polymer solutions in this work were an oil-phase, water was utilized as a nonsolvent carrier stream. In contrast, when the hydrophilic polymer such as hydrogel is employed, the carrier stream needs to be an oil phase.

2.2 Prevention of Agglomeration

To minimize the surface energy, smaller drops tend to agglomerate to form larger ones. Because of this tendency, the drops, once generated, need to be separated to retain their uniform original size. One way to achieve this separation is to use a surfactant and reduce the surface tension force of the drops. In our previous work, the drops of oil-soluble polymers were seen not to agglomerate when a surfactant, polyvinyl alcohol (PVA) was incorporated [2, 52-54]. However, with hydrophilic polymers, various attempts using surfactants failed to prevent the

drops suspended in oil phase from coalescing [55, 56].

To resolve this difficulty, an electric field was employed to charge the drops with the same polarity. As is well known, the repulsive force between the two point charges with the same polarity and amount of charge is [57]:

$$F = Q^2 / 4\pi\epsilon R^2 \quad (2.2)$$

where F is the force, Q the amount of charge, ϵ the permittivity of the media, and R the distance between two points. We utilized both direct and indirect charging methods to prevent the drop coalescence. For direct charging, hydrogel solution was connected to a high voltage (Figure 2.2(A)) injecting the charge directly through induction. However, it might not be safe for a large-scale system because the whole apparatus in contact with the hydrogel solution could also experience high electric potential if not heavily insulated. To avoid such a problem, an indirect charging method (Figure 2.2(B)) was suggested. A conductive ring at a high electric potential was placed on the path of a hydrogel solution jet without contact. An electric field formed between the ring and the electrically grounded hydrogel solution induced the charge into the drops. By this method, only the ring has a high electric potential, thereby resolving the possible safety issue caused by direct charging

To successfully spread the drops using an electric force, the selection of the collection media is critical. While the drops were separated in the media, discharge needed to take place very slowly allowing for the drops to harden without losing their uniformity. For fabrication of oil-soluble polymer MS, the method was not applicable. The solution drops were suspended in aqueous media, which were highly conductive, rapidly losing their charge before being hardened. In contrast, the solution drops of hydrophilic polymers such as hydrogel were collected in non-

conducting oil allowing the drops to maintain their charges.

2.3 Particle Hardening

While separated in the collection media, the drops were subjected to hardening to convert them into dried MS. The phase of the collection media was selected to be immiscible with the polymer solution so that it helped to achieve smooth spherical shape of the MS due to the high surface tension force. In contrast, air-dried MS were often reported to exhibit nonuniform and rough morphologies due to the low interfacial tension between the air and the polymer solution [39, 40].

In this study, we employed three different hardening methods depending on the solvent characteristics and the polymer kinds (Figure 2.3). The solvent with high vapor pressure was evaporated at room temperature without any other treatment while the drops were suspended in the collection media (Figure 2.3(A)). In our previous study, the solvent with high vapor pressure, such as methylene chloride (350 mmHg at 20 °C), was evaporated at room temperature to obtain dry PLG and/or polyanhydride MS [2, 52-54]. However, for the solvent with low vapor pressure such as water (17.54 mmHg at 20 °C), the solvent evaporation was facilitated by the collection bath heated above their boiling point (140 ~ 160 °C), as shown in Figure 2.3(B). This evaporation method, however, was inapplicable to a polymer such as gelatin because of its degradation at high temperatures. Instead, as shown in Figure 2.3(C), a low temperature (0 ~ 4 °C) was used for the collection bath to cause gelation of the solution drops. These gelled drops were rigid enough not to recombine even after charge disappeared. The resulting suspension was mixed with acetone afterwards to extract the solvent (water) and obtain the dried MS as previously reported [27].

2.4 Apparatus for Precision Particle Fabrication

The apparatus was designed so as to be specially suited to fabrication of uniform biocompatible polymer MS as shown in Figure 2.4. A dual nozzle was utilized to generate the solution jet thinner than the nozzle orifice, with help of the carrier stream. A typical size of the nozzle opening utilized in this study was about 250 μm . The nozzle was attached to an ultrasonic wave launcher to introduce a mechanical force (acoustic excitation) into the source jet. The energy and frequency of the acoustic wave were managed by the electric power supply. The drop generation was monitored on a TV screen via a camera and an optical microscope. To measure the size of the drops during generation, the still image was obtained by using a stroboscope by synchronizing it with the acoustic wave. The resulting drops were collected in the nonsolvent media, which were stirred slowly to expedite the solvent evaporation or the drop gellation. All the parameters, such as the flow rates of the polymer solution and the carrier stream, the acoustic energy, and the frequency, were precisely controlled using a computer interface to improve accuracy and reproducibility. Figure 2.5 shows the control panel of the PPF apparatus, where all the critical parameters could be controlled remotely.

2.5 Figures

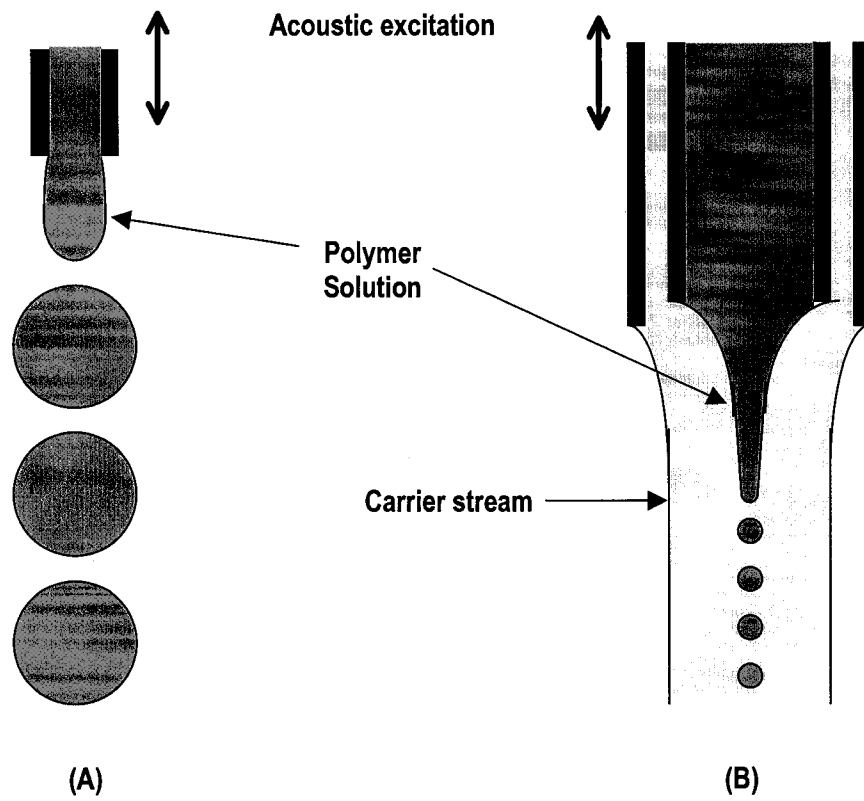


Figure 2.1 Generation of uniform solution drops (A) from a single nozzle, and (B) a dual nozzle employing a carrier stream.

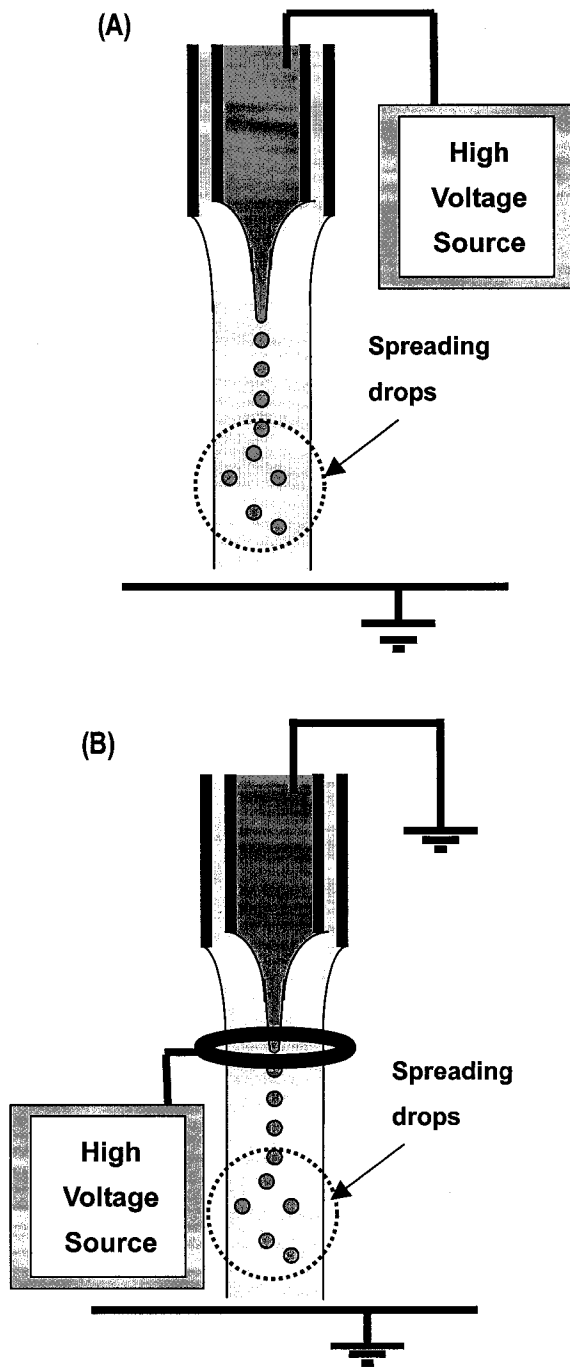


Figure 2.2 Drop separation by an electric force. Two different charging methods were employed: (A) direct charging, and (B) indirect charging.

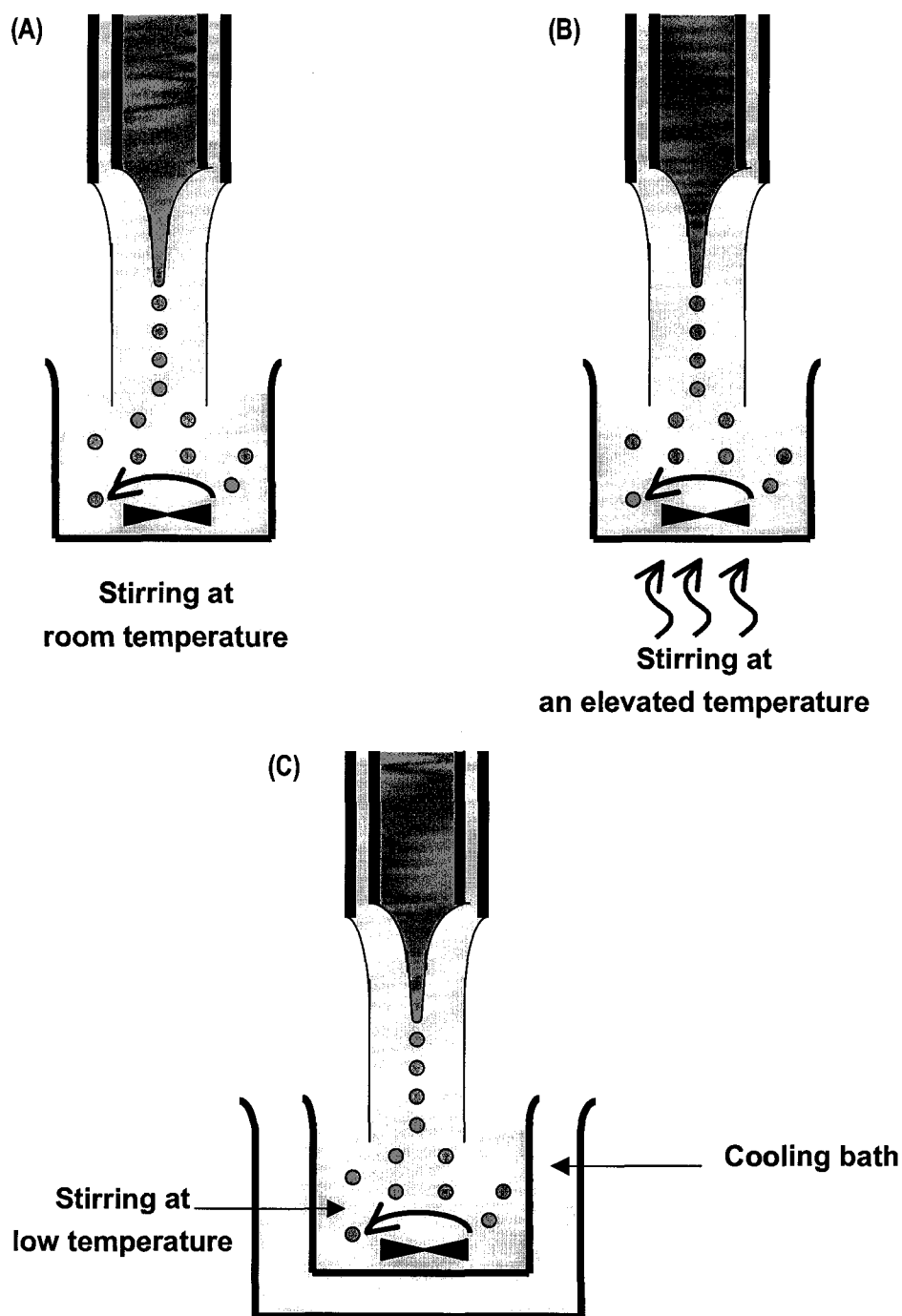


Figure 2.3 Schematic illustrations of different hardening methods: (A) solvent evaporation at room temperature, (B) solvent evaporation at an elevated temperature, and (C) gellation of the polymer solution drops at low temperature.

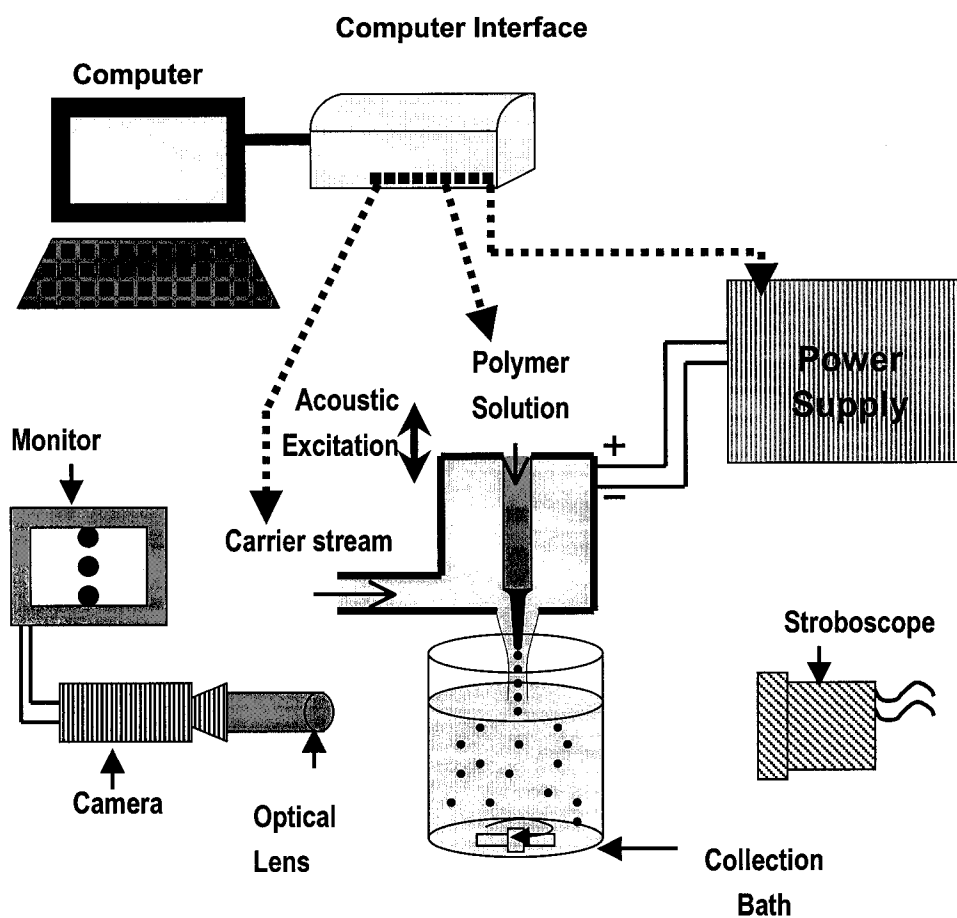


Figure 2.4 Simplified schematic of the PPF apparatus for fabrication of uniform MS of biocompatible polymers. All the parameters were controlled by a computer to improve the reproducibility.

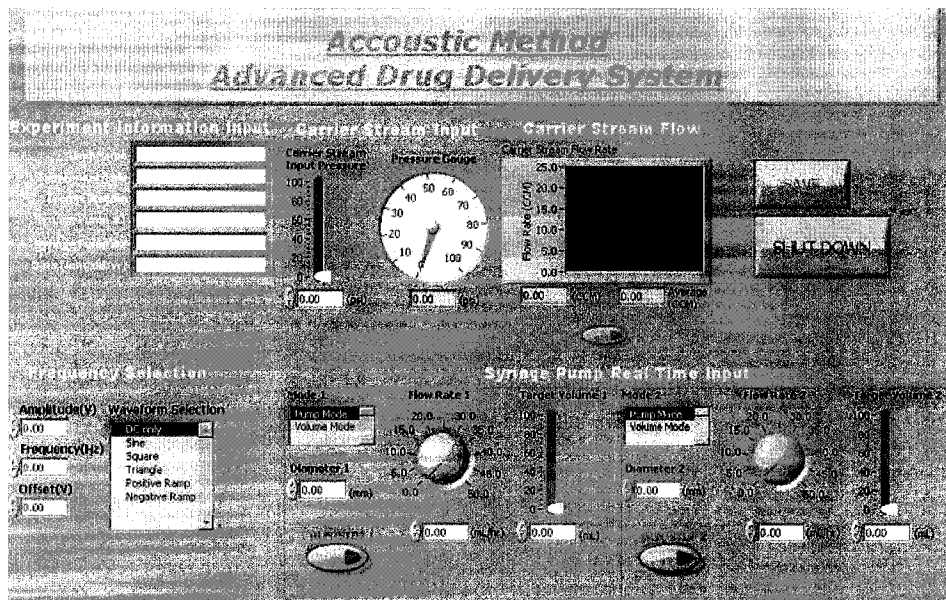


Figure 2.5 Control panel of computer-based PPF apparatus.

CHAPTER 3

UNIFORM ETHYL CELLULOSE MICROSPHERES OF CONTROLLED SIZES AND POLYMER VISCOSITIES AND THEIR DRUG RELEASE PROFILES

Monodisperse EC MS were fabricated by the PPF methodology described in Chapter 2, which combines mechanical and hydrodynamic forces. Due to the excellent uniformity and sphericity of the particles, the drug release profiles obtained with the resulting EC MS were free from the uncertainties caused by the uncontrolled particle size and morphology. The effect of polymer viscosity was examined by employing EC with two distinct viscosities (4- and 45-cp). Piroxicam and rhodamine B were used as the model drugs. The drug distribution in the MS was examined to see the effect on drug release.

3.1 Purpose

EC, a water-insoluble and pH-independent polymer, has been widely used as a material for controlled drug release for various administration routes [8-12, 58, 59]. Several methods of fabricating drug-loaded EC MS, including coacervation [11, 33, 34, 60], spray drying [41, 42], and emulsion techniques [13, 37, 38, 60-64], have been investigated and the factors affecting the drug release profiles studied. The nonsolvents used [37, 60, 61], the amount of emulsion stabilizer [63], the rate of agitation [12, 63, 65], and the molecular weight of EC [38, 41] were varied to examine their respective effects on drug release. However, none of these release studies was carried out without the uncertainty stemming from the inability to precisely control the size and size distribution of the MS.

It is well known that the shape, size, and size distribution of drug-loaded MS are critical determinants of drug release profiles because the surface area-to-

volume ratio of the MS strongly affects the rate of drug release and/or polymer degradation. For example, MS with distorted spherical shape should show different drug release from those with smooth spherical shape, even with the same volume due to difference in the surface areas. EC MS obtained from coacervation and spray drying exhibited irregular shapes with wide size distributions [34, 41]. Most of the MS obtained from the emulsion method exhibited smooth spherical shapes [13, 37, 38, 60-64] but still wide size distributions. The reported standard deviations of the size distributions were 20~50% of the average diameters.

We recently fabricated monodisperse MS of poly(D,L-lactide-co-glycolide) (PLG) and a few other polymers for use as drug delivery systems using the PPF technique [2, 52-54]. Following the basic PPF scheme, drug-loaded EC MS with uniform size and precisely controlled size distribution were fabricated in this work. Piroxicam, a nonsteroidal anti-inflammatory drug (NSAID), and rhodamine B were encapsulated as model drugs. Although the two drugs are similar in molecular weight, piroxicam was chosen as a representative for water-insoluble drugs (53.3 µg/ml at pH ~7) and rhodamine for water-soluble drugs (7.8 mg/ml) [53]. By fabricating monodisperse EC MS with different sizes from two distinct viscosities of EC, we were able to investigate the effects of particle size and polymer viscosity on the drug release, without the uncertainties associated with the particle size variation. EC stocks with viscosities of 4 cp and 45 cp were used. The effects of particle surface morphology and drug distribution on drug release were studied. The *in vitro* drug release studies were performed over 24 h mainly to investigate the effectiveness of the EC MS as oral/rectal delivery vehicles.

3.2 Materials and Experimental Methods

3.2.1 Materials

EC with two different viscosities (48% ethoxy, 4 cp; and 49.3% ethoxy, 45 cp) were obtained from Aldrich. PVA (88% hydrolyzed) was purchased from Polysciences. Rhodamine B chloride was acquired from Sigma. Piroxicam freebase was a gift from Dongwha Pharmaceuticals (Korea). HPLC-grade dichloromethane (DCM) was purchased from Fisher Scientific.

3.2.2 Microsphere preparation

Uniform EC MS with drug loading were fabricated as described in Chapter 2 (Figures 2.1, 2.3(A), and 2.4). Briefly, to fabricate the drug-loaded EC MS, EC was dissolved in methylene chloride (5% w/v) followed by an initial loading of the drugs (piroxicam: 5% w/w and rhodamine: 10% w/w). The resulting EC solution was fed into a nozzle structure with a syringe pump to produce a smooth liquid jet exiting the nozzle opening. A carrier stream (1% w/v PVA in DI water) surrounding, and moving faster than, the jet was introduced, accelerating the jet to a desired smaller size below the nozzle opening. An acoustic excitation of controlled frequency and amplitude was launched into the jet using a piezoelectric transducer (Branson Ultrasonics) controlled by a frequency generator (Hewlett Packard model 3325A). The jet was broken into a train of uniform droplets, which were collected in a beaker containing a PVA solution and subsequently hardened for 2 ~ 5 h. The resulting microspheres were filtered, washed several times with DI water, and lyophilized.

3.2.3 Particle size distribution

A Coulter Multisizer 3 (Beckman Coulter, Inc.) equipped with a 200- μ m

aperture was used to determine the size distribution of the resulting EC MS. The EC MS were suspended in Isoton electrolyte with a dispersant to prevent aggregation. More than 5000 MS were counted for each sample.

3.2.4 Scanning electron microscopy (SEM)

The uniformity and surface morphology of the microspheres were examined using a Hitachi S-4700 scanning electron microscope. A droplet of an aqueous suspension of EC MS was placed on a small piece of silicon wafer attached onto a scanning electron microscope sample holder. The samples were dried overnight and sputter-coated with gold to facilitate SEM imaging. The MS were imaged at 2-10 kV.

3.2.5 Confocal Microscopy

A small amount of drug-loaded EC MS (~1 mg) was suspended in distilled water. A droplet of the resulting suspension was placed on a microscope slide and dried overnight. The drug-loaded MS were imaged using a laser scanning confocal microscope (Olympus Fluoview FV 300 Laser Scanning Biologic Microscope). Krypton and helium/neon lasers were used to excite rhodamine and piroxicam, respectively. The midsections of the MS were analyzed to determine the drug distribution at the center.

3.2.6 In vitro drug release

A known amount of EC MS loaded with piroxicam or rhodamine (~5 mg) was suspended in 1.5 ml of a PBS solution (pH = 7.4) containing 1% Tween 20. The suspensions were incubated at 37 °C for 24 h while continuously agitated by inversion (~8 rpm). At certain time intervals, the supernatant was sampled and the same volume refilled with a fresh buffer solution. Absorbance of the sampled

supernatant was measured at 350 nm for piroxicam and 550 nm for rhodamine, respectively. The amount of drug release at each time interval was cumulatively added to the amount measured at the previous time interval and divided by the actual loading in the MS, resulting in cumulative percent release. The samples prepared with the same amount of blank MS were treated identically, and the absorbance values thus obtained were subtracted from all measurements.

3.3 Results

3.3.1 Preparation of drug-loaded microspheres

Uniform EC MS with drug loading were fabricated using the PPF method. The model drugs, piroxicam and rhodamine, were encapsulated as the representatives of water-insoluble and water-soluble drugs, respectively. For each viscosity of EC, three different sizes of MS were fabricated to study the effects of particle size and viscosity on drug release. Figure 3.1 shows the pictures of the resulting MS with two different viscosities (4 cp and 45 cp) taken by a scanning electron microscope (SEM), which provide clear visual evidence of the uniformity of the MS. Piroxicam-loaded MS of 35-, 55-, and 85- μm diameters were fabricated using 4-cp EC and 30-, 55-, and 90- μm diameters using 45-cp EC (Table 3.1). Rhodamine-loaded MS were fabricated with 30-, 60-, and 105- μm diameter using 4-cp EC and 20-, 60-, and 90- μm diameter using 45-cp EC (Table 3.1). All MS exhibited much smaller sizes than the nozzle opening (250 μm) used for the fabrication in this study, which showed that the carrier stream functioned properly reducing the thickness of the EC solution jet. To further prove the uniformity and narrow size distribution of the EC MS, four different batches of the MS were measured using a Coulter Multisizer. As shown in Figure 3.2, uniform EC MS of various sizes were fabricated with more than 90% of the MS within $\pm 3 \mu\text{m}$ of the

average diameter.

3.3.2 Drug distribution in the microspheres

The drug distribution inside of the MS is one of the critical factors governing drug release. To examine the drug distribution, the mid-section of the drug-loaded MS was inspected using confocal fluorescent microscopy. The intensity of the emission light corresponded to the relative concentration of the drug. Grattard et al. [41] previously examined the distribution of fluorescein-labeled protein in spray-dried EC MS and observed uncontrolled distribution profiles possibly due to the polydispersity of the EC MS. The monodisperse EC MS fabricated in the present work exhibited drug distributions specific to each precisely controlled size.

Figure 3.3 shows piroxicam and rhodamine distributions inside the EC MS. It appears that rhodamine is more hydrophilic than piroxicam, which, in turn, is more hydrophilic than EC. As a result, only the small EC MS (30- and 35- μm) exhibited relatively homogeneous piroxicam distributions, where, due to the rapid particle hardening, the drug had little time to diffuse outwardly toward the aqueous media. Larger MS, therefore, showed higher piroxicam concentrations near the particle surface. For rhodamine, possibly due to its hydrophilicity, the high drug concentrations near the surface were more notable regardless of the MS size and EC viscosities. Still, due to rapid hardening, the 20- and 35- μm MS showed more evenly distributed rhodamine.

The above results are consistent with our previous observations with PLG MS, which showed that piroxicam in the PLG MS exhibited higher concentrations at the center while rhodamine localized at the surface, due to the different affinities of the drugs for the polymer and aqueous phase [52]. Piroxicam might be more hydrophobic than PLG, causing it to localize toward the center while rhodamine,

being less hydrophobic (or more hydrophilic) than PLG, may have moved outwardly toward the aqueous media during hardening.

3.3.4 In vitro drug release study

Figure 3.4 shows the results from the in vitro drug release experiments, which elucidate the effects on the release kinetics of the particle size, viscosity of EC, and intraparticle drug distribution. The effects of MS size were dominant in piroxicam release, which could be explained by the relationship between the MS size and the surface-area-to-volume ratio (Figures 3.4(A) and (B)). The larger the MS, the smaller the surface-area-to-volume ratio, reducing the flux of piroxicam out of the particles. For 4-cp EC, however, the release from the 55- μm MS at the beginning was faster than that from the 35- μm MS. The drug, highly concentrated near the surface as shown in Figure 3.3(B), seemed to cause faster release from the 55- μm MS [66]. The initial burst of piroxicam from the 55- μm MS of 45-cp EC could also be explained by the high drug concentrations at the surface. For the 90- μm MS of 45-cp EC, the large size and high polymer viscosity appeared to suppress the release during the initial 8 h.

The effect of polymer viscosity on rhodamine release was quite dramatic. As shown in Figures 3.4(C-D), the total percent release during the first 24 h for the 45-cp MS was below 8% while that for the 4-cp MS was 20 – 60 %. For the 60- μm MS, the total release increased from 8 to 40% as the viscosity decreased from 45- to 4-cp. For 45-cp MS, 60- μm particles exhibited faster release ($\sim 8\%$) than the other sizes ($< 2\%$). However, due to the overall slowdown in release, the size effect of the 45-cp MS was minimal. On the other hand, the release of rhodamine from 4-cp MS exhibited a stronger dependence on MS size (Figure 3.5(C)). For instance, the total percent release during the first 24 h for 105- μm MS was 20% whereas it was 60 % for 30- μm MS.

3.4 Discussion

The size, size distribution, and viscosity of the EC MS strongly influence the in vitro drug release profiles. Given a particular drug and carrier polymer, the surface area-to-volume ratio (i.e., the particle size) most critically influences the intraparticle drug distribution and the diffusive drug release, which, in turn, dictate the drug release kinetics. The PPF method provided us the means by which to fabricate piroxicam- and rhodamine-loaded uniform EC MS with precisely controlled sizes, as shown in Figures 3.1 and 3.2. This, in turn, enabled us to elucidate the parameters affecting the drug release without the uncertainties resulting from non-uniform particle size.

The effects of MS size and polymer viscosity on the drug release have been investigated by many researchers. For instance, the release of isosorbide dinitrate or potassium chloride in EC MS was reported to increase as the MS size decreased [10, 63]. Arabi et al. [67] showed that higher polymer viscosity retarded the allopurinol release more. However, these investigators could not accurately control the MS size by varying the surfactant concentration, agitation rate, or sieve size and had to settle with wide size distributions. As a result, accurate analysis of the effects of MS size and polymer viscosity was not possible. In the present work, the uncertainties originating from MS size variation were eliminated using uniform EC MS (Figures 3.1 and 3.2) fabricated by the PPF method and a release profile specific to each MS size was obtained.

The drug release profiles are influenced by the properties of the MS such as the particle size, polymer viscosity, and intraparticle drug distribution. For example, due to high EC viscosity, as shown in Figures 3.4(C) and (D), the total percent release of rhodamine during the first 24 h was minimal (< 8%) for all MS of 45-cp EC while more than 60% of release was obtained with the 30- μ m MS of 4-cp EC. The effects of MS size were also notable in drug release from the MS of

4-cp EC (Figures 3.4(A) and (C)). That is, the larger the MS, the slower the drug diffusion out of the particles. . However, interestingly, the release from the 30- and 35- μm MS was more sustained than that from the larger MS, 55- and 60- μm in diameters, respectively. The drug, highly concentrated near the surface as shown in Figure 3.4(B), seemed to be responsible for the fast drug release at the beginning from the 55- and 60- μm MS resulting in less sustained drug release than the smaller MS [66].

Reduction of initial burst and sustained release of the drug has been widely studied for hydrophilic drugs such as proteins and peptides since significant initial burst is not only dangerous to the body but also undesirable for a long-term release [68]. To realize zero-order release, which is considered the optimal release of nonsteroidal anti-inflammatory drugs such as ketoprofen, the reduction of initial burst is necessary [69]. It was reported that the release of fenoterol HBr, a highly water-soluble drug, from EC MS exhibited a reduced initial burst with the addition of nonsolvent such as petroleum benzene during the microsphere hardening [65]. Yamada et al. [69] realized an approximate zero-order release of ketoprofen by coating the Eudargit particles with a mixture of carboxymethylethylcellulose and EC. However, the size distributions of their microspheres were not precisely controlled, thereby still leaving the unresolved issue of reproducibility due to the polydispersity of MS.

The monodisperse EC MS of 30- and 35- μm size, fabricated with the PPF method reported herein, exhibited approximate linear release with reduced initial bursts. As mentioned above, the fast hardening of the small MS might give rise to more even drug distributions and prevent massive dissolution of the drug from the surface at the initial stage of the release of both hydrophobic and hydrophilic model-drugs. Most importantly, due to the precise control of the size and size distribution, the critical parameters governing the drug release, such as the surface-

area-to-volume ratio and intraparticle drug distribution, could be controlled highly consistently and reproducibly for each specific size of the MS.

3.5 Conclusion

We have developed a novel method of fabricating drug-loaded uniform EC MS with precisely controlled sizes and size distributions. Both acoustic and hydrodynamic forces were used to produce the MS. The effects of the MS size and EC viscosity on the drug release kinetics were examined. The size effects were quite evident with the piroxicam release. The initial burst of piroxicam from the 55- μm MS may be explained by the high drug concentrations at the MS surface. The rhodamine release from 4-cp MS varied according to the MS size. The release from the 45-cp MS was slow due to the higher viscosity. The 30- and 35- μm MS of the lower viscosity showed approximate linear release with a reduced initial burst possibly due to the relatively uniform drug distributions. The EC MS prepared by the PPF method could realize sustained drug release with high reproducibility.

3.6 Figures and Table

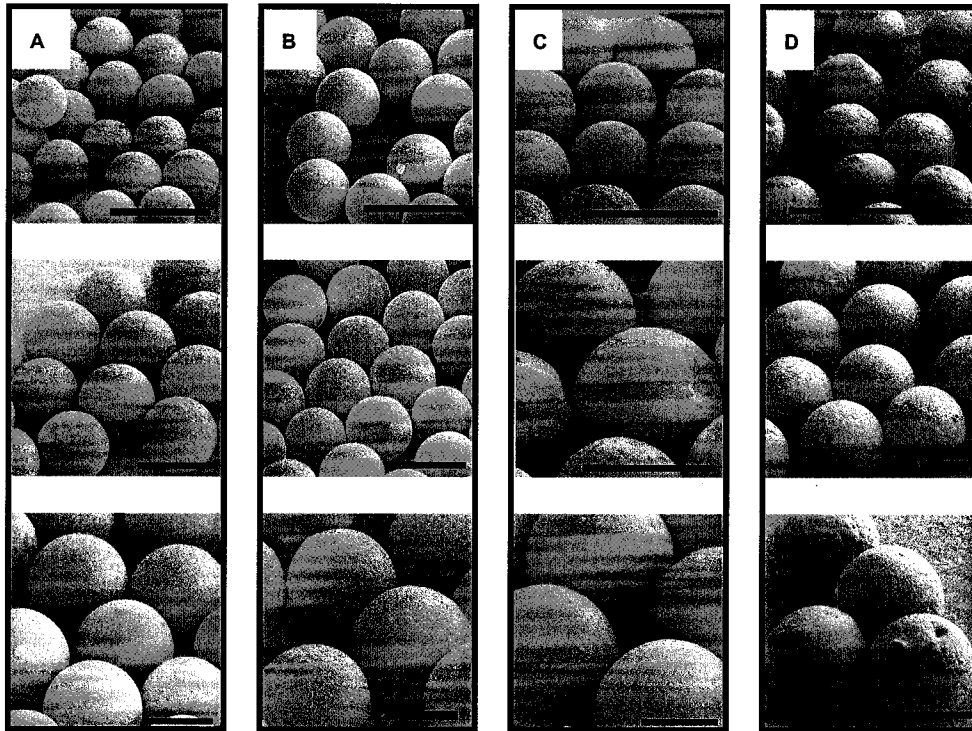


Figure 3.1 SEM pictures of drug-loaded uniform EC MS with different sizes and EC- viscosities. The drugs loaded and EC viscosities are (A) piroxicam, 4 cp; (B) piroxicam, 45 cp; (C) rhodamine, 4 cp; and (D) rhodamine, 45 cp. The diameters of the MS are, from top to bottom, (A) 35, 55, 80 μm ; (B) 30, 55, 90 μm ; (C) 30, 60, 105 μm ; and (D) 20, 60, 90 μm . The scale bars are 50 μm .

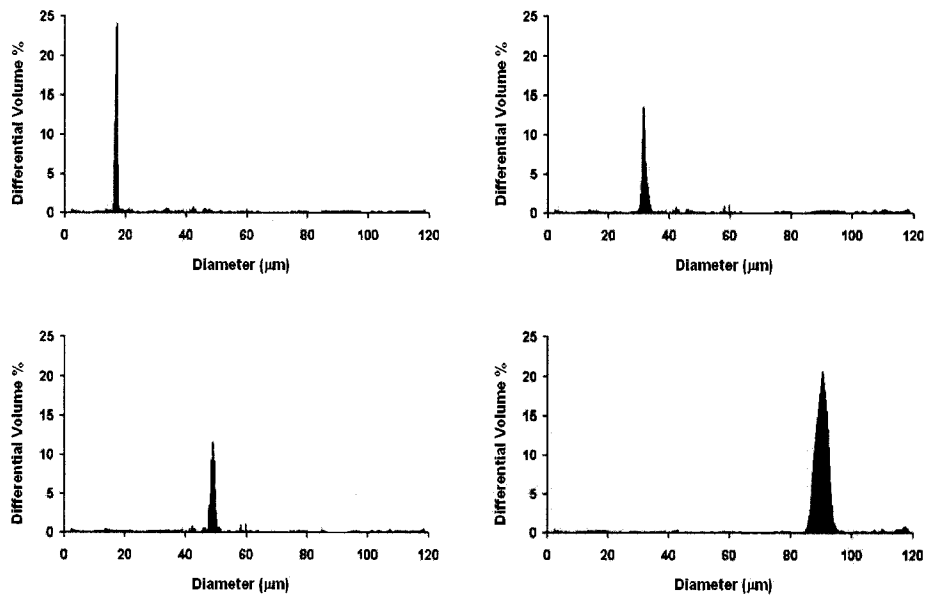


Figure 3.2 Size distributions of four different batches of EC MS fabricated with the PPF method.

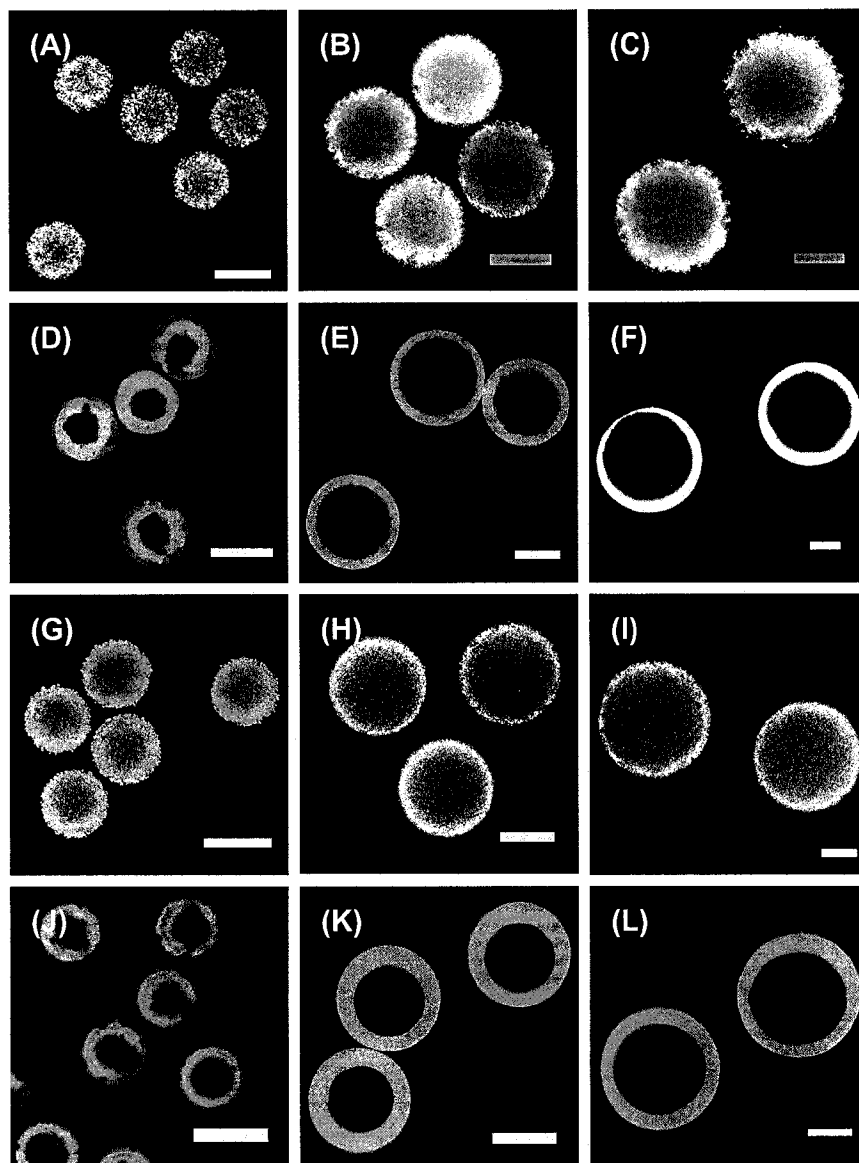


Figure 3.3 Confocal laser micrographs of drug-loaded EC MS with different sizes and EC viscosities. The light intensity indicates piroxicam and rhodamine distributions. The scale bar is 30 μm . The drugs loaded are (A)-(C) piroxicam, (D)-(F) rhodamine, (G)-(I) piroxicam, and (J)-(L) rhodamine. The EC viscosities are (A)-(F) 4cp, and (G)-(L) 45 cp. The diameters are (A) 35 μm , (B) 55 μm , (C) 80 μm , (D) 30 μm , (E) 55 μm , (F) 90 μm , (G) 30 μm , (H) 60 μm , (I) 105 μm , (J) 20 μm , (K) 60 μm , and (L) 90 μm .

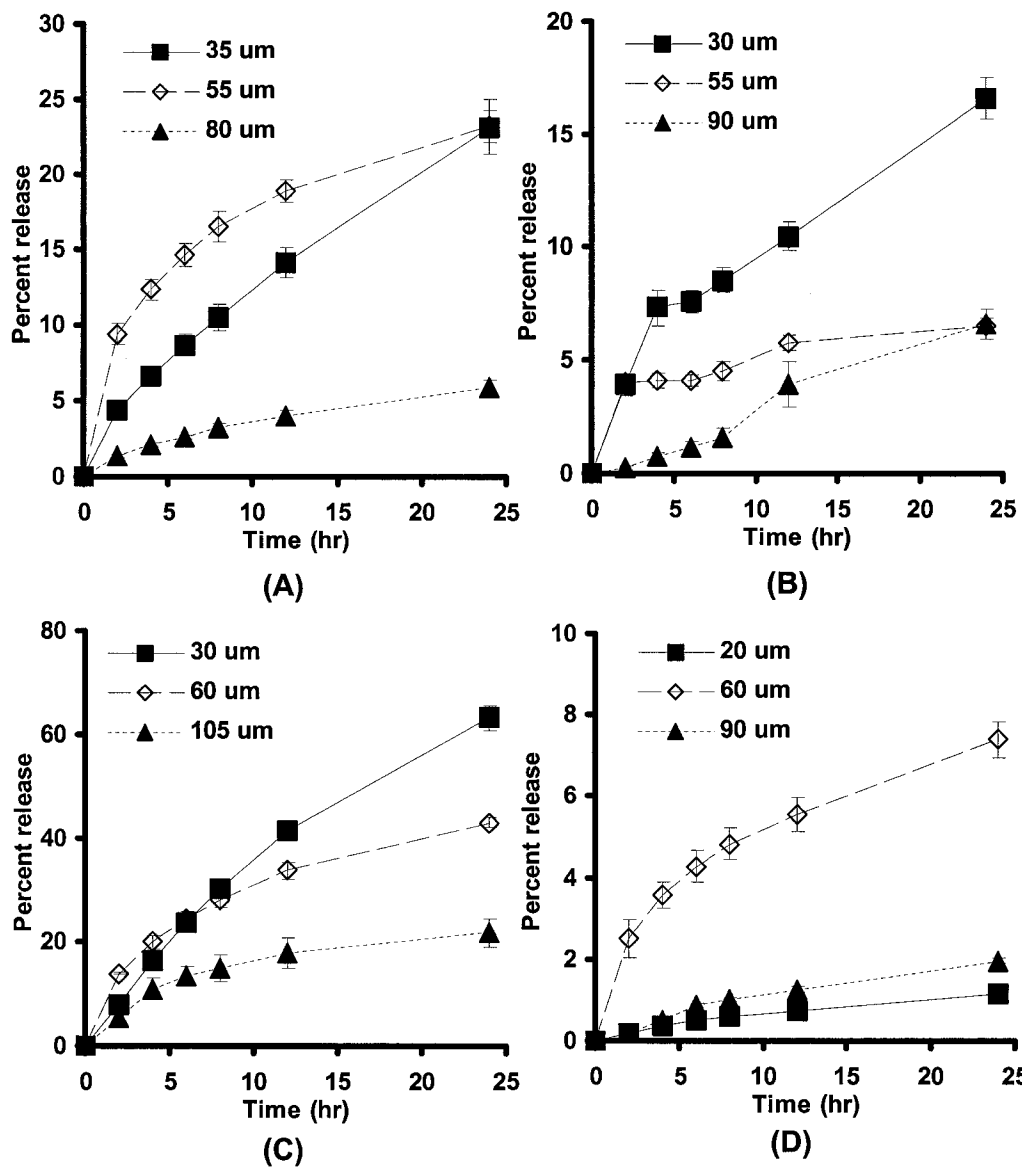


Figure 3.4 Drug release profiles from EC MS with different sizes and EC viscosities. The drugs and EC viscosities are (A) piroxicam, 4 cp; (B) piroxicam, 45 cp; (C) rhodamine, 4 cp; and (D) rhodamine, 45 cp.

Table 3.1 Average diameters EC microspheres fabricated by the present method

Polymer	Viscosity	Average Diameter (μm)
Piroxicam	4 cp	35(\pm 1.5)
		55(\pm 2.6)
		80(\pm 3.0)
	45 cp	30(\pm 2.4)
		55(\pm 3.0)
		90(\pm 2.5)
Rhodamine B	4 cp	30(\pm 1.5)
		60(\pm 1.5)
		105(\pm 2.3)
	45 cp	20(\pm 1.0)
		60(\pm 2.0)
		90(\pm 2.5)

CHAPTER 4

A NOVEL ELECTRIC FIELD ASSISTED METHOD FOR FABRICATION OF UNIFORM BIODEGRADABLE HYDROGEL MICROSPHERES

A modified PPF method enabling fabrication of uniform biodegradable hydrogel microspheres of precisely controlled size has been developed. Especially, with the use of electric force, the method allows surfactant-free and nontoxic particle fabrication. Four different hydrogels, including chitosan, starch, and gelatins with two distinct polarities, were utilized as the model polymers.

4.1 Hydrogel Microspheres for Controlled Drug Release

Hydrogel MS were widely investigated as drug delivery vehicles due to their advantages including tissue compatibility and ease of swelling and, solute permeability [14]. The MS using hydrogel polymers such as chitosan and starch have been of particular interest for controlled drug release.

Chitosan is a natural cationic hydrogel and has been used as the encapsulation materials for biodegradable microspheres [15, 16]. The drugs such as prednisolone sodium phosphate, melatonin, and theophylline were encapsulated in CMS resulting in prolonged drug release [16, 70-73]. Due to the bioadhesiveness of chitosan, CMS were used for site specific delivery [19, 20, 35]. Morphine, which has low bioavailability administered in simple solution, was loaded in CMS and exhibited rapid adsorption to the lung with high bioavailability [19]. In eradicating *Helicobacter pylori*, which is etiologically linked to chronic gastritis, peptic ulcer disease, and gastric cancer, the CMS containing tetracycline increased the residence time in the stomach, thus resulting in high drug efficacy [20, 35].

CMS are also well known as a good protein and/or as DNA delivery vehicle because of their cationic charge [15, 17, 18]. Positively charged CMS can

form a polyion complex with a negatively charged protein thus prolonging the release. The plasmid DNAs such as pGL2 and pMK3 showed sustained and high protein production using CMS as carrier [17]. The CMS containing transforming growth factor- β 1 (TGF- β 1) were incorporated into the tissue scaffold augmenting the cell proliferation and production of extracellular matrix [15, 18].

Starch, another natural hydrogel, has been explored for its use as a drug delivery vehicle because it is inexpensive, inert, biocompatible, and biodegradable [21]. The MS of various starches were studied as adjuvant in oral immunization and protein delivery system [22, 23, 74-77]. Polyacryl starch MS were examined as a drug delivery system for vaccination and successfully induced mucosal and systemic immune responses using antigens such as rotavirus, human serum albumin, and diphtheria toxin [22, 23, 74, 77]. The proteins such as bovine serum albumin, horseradish peroxidase, and insulin, were encapsulated in poly(acryloyl-hydroxyethyl starch) MS and exhibited good stability and prolonged release [75, 76].

Gelatin microspheres (GMS) have been of great interest in recent years because of its excellent biocompatibility and degradation to non-toxic products [24]. The administration routes such as nasal, gastrointestinal and rectal ways were suggested in conjunction with using GMS as drug carrier due to their good mucoadhesive properties [26, 78-80]. Carboplatin, an antitumor drug was encapsulated in GMS and successfully delivered via the nasal route with very high lung-targeting efficiency [56] and calcitonin, which has a low bioavailability when administered via the oral route, also resulted in enhanced nasal adsorption [81]. Interleukin-10 (IL-10), an anti-inflammatory cytokine, was delivered via rectal routes of female mice and inhibited colonic mucosal inflammation more efficiently when GMS were used as delivery vehicles [26].

In addition to bioadhesiveness, GMS are well known as good protein

delivery vehicles since they can be positively or negatively charged and can form a polyion complex with an oppositely charged protein thus prolonging the protein release [27, 28]. Proteins complexed with gelatin hydrogel are known to be released through the degradation of gelatin. Due to these properties, GMS have been widely used as a delivery vehicle for growth factors in tissue engineering [25, 30, 82-88]. Growth factors are known to contribute to tissue regeneration at different stages of cell proliferation and differentiation [88, 89]. However, due to their short half-lives, an appropriate delivery vehicle is needed to maintain therapeutically efficacious levels of the growth factors in vivo. Basic fibroblast growth factor (bFGF) was impregnated in gelatin sponge or GMS with isoelectric point (IEP) of 5.0 (acidic gelatin) and exhibited prolonged vascularization, accelerated tissue regeneration and improved therapeutic efficacy of cardiomyocyte transplantation [25, 82, 84, 85]. Adipose or periodontal tissue regeneration was also enhanced with bFGF-impregnated GMS [86, 87, 90]. Other basic growth factors, such as transforming growth factor- β 1 (TGF- β 1) and hepatocyte growth factor (HGF), were also encapsulated in acidic GMS and released in a controlled manner, demonstrating that it is a promising therapy for the articular cartilage defect and the liver cirrhosis [30, 83, 88]. For bone morphogenic protein (BMP), basic gelatin (IEP = 9.0) was used as the carrier to form polyionic complex and demonstrated enhanced alkaline phosphatase (ALP) activity [29].

4.2 Conventional Fabrication Methods and Their Problems

To fabricate hydrogel MS, various methods, such as aqueous precipitation [16, 20, 36], classic emulsion [24, 30], and spray drying [40, 91], were often employed. The hydrogel solution drops were formed by agitating, with high-pressure air, the suspension or the hydrogel solution resulting in random breakup of the droplets. Thus, the resulting MS exhibited wide size distributions, which caused

possible uncertainties in drug release profiles. Various other approaches with better control have also been attempted by using a membrane with uniform pores [92], a microreactor [93, 94], and a spinning disk [95]. Although fairly uniform MS were obtained with these methods, the difficulties still remained because the drop size depended on the solution viscosity, the reactor shape, and the size of pore or disk-tooth. For example, to fabricate small MS of a viscous polymer, one might need a very high pressure to allow the solution to pass through the small pores of the membrane and/or the micro-reactor. For the same reason, a spinning disk might require high rotating velocity to generate strong centrifugal force, which could be limited by the capacity of a motor. Occasionally, aqueous hydrogel solution caused the wetting on the membrane surface hindering the drop formation at each pore.

4.3 Fabrications and Characterization of Uniform Hydrogel Microspheres

The PPF scheme was suggested as a means to overcome the limitations described above. Although the basic PPF scheme worked well, for the following reasons the fabrication of hydrogel MS was challenging and required further improvement of the method. First, hydrogel materials were dissolved in water to make the working polymeric solutions, which were often highly viscous. To appropriately introduce the hydrodynamic force, therefore, an oil phase was chosen as a carrier stream, which exhibited viscosity comparable to that of the hydrogel solution. Aqueous carrier stream would mix rapidly with hydrogel solution before it functioned properly [2, 52-54, 96]. Second, solvent removal from the hydrogel solution drops was more demanding than that from the oil-soluble polymer drops wherein the solvents were volatile. For instance, methylene chloride used for the PLG MS fabrication could be removed efficiently at room temperature without employing any extra process [2, 52-54]. Third, various attempts, including the use of surfactants, failed to prevent the drops suspended in oil phase from coalescing

[55, 56]. Thus, a new approach was required to separate the hydrogel drops and avoid their agglomeration. Finally, to be practically useful, the apparatus and the processing protocols must be suitable for scale-up production.

In this section, we report on first successful fabrication of monodisperse MS of biodegradable hydrogels and an apparatus enabling it. The hydrogel polymers tested included chitosan, hetastarch, and gelatin. Gelatins with two different isoelectric points (IEPs = 5 and 9) were used because they are well known for delivery of oppositely charged proteins [27, 30].

4.3.1 Materials

Chitosan (75-85% deacetylated) was purchased from Aldrich. Hetastarch solution (6% hetastarch in 0.9% sodium chloride injection; Abbott laboratories), hetastarch was a gift from Professor Timothy M. Fan of the Department of Veterinary Clinical Medicine, and gelatins of two different IEPs (IEPs = 5.0 and 9.0; Mw = 100 kDa; Nitta Gelatin Co., Osaka, Japan) were a gift from Professor Russell D. Jamison of the Department of Materials Science and Engineering. Professors Fan and Jamison are with the University of Illinois at Urbana-Champaign.

4.3.2 Preparation of uniform hydrogel microspheres

Herein, we report a novel method for fabricating monodisperse MS of biodegradable hydrogels. The hydrogel materials used in this work were chitosan, hetastarch, and gelatins with IEPs of 5 and 9, respectively. To generate uniform hydrogel solution drops, canola oil was chosen as a nontoxic and nonsolvent carrier stream material to effectively apply the hydrodynamic force [2, 52-54]. As the hydrogel solution was fed through the nozzle, it formed a smooth jet of a size smaller than the nozzle opening, which subsequently was broken up into uniform

droplets by the acoustic excitation as described in Chapter 2 [50, 51]. Figure 4.1 shows the thus-produced uniform hydrogel drops of 200-, 150-, 100-, and 50- μm in diameter using a nozzle with 250- μm opening. All drops exhibited smaller sizes than the nozzle orifice.

Once generated, the hydrogel drops were collected in an oil bath and subjected to hardening. Unfortunately, to minimize the surface tension energy, liquid drops are inclined to recombine and form larger drops unless prevented. However, even with the use of surfactants it has been extremely difficult to prevent the drops suspended in oil phase from coalescing [55, 56]. In this work, we introduced an electric field to charge the drops so that they could repel each other and maintain their integrity (Figure 2.2). Due to the coulombic repulsion, the charged hydrogel solution drops were prevented from agglomeration during the hardening process resulting in uniform dry MS. The fact that this process involved no toxic surfactants qualified the method to be particularly attractive for biomedical applications such as advanced drug delivery and tissue engineering. Figure 4.2 shows the effect of charging on the hydrogel solution drops 150- μm in diameter. As the electric field was applied, the drops were repelled due to the coulombic force. With more charging, the separation of the drops increased.

While separated in oil, the drops were subjected to hardening to give dried hydrogel MS. The oil, utilized as the hardening media, helped the MS to attain smooth surface morphology due to its high surface tension force. In general, air-dried microparticles exhibit nonspherical and rough morphologies due to the low interfacial tension between the air and the hydrogel solution [39, 40, 97]. For the chitosan and hetastarch MS, water used as the solvent was boiled off by elevating the temperature of the oil bath. This evaporation method, however, was inapplicable to gelatin because of its degradation at high temperatures. Therefore, gelatin solution drops were gelled by lowering the temperature of the oil bath to 0 ~

4 °C, followed by extraction of water using acetone to obtain dried MS [27]. The gel-drops were rigid enough not to agglomerate even after charge disappeared.

4.3.3 Characterization

The MS were examined using a Hitachi S-4700 scanning electron microscope (SEM). A droplet of MS samples suspended in hexane was placed on a small piece of silicon wafer attached on top of the SEM sample holder and dried overnight with desiccant. The samples were sputter-coated with gold. The MS were imaged at 2-10 eV.

4.4 Results and Discussions

Figure 4.3 shows thus-fabricated MS of chitosan, hetastarch, and gelatin. Regardless of the materials used, all MS exhibited excellent uniformity and sphericity. The average diameters of the CMS (Figure 4.3(A1-3)) were 15 μm , 20 μm and 28 μm ; hetastarch MS (Figure 4.3(B1-3)) were 17 μm , 30 μm , and 45 μm ; GMS of IEP = 5 (Figure 4.3(C1-3)) were 25 μm , 40 μm , and 50 μm ; and GMS of IEP = 9 (Figure 4.3(D1-3)) were 20 μm , 30 μm , and 40 μm . The size uniformity was further verified with a Coulter Multisizer. Figure 4.4 illustrates the precisely controlled size and narrow size distributions for the four different batches of the CMS. More than 90% of the MS were fabricated within ± 3 μm of the average diameter.

To verify that the MS of chitosan and hetastarch were properly formed as solid particles through solvent evaporation, their cross-sections were examined. As shown in Figure 4.5, the insides of the MS were densely packed regardless of the MS sizes, which proved that for both hydrogel polymers, the use of a high-temperature oil bath removed the solvent appropriately. The porosity of the MS was known to be a critical factor in determining the drug release profile [7, 98, 99].

The smooth and dense structures of both CMS and HMS could allow one to tailor the drug release with better control.

The GMS, when suspended in water at body temperature, dissolve rapidly, thus are not suitable as vehicles for sustained drug delivery. Therefore, crosslinking was often carried out to prepare nondissolving GMS (0.125% glutaraldehyde). Figure 4.6 shows the dry GMS after crosslinking, which were no longer spherical but exhibited rough surfaces (Figures 4.6). Although the IEP = 9.0 GMS exhibited smoother surfaces than those of IEP = 5, the dimples were still shown. However, the crosslinked GMS after water uptake retained their uniformity and sphericity as shown in Figure 4.7, which was meaningful from the perspective of controlled drug release because the actual drug release occurred in aqueous environment. The most important advantages of the PPF drop generation method described in this work would be the flexibility in controlling the drop size and the capability to perform large-scale production. The use of carrier stream enabled the PPF to overcome the limitations imposed by solution viscosity and nozzle dimension. Therefore, drops of different sizes could be generated with a fixed nozzle simply by varying the flow rate of the carrier stream and/or the frequency of acoustic excitation. With a single set of nozzle, the achievable size range was quite wide. By increasing the number of nozzles subjected to acoustic excitation, the amount of hydrogel MS produced would increase by the same number. Therefore, scale-up could be easily established with the present method. Also, the production rate would not change with the changing target drop size because, at a fixed flow rate, uniform drops of wide size-range could be obtained by varying the frequency of acoustic excitation.

4.5 Conclusion

We have developed a novel method particularly suited to fabricating uniform hydrogel MS of precisely controlled size and size distribution. Chitosan,

hetastarch, and gelatins (IEPs = 5.0 and 9.0) were used as the model hydrogel materials. Use of carrier stream in combination with acoustic excitation facilitated the fabrication of uniform solution drops so that the solution viscosity and nozzle size would no longer limit the uniform MS fabrication of controlled size. By applying electric charge, the hydrogel solution drops could be prevented from coalescing during the hardening process, requiring no surfactant. In addition, with the present method, scaling-up could be easily realized by increasing the number of nozzles. Excellent uniformity and smooth spherical shape were exhibited for the hydrogel MS fabricated herein, both dry and swollen containing drug solution, which may provide accurate control in the drug delivery mediated by hydrogel particles. This study demonstrated that the fabrication of MS could be extended to a wide range of hydrogel materials with excellent control in size.

4.6 Figures

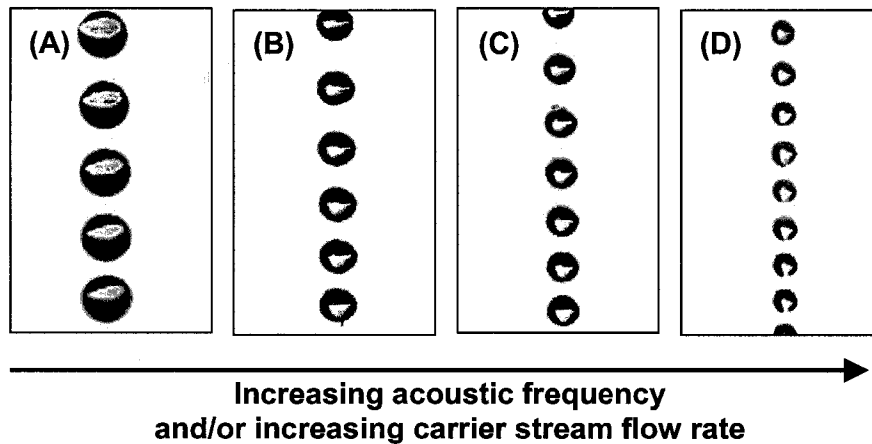


Figure 4.1 Generation of uniform hydrogel solution drops. Four different sizes of uniform drops generated by the present method. Drop diameters are (A) 200 μm , (B) 150 μm , (C) 100 μm , and (D) 50 μm .

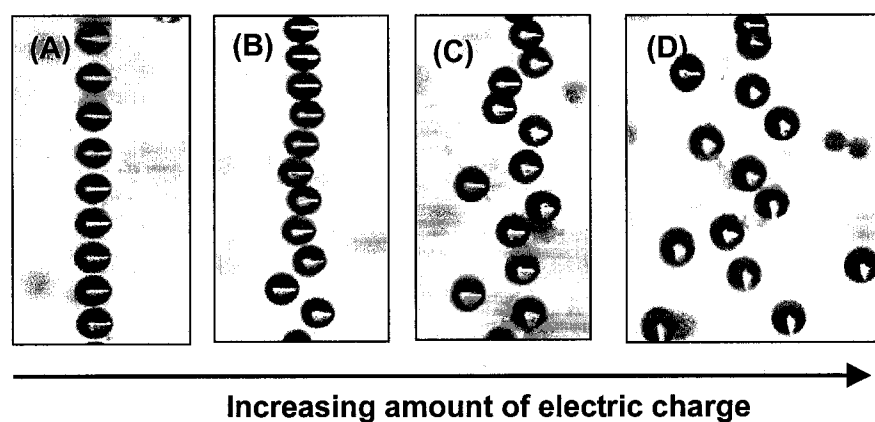


Figure 4.2 Charging was used to prevent chitosan drop agglomeration via coulombic repulsion. The applied electric fields were (A) 0 V/cm, (B) 50 V/cm, (C) 100 V/cm, and (D) 150 V/cm. The drop diameters are 150 μm .

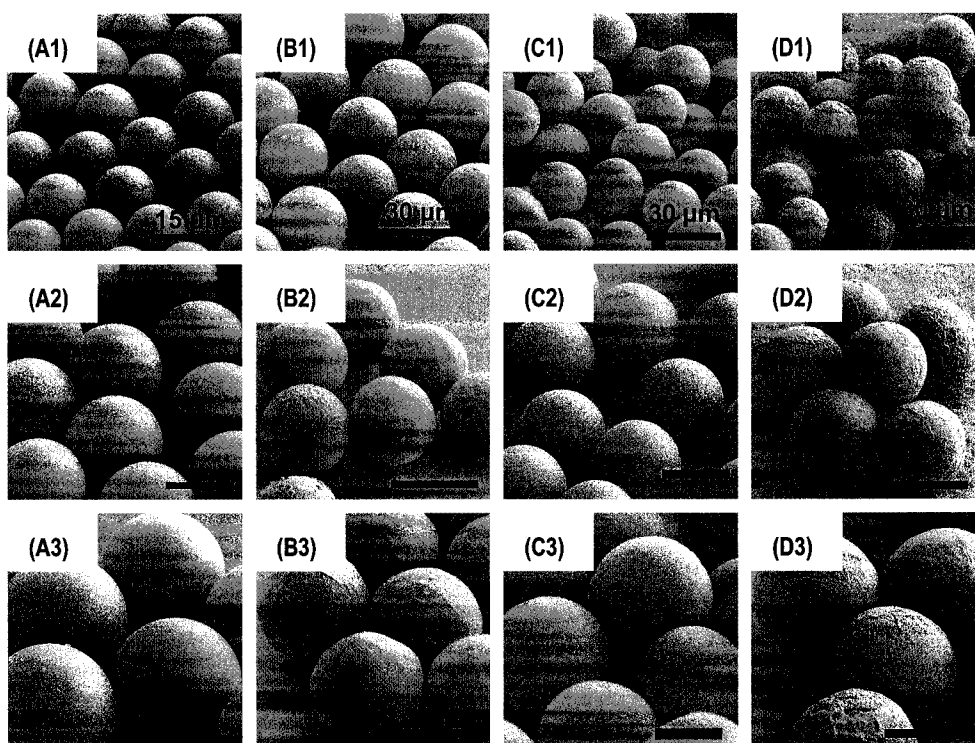


Figure 4.3 SEM pictures of uniform hydrogel microspheres. The polymers used are (A) chitosan, (B) hetastarch, (C) IEP = 5 gelatin, and (D) IEP = 9 gelatin. The diameters are (A1) 15 μm , (A2) 20 μm , (A3) 28 μm , (B1) 17 μm , (B2) 30 μm , (B3) 45 μm , (C1) 25 μm , (C2) 40 μm , (C3) 50 μm , (D1) 20 μm , (D2) 30 μm , and (D3) 40 μm . The scale bars are (A) 15 μm and (B-D) 30 μm .

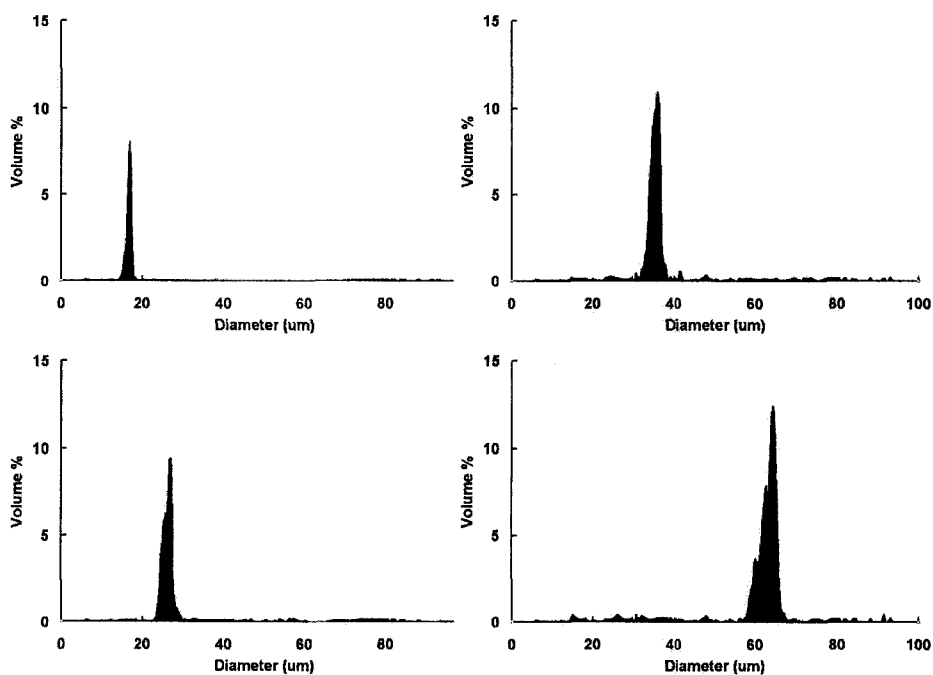


Figure 4.4 Size distributions of hydrogel MS (chitosan) prepared by PPF method. Four different batches were measured by Coulter Multisizer and exhibited narrow size distributions.

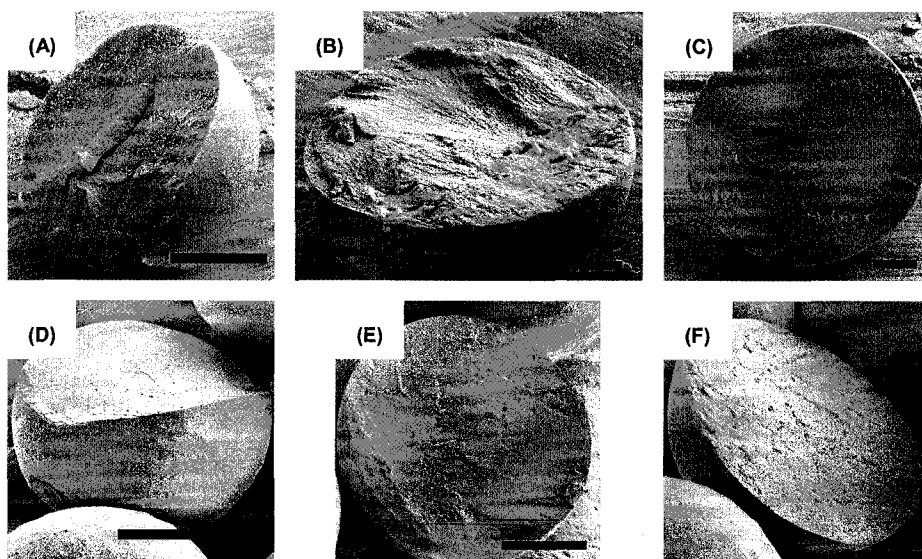


Figure 4.5 SEM pictures of the cross sections of the MS. The polymers used were (A)-(C) chitosan and (D)-(F) hetastarch. The diameters are (A) 15 μm, (B) 20 μm, (C) 28 μm, (D) 17 μm, (E) 30 μm, and (F) 45 μm. The scale bars are (A)-(C) 5 μm and (D)-(F) 10 μm.

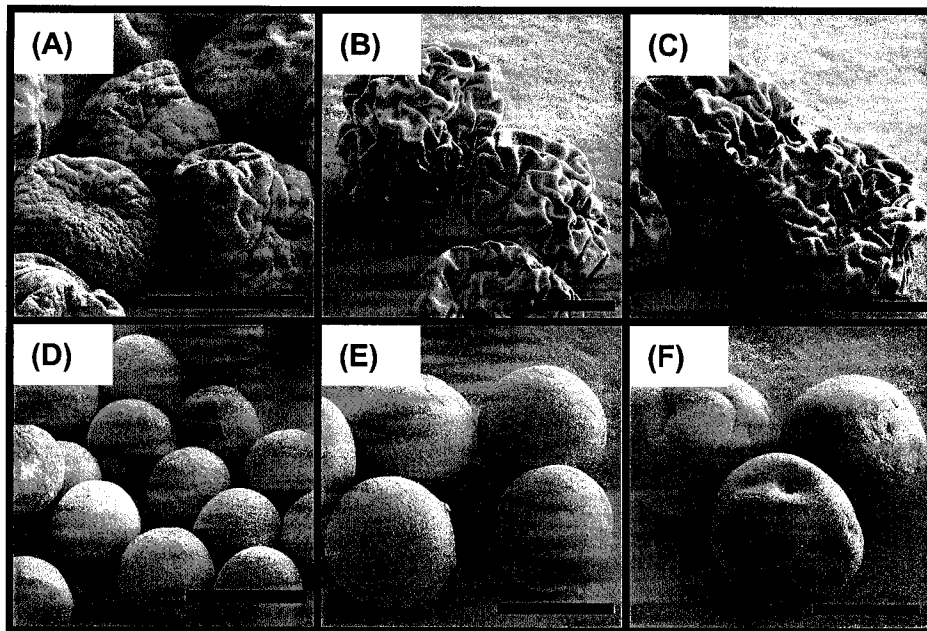


Figure 4.6 SEM pictures of dry GMS after crosslinking. The GMS at dry state were shown. The gelatins are IEP = 5.0 from (A) to (C) and IEP = 9.0 from (D) to (F). The scale bar = 30 μm .

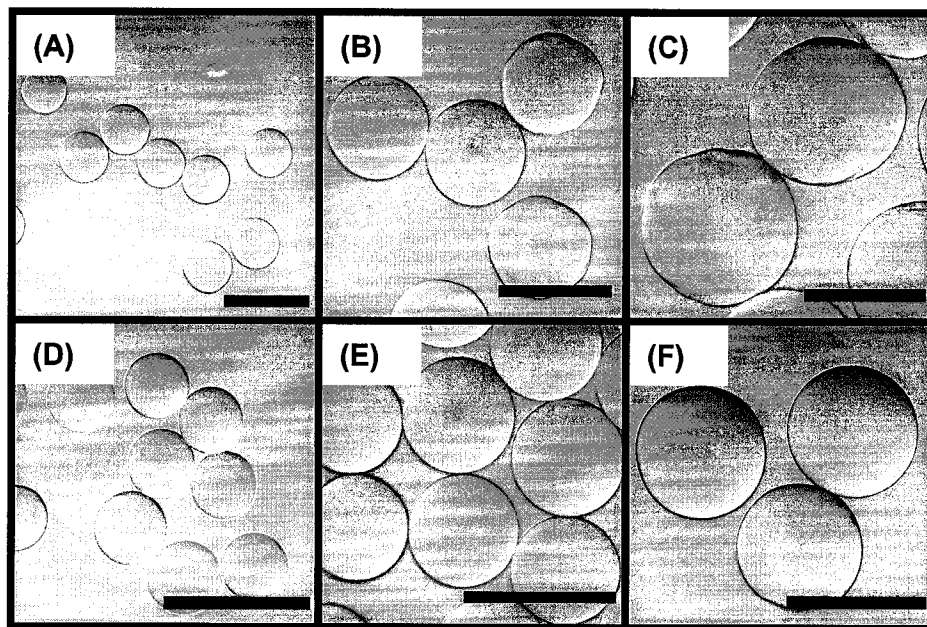


Figure 4.7 Optical micrographs of uniform GMS after crosslinking. The GMS after water-uptake were shown. The gelatins are IEP = 5.0 from (A) to (C) and IEP = 9.0 from (D) to (F). The diameters after swollen are (A) 55 μm , (B) 90 μm , (C) 120 μm , (D) 45 μm , (E) 70 μm , and (F) 80 μm . The scale bar = 100 μm .

CHAPTER 5

DRUG RELEASE PROFILES OF UNIFORM GELATIN MICROSPHERES UNDER DIFFERENT CROSS-LINKING CONDITIONS

GMS were often crosslinked using glutaraldehyde to form nondissolving MS for sustained drug delivery. Due to the diffusion of glutaraldehyde, the crosslinking density in the MS could be heterogeneous, influencing their drug release kinetics. In this study, uniform GMS were fabricated with the PPF method and the effects of crosslinking elucidated without possible uncertainties caused by the particle polydispersity.

5.1 Crosslinked Gelatin Microspheres

Cross-linking density is one of the critical parameters affecting the degradation of GMS [100, 101], which would consequently determine the drug-release profile. Glutaraldehyde has been used as one of the most effective cross-linking agents. However, due to its cytotoxicity [102, 103], it is desirable to minimize the use of glutaraldehyde in the cross-linking of gelatin. Although less toxic agents, such as genipin and D,L-glyceraldehyde, have been used, they were not as efficient as glutaraldehyde [24, 104]. For practical application of GMS as a delivery vehicle, it is important to understand the drug-release profile as a function of cross-linking, which, in turn, would allow tailoring of the release profile.

Conventionally, GMS are fabricated by the emulsion method and cross-linked in an aqueous solution of glutaraldehyde [27]. The cross-linking reaction takes place as glutaraldehyde diffuses through the GMS, which may give rise to a concentration gradient of glutaraldehyde along the path and lead to heterogeneity of the cross-linking density in the GMS. This could be a significant factor affecting the drug release profile of GMS. However, to study such phenomenon,

monodisperse GMS are required so that any uncertainties resulting from size nonuniformity of the spheres could be eliminated. For instance, the diffusion of glutaraldehyde and drug and the decomposition of GMS would depend on microsphere size. Unfortunately, due to the difficulty in controlling the GMS size, such well-defined GMS have not been available to date. As a result, the study on drug-release profile of GMS as a function of cross-linking has been hampered.

In this work, we fabricated uniform-sized GMS of IEP = 9 as described in Chapter 4 using glutaraldehyde as the cross-linking agent [105] and studied the effect of cross-linking on the drug distribution inside the GMS and the drug-release profile. The concentrations of glutaraldehyde used for the cross-linking reaction were 0.125 – 0.875 % as summarized in Table 5.1. The in vitro drug-release study was performed utilizing trypan blue, an acidic model drug, to effect the formation of charge complex. The critical parameters governing the drug release, such as the drug distribution in the microspheres and the in situ degradation profile of the MS, were examined.

5.2 Experimental

5.2.1 Cross-linking uniform gelatin microspheres

Uniform GMS, 60 μm in diameter, were fabricated as described in Chapter 4. The resulting GMS were cross-linked using galutaraldehyde. The un-cross-linked GMS were first suspended in cold water (0 ~ 4°C) of different glutaraldehyde concentrations (Table 5.1) and cured for 24 h. The resulting GMS were filtered, washed with DI water, and agitated in glycine solution to block excessive aldehyde groups. After 2 h, the GMS were washed again with DI water and lyophilized.

5.2.2 Drug loading

An acidic model drug (trypan blue) was impregnated into IEP = 9 GMS to form polyion complex. Briefly, an aqueous solution containing the drug (0.1% w/v) was dropped onto the known amount of GMS (5 $\mu\text{L}/\text{mg}$) and left for 2 h at room temperature. The drug solution was completely absorbed by the GMS because the volume of the solution was less than that required for the theoretical equilibrium swelling of the GMS.

5.2.3 In vitro drug release study

The in-vitro drug release study was preformed utilizing two distinct release media of PBS with and without an enzyme (Collagenase 1A) [30]. The enzyme concentration used in this work (373 ng/mL) mimicked the synovial fluid of a patient with osteoarthritis disease. Drug-loaded GMS were suspended in 1.5 mL of the release media and incubated at 37 °C for 18 days with continuous agitation. The supernatant was sampled at scheduled time intervals. Optical absorption of the sampled supernatant was measured spectrophotometrically.

5.2.4 Observation of intraparticle drug distribution

To examine the drug distribution in the MS, the GMS were loaded with acid fluorescent dye (Aexa Fluor 430), and the intensity of the emitted light at the cross-sections was observed using the confocal fluorescent microscope (Olympus Fluoview FV 300 Laser Scanning Biological Microscope). The initial drug distribution was obtained of the GMS 2 h after the drug loading. To examine ionically complexed drug distribution, the drug-loaded GMS were suspended in phosphate buffered saline (PBS) without enzyme for 15 days to remove the nonbonded drug.

5.2.5 Zeta-potential measurement

Zeta potential is a measure of the charge that develops at the interface between a solid surface and its liquid medium. Thus, by measuring the zeta-potential of homogeneously cross-linked gelatin particles, the change in the charge of gelatin molecules due to cross-linking density could be identified. The gelatin solution (5% w/v) was cross-linked under different glutaraldehyde concentrations (Table 5.1) at 50 °C for 5 h. The resulting solutions were rapidly cooled down at –50 °C and lyophilized. The cross-linked gelatin was ground into small particles and suspended in PBS (pH = 7.4) after filtration (5- μ m pore). The zeta-potential of the suspension was measured five times using Malvern Zetasizer 3000.

5.2.6 In situ degradation study

In situ degradation profiles of the GMS were examined to study the effect of crosslinking conditions. Differently cross-linked GMS were placed in the enzyme-containing PBS solution. At scheduled intervals, the GMS were drawn and observed under an optical microscope.

5.3 Results and Discussion

Figure 5.1 shows the SEM and optical microscope images of the GMS before and after cross-linking. The GMS before cross-linking exhibited excellent uniformity and smooth surface with an average diameter of 60 μ m. However, regardless of the glutaraldehyde concentrations used, the dry GMS after cross-linking exhibited “crumpled” shapes although the size appeared to be alike. Because the drug release occurred in an aqueous environment, the integrity of the GMS upon water uptake was more important. Thus, the dry crosslinked-GMS were suspended in a phosphate buffered saline solution (PBS, pH = 7.4) for one day and observed using an optical microscope. As shown in Figure 5.1(C), the wet GMS

restored the spherical shape and uniformity regardless of the cross-linking conditions, which proved that the control on the size and morphology were still viable with the crosslinked GMS. The average diameter of the swollen GMS was restored to 100 μm regardless of the cross-linking conditions.

Figure 5.2 shows the *in vitro* drug release profiles of the drug-loaded GMS with and without the enzyme (i.e., collagenase 1A) in the release-media [30, 83]. The concentration of the enzyme used herein was 373 ng/mL to mimic the synovial fluid of the patient with osteoarthritis disease. Without the enzyme, about 40% of the drug was released in 3 days, and no significant amounts afterwards. All the samples exhibited similar release-profiles regardless of the glutaraldehyde concentrations used for the cross-linking. This was not unexpected since the drug bound to the gelatin matrix would not be released without the decomposition of the gelatin and consequently the drug-release would be a diffusion-controlled process.

In the presence of enzyme, the total release was increased to 100% for all the samples (Figure 5.2(B)) due to the degradation of gelatin. The samples, C1 and C2, exhibited a 100% total release in 9 and 10 days, respectively, and C3 in 15-18 days, indicating that the release was retarded as the glutaraldehyde concentration increased. Interestingly, no further retardation was observed for the samples C4 and C5 in spite of their higher glutaraldehyde concentrations. With the C6 sample, the total release seemed to be retarded further, but its release profile was similar to those of the samples C3, C4, and C5. This was intriguing since the cross-linked gelatin was reported to become more resistant to degradation with higher glutaraldehyde concentrations, resulting in prolonged release [29, 100]. To elucidate the release profile of the cross-linked GMS, it is crucial to understand the drug-distribution in the GMS as a function of the glutaraldehyde concentration since the heterogeneous cross-linking density in the GMS described previously might have caused a nonuniform drug-distribution in the sphere, affecting the

release profile.

An acidic fluorescent dye, Alexa fluor 430, was used as a model drug to study the drug distribution within the GMS using a confocal fluorescent microscope. The intraparticle drug distribution was measured before and after suspending the drug-loaded GMS in a PBS solution (pH = 7.4) for 15 days to ensure the release of the drug that was not bound to the gelatin. No enzyme was used to eliminate the effects resulting from the enzymatic degradation of the gelatin. Figure 5.3 shows the drug distribution in the GMS after 2 h and 15 days, which represent the initial drug distribution and the distribution of the drug complexed to the gelatin, respectively.

The initial drug distribution curve of the sample C1, which was concave-downward, indicated that the drug was populated more at the center. As the glutaraldehyde concentration increased, the amount of the drug near the surface increased and the shape of the intraparticle drug distribution curve changed to concave-upward for the sample C3. This could be attributed to the facile diffusion of the drug during its loading into the GMS center at the lower degrees of cross-linking. Interestingly, no significant change was observed for the samples C4 – C6 although the glutaraldehyde concentration increased further. On the other hand, the relative amount of the drug complexed to the gelatin matrix near the surface decreased as the glutaraldehyde concentration increased for the samples C1 – C6. This could be explained by the inhomogeneous cross-linking, i.e., higher cross-linking at the GMS surface and lower toward the surface, caused by the concentration gradient of the glutaraldehyde along the diffusion path of the GMS.

The basicity of the gelatin would be weakened as its ϵ -amino groups reacted with glutaraldehyde during the cross-linking process [106, 107]. Consequently, the driving force for the complexation of the acidic drug with the basic gelatin would be reduced with higher cross-linking. The effect of the cross-

linking density on the charge of the basic gelatin was investigated by measuring the zeta-potential of the bulk gelatin as a function of cross-linking. To induce homogeneous cross-linking, gelatin was cross-linked in an aqueous solution using the glutaraldehyde concentrations in Table 5.1 followed by the removal of water. Figure 5.4 shows the zeta-potentials of the cross-linked bulk gelatin as a function of the glutaraldehyde concentration. The label corresponded to the glutaraldehyde concentration used for cross-linking (Table 5.1). The results indicated that the zeta-potential of the gelatin decreased significantly as the cross-linking density increased. As a result, the samples with the glutaraldehyde concentration higher than 0.325% exhibited negative zeta-potential. This supports the intraparticle drug distribution in Figure 5.3. The increase in the glutaraldehyde concentration would be more effective near the GMS surface. Therefore, at higher glutaraldehyde concentrations, the lowering of the zeta-potential would be more prevalent near the surface than the center, reducing the complexation of the drug to gelatin even if the initial drug distribution was higher near the surface.

To study the effect of cross-linking on the GMS degradation, the morphology of the GMS during the enzymatic degradation process was monitored using the optical microscopy. It is well known that the gelatin with higher cross-linking would be more resistant to the enzymatic degradation. Figure 5.5 shows the optical micrographs of the degradation profiles of the GMS cross-linked with different amounts of glutaraldehyde. At day 6, the samples C1 and C2 eroded into fragments while C3–C6 maintained their integrity with some deformation. C3 lost its integrity at day 9 and C4–C6 at day 12. It was rather intriguing to observe a similar decomposition pattern for the samples C4–C6 regardless of the glutaraldehyde concentration used for the cross-linking. While the bulk behavior of the samples C4–C6 were similar, the optical images at day 6 revealed interesting details of their decomposition pattern: C3 and C4 exhibited cracked surface and C5

and C6 elongated opening on the surface with significant reduction in size. For comparison, the GMS suspended in a PBS solution without enzyme retained their integrity without any visual evidence of degradation.

Since the amount of drug complexed to the gelatin would be higher at the center and lower at the surface, the decomposition and release of the gelatin from inside the sphere would play a critical role in the drug release process of the GMS. This may explain the similar drug release profiles for samples C3–C6 regardless of the different glutaraldehyde concentrations used for the cross-linking. To explain such effect, the net release of the ionically complexed drug was examined. Figure 5.6 shows the plot of the amount of drug release without enzyme (i.e., the diffusional release) subtracted from that with enzyme. Because the drug release by diffusion was removed, such plot would represent the release of ionically complexed drug solely incorporated with the GMS degradation.

For the first 2 days, the release profiles did not show much difference regardless of glutaraldehyde concentrations, which corresponded to the results shown in Figure 5.5. The GMS at day 2 did not exhibit discernible difference in erosion regardless of glutaraldehyde concentrations. However, at days 3–6, the difference became noticeable. Especially at day 6, the differences in the release were maximal because of the distinctive decomposition patterns of the GMS. As shown in Figure 5.5, C1 and C2 eroded into fragments while C4-6 still retained the integrity of the surface. However, because the center of the GMS eroded into fragments, continuous drug release was seen until day 9. Although C4-6 swelled back to the original size and spherical shape, the drug release was minimal possibly due to the small amount of complexed drug near the surface of the GMS.

One of the factors causing the different decomposition patterns of these samples would be the concentration gradient of glutaraldehyde in the microsphere. For the samples with high glutaraldehyde concentrations, the increase in

glutaraldehyde concentration would lead to more cross-linking at the surface, which would retard the diffusion of glutaraldehyde into the center even further. Figure 5.5 supports the lower cross-linking density at the center. As a result, the decomposition would take place at the center while the surface remained intact, resulting in pressure build-up inside the sphere to develop cracks or openings depending on the cross-linking density at the GMS surface. The shrinkage of the GMS could be due to the release of the decomposed gelatin-matrix through these cracks or openings.

The intraparticle drug distribution patterns in Figure 5.3 may provide further insight on the decomposition pathways, wherein the curve for the initial drug distribution was changed from concave-downward to concave-upward as the sample switched from C2 to C3. This, in conjunction with the decrease in the amount of complexed drug at the surface, indicated a drastic increase in the cross-linking density at the surface, leading to the retarded decomposition of the GMS surface. Therefore, one may envision the decomposition pattern of a GMS based on its intraparticle drug distribution and estimate the glutaraldehyde concentration needed for a desired drug release profile.

5.4 Conclusion

We investigated the drug release profiles of the GMS cross-linked with different glutaraldehyde concentrations. It was found that the effect of the glutaraldehyde concentration on the drug release profile was not linear, which was significant at its low end but negligible at its high end. The intraparticle drug distribution patterns indicated that the population of the complexed drug near the GMS surface decreased as the glutaraldehyde concentration increased. The zeta-potential measurements revealed that the low drug-gelatin complexation near the GMS surface reflected its high cross-linking density. The degree of cross-linking at

the surface seemed to be an important factor determining the decomposition pattern of the GMS, affecting the drug release profile. At higher glutaraldehyde concentrations, the GMS surface would be more cross-linked, leading to more resistant to degradation and less drug complexation. Under this situation, the drug-release profile would be mostly governed by the decomposition and release of the inner mass via the cracks or openings on the surface. Therefore, above the threshold value wherein the GMS would follow such decomposition pattern, the effect of glutaraldehyde concentration on the drug release profile would be negligible. The threshold glutaraldehyde concentration would vary as the GMS size varies, however, one may estimate it based on the intraparticle drug distribution patterns, which reveal the cross-linking profiles of the GMS. This study elucidated the factors affecting the drug release profile and demonstrated that the tailoring of the drug release profile could be realized using the uniform sized GMS.

5.5 Figures and Table

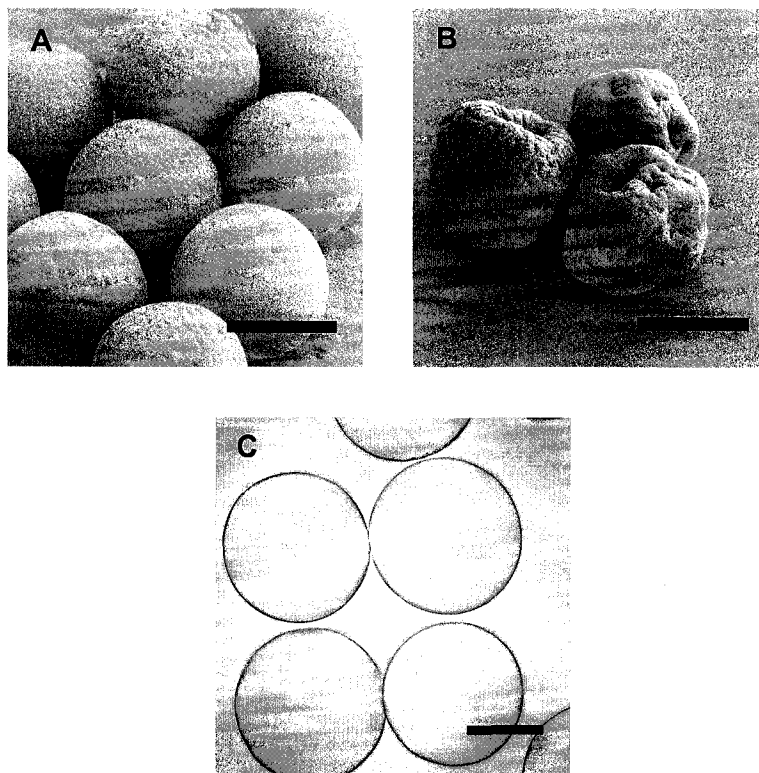


Figure 5.1. SEM and optical micrographs of uniform GMS prepared by the PPF method: (A) dry GMS before cross-linking, (B) dry GMS after cross-linking, and (C) wet GMS after cross-linking. The scale bars are 50 μm .

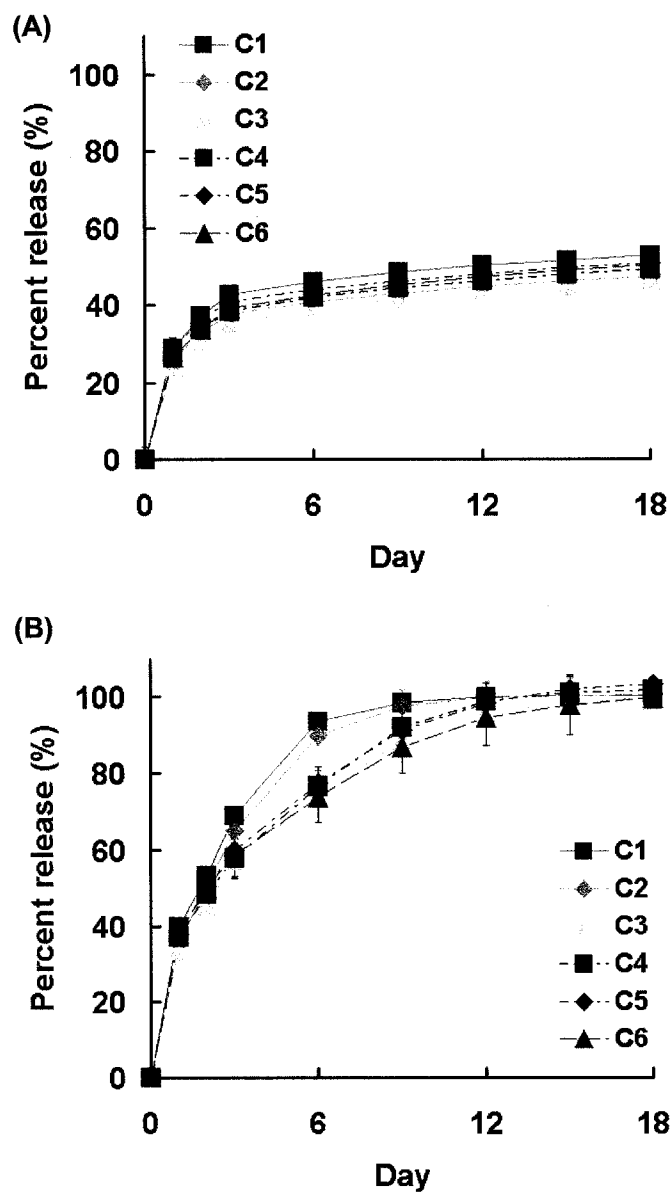


Figure 5.2 In vitro drug release from uniform GMS with different cross-linking conditions. The release media used are pH = 7.4 PBS solutions (A) with enzyme and (B) without enzyme.

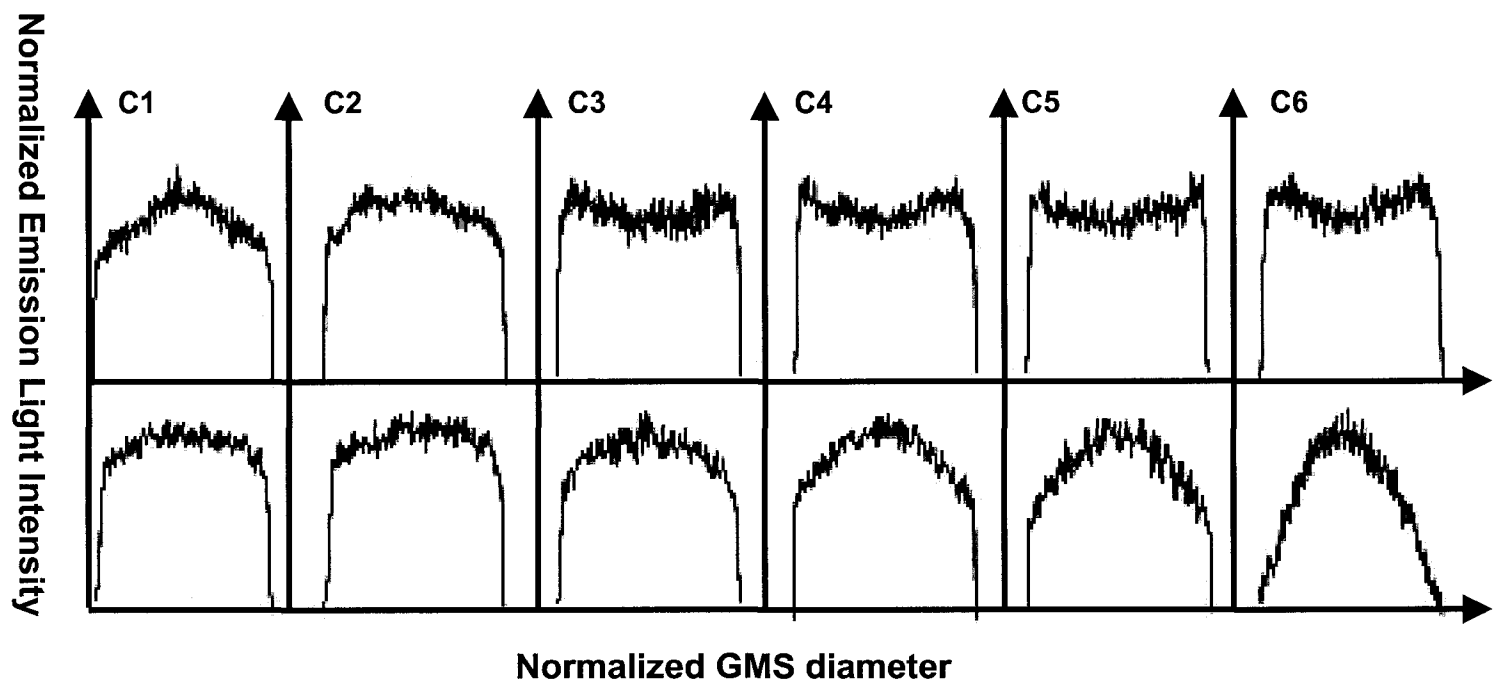


Figure 5.3 Drug distribution profiles inside of the GMS. The GMS were loaded with acid fluorescent dye (Alexa Fluor 430), and the light intensity at the cross-sections was observed using the confocal fluorescent microscope. The top row corresponded with the initial drug distributions and the bottom row the ionically complexed drug distributions.

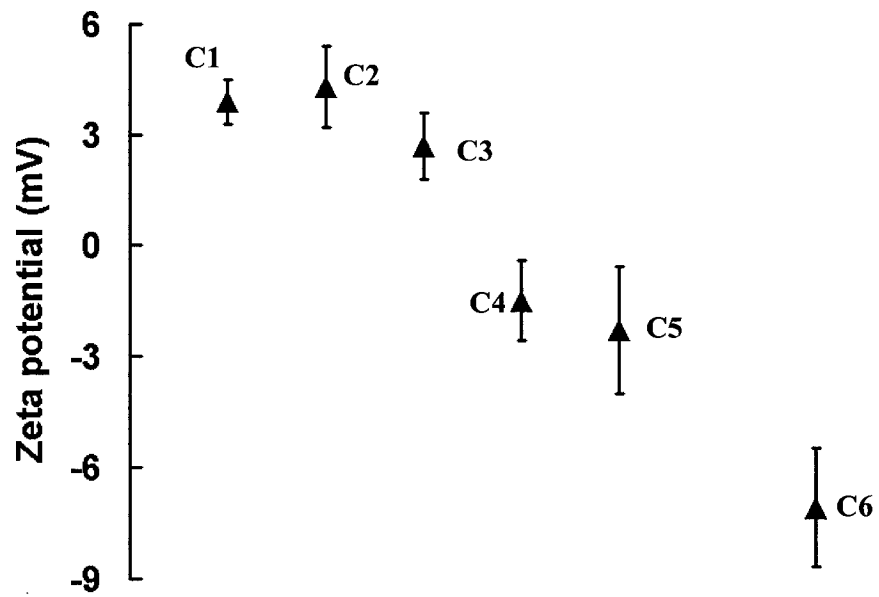


Figure 5.4 Zeta potentials of differently crosslinked gelatin. The label corresponds to the GA concentration used for crosslinking

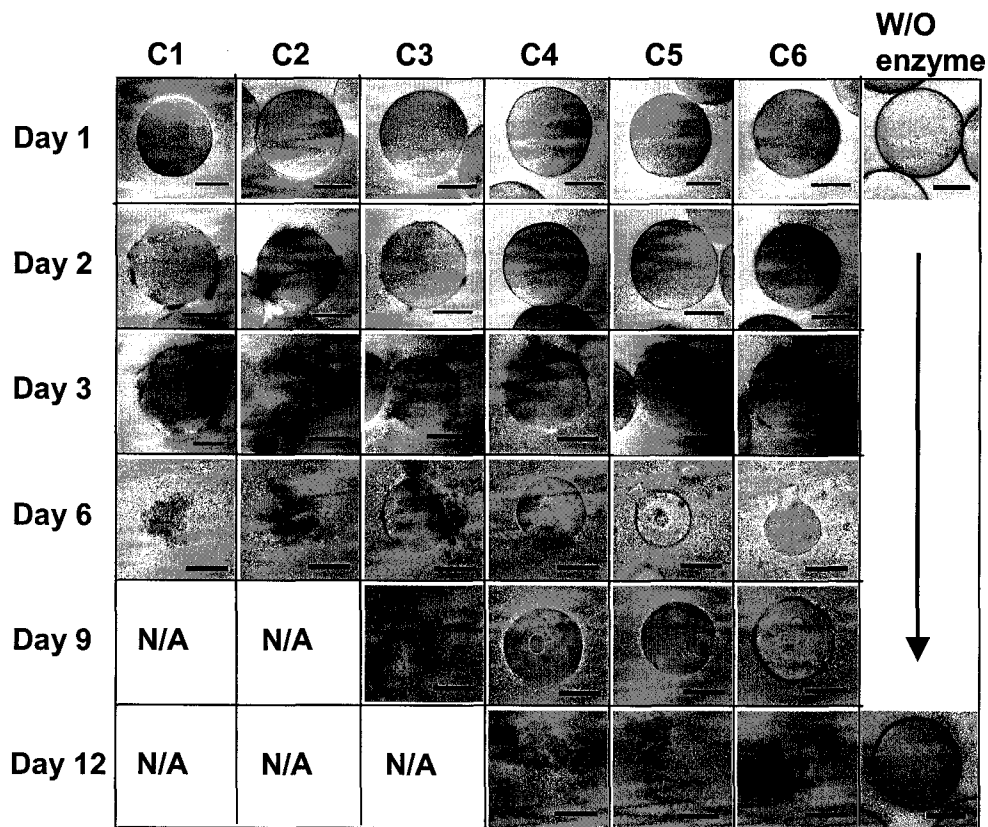


Figure 5.5 In situ degradation study with uniform GMS prepared under different crosslinking conditions. The PBS with enzyme was utilized as the suspension media. Each column represents a specific crosslinking condition employed for the GMS and each row the time of observation. For comparison, the GMS suspended in the media without enzyme were shown on the right-most column. The scale bars are 50 μm .

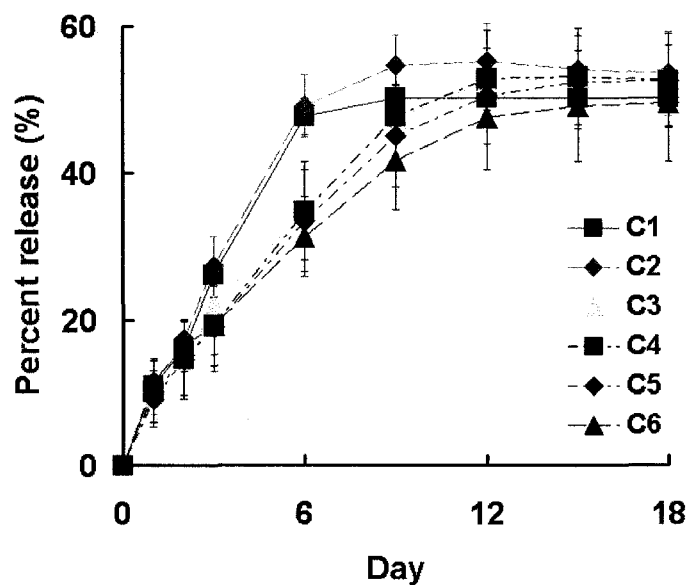


Figure 5.6 Net release profiles of ionically complexed drug. The values of the diffusional release subtracted from those of enzymatic release were plotted.

Table 5.1 Different glutaraldehyde concentrations utilized to cross-link the uniform GMS

Sample Name	C1	C2	C3	C4	C5	C6
Glutaraldehyde Conc. (%)	0.125	0.250	0.325	0.500	0.625	0.875

CHAPTER 6

UNIFORM CHITOSAN MICROSPHERES WITH DIFFERENT CROSSLINKING DENSITIES FOR ORAL DRUG DELIVERY

Uniform CMS with different cross-linking densities were fabricated to investigate their suitability as oral delivery vehicles. Drugs with three different polarities (base, weak acid, and strong acid) were utilized to examine the effect of polyion complex. The drug release profiles were investigated by using media with continuously changing pHs to mimic the gastrointestinal fluids.

6.1 Chitosan Microspheres for Oral Drug Delivery

CMS have been widely used as drug-delivery vehicles due to their biocompatibility, biodegradability, and bioadhesiveness [108-113]. Especially, the CMS with bioadhesiveness were known to increase the residence time at the mucosal surfaces in the stomach or intestine, improving the drug adsorption. For this reason, various therapeutic agents, such as Vitamin C, theophylline, aspirin, and griseofulvin, were encapsulated in the CMS for oral administration, resulting in sustained release [109, 114, 115]. The CMS were also investigated for oral immune delivery. The antigen encapsulated in CMS was protected from degradation and was gradually released enhancing the immune response [108, 116-118].

In addition, the CMS were favored due to their cationic property. An anionic drug complexed with CMS was shown to prolong the release. Especially for proteins and peptides, the interactions with CMS were reported to improve loading capacity, drug stability, and bioactivity [119, 120]. Due to such ionic effect, the CMS often exhibited pH-dependent release [114, 121], which could be applied to various drugs for colon-specific delivery. For viral gene delivery, DNA needed to be protected through the gastrointestinal tract until it was delivered to a specific

colonic site [109]. The drug known to have an adverse effect on the stomach needed to suppress its release at low pH but be continuously released from the small intestine [122]. Such control was governed by both ionic interaction between chitosan and the drug, and the pH of the release media. Unfortunately, the CMS passing through the gastric media often exhibited considerable amount of drug release due to their higher swelling and/or dissolution at low pH [109, 123].

6.2 Purpose

Various attempts were made to control the pH-dependent drug release from CMS. One approach was to incorporate anionic polymer such as alginate. The MS were fabricated with a combined use of both chitosan and alginate, whose bonding strength varied due to the pH [124, 125]. Thus, the drug release was determined by the mass ratio of the two polymers. Coating the CMS with various polymers, such as cellulose acetate butyrate, ethyl cellulose, and Eudragits, was also suggested to suppress the burst of drug release in gastric fluid [118, 122, 126, 127]. Because of the additional polymer barrier formed on the CMS, the drug by-passed the stomach but was released afterwards.

Although such methods could provide better control, there were several disadvantages. Firstly, additive polymers could change the cationic property of chitosan, thus degenerating the bioadhesiveness, and/or the polymer-drug interaction. The weaker polymer-drug interaction might lower drug stability and loading capacity. Secondly, the method often required an unfavorable process. To coat the CMS with hydrophobic polymers, an organic solvent was needed [118, 122, 126, 127], which would not be suitable for encapsulation of proteins, peptides, and DNA due to their degradation. Most of all, the size of the MS was not precisely controlled resulting in possible uncertainties and poor reproducibility in drug release.

As noted before, drug release from MS-based delivery systems critically depends on the size and size distribution of the MS because the surface area-to-volume ratio strongly influences the rate of out-diffusion of the drug and/or degradation of the polymer matrix. The MS size was also known to be a critical determinant in site-specific delivery. The MS less than 10 μm were reported to be effective for the particle transportation via Peyer's patches [31]. However, the methods often employed for fabrication of CMS, such as aqueous precipitation [16, 35], classic emulsion [124, 128] and spray drying [40, 129], did not produce uniform MS due to lack of control over atomization. Membrane with uniform pores was utilized to control the size of chitosan solution drops [113, 130]. Although the resulting CMS exhibited a fairly uniform size, the method still depended on pore dimension and solution viscosity, which did not provide enough flexibility in size control.

In this study, we have fabricated monodisperse CMS for oral delivery vehicles as previously reported [105]. Due to the excellent uniformity and narrow size distribution, the drug release from the resulting CMS could be accurately tailored. In addition, the present method did not involve any organic solvent or toxic surfactant, which would be favorable for biomedical applications aimed in this work. As stated above, the CMS were known to cause burst release at lower pH due to their swelling and dissolution. Thus, the crosslinking agent, glutaraldehyde was employed to fabricate acid-resistant CMS [130, 131]. To minimize the adverse effect of glutaraldehyde [103], all CMS used in this study were weakly crosslinked (Table 6.1). Due to the cationic nature of chitosan, therapeutic agents, such as anionic proteins and DNA, could be well encapsulated in and protected by CMS while passing through the GI tract. To examine such electric interaction and its effect on drug release, model drugs with three different polarities were employed, which were toluidine blue (TO; basic), trypan blue (TR; strong acid), and

diclofenac sodium salt (DS; weak acid). TR represented the drug containing multiple anionic functional groups, such as protein. DS is known to cause the adverse effect on the gastric cavity but well adsorbed in the colon [132, 133], which would be advantageous if released less at the stomach but continuously near the colon.

6.3 Materials and Methods

6.3.1 Materials

Chitosan (75-85% deacetylated) was purchased from Aldrich, and the model drugs (TR, TD, and DS) and glutaraldehyde (25% in aqueous solution) from Sigma. Glacial acetic acid and acetone with high purity were obtained from Fisher Scientific.

6.3.2 Preparation of uniform chitosan microspheres

Uniform CMS were prepared following the method described in Chapter 4. Briefly, to fabricate uniform CMS, the chitosan solution (1% w/v) was prepared in 0.2 M acetic acid solution, which was subsequently crosslinked using glutaraldehyde (Table 6.1). A smooth liquid jet of this solution, much thinner than the nozzle opening was generated with the use of carrier stream and subsequently broken up into uniform droplets using acoustic excitation. To prevent the agglomeration, the drops were electrically charged so that coulombic repulsion kept them separated. The uniform chitosan-solution drops were suspended in a hot oil bath (150 ~ 160 °C) to boil off water. The resulting CMS were collected by filtration, washed with acetone to remove the residual oil, and lyophilized.

6.3.3 Drug loading in chitosan microspheres

The model drugs with different polarities were impregnated in CMS. Briefly, the PBS solution (pH = 7.4) containing the drug (TR, 5% w/v; TD, 5%; SD, 0.5%) was dropped onto the known amount of CMS (1 μ l/mg) and cured for 3 h at room temperature. The solution volume was less than the theoretical equilibrium swelling volume of the CMS resulting in complete absorption.

6.3.4 Characterization

The uniformity and morphology of the dry CMS were observed using a Hitachi S-4700 scanning electron microscope. A droplet of CMS suspended in hexane was placed on a small piece of silicon wafer attached on top of a scanning electron microscope sample holder and dried overnight with desiccant. The samples were sputter-coated with gold. The GMS were imaged at 2–10 eV. The swollen CMS were observed using an optical microscope. To prepare the completely swollen MS, a small amount of CMS (~ 1 mg) was suspended in 1 mL of two distinct buffer solutions at pHs = 7.4 and 1.0 and left for 24 h at room temperature. To observe the size change due to swelling, more than 50 MS were measured for three different cases: dry, wet at pHs = 7.4 and 1.0.

6.3.5 Drug distribution in the microspheres

The midsections of the MS were analyzed to determine the drug distribution at the center. To examine the effect of the drug polarity, two different fluorescent dyes were employed. Rhodamine B and Eosin Y represented the basic and acidic drug, respectively. The drug-loaded CMS were imaged using a laser scanning confocal microscope (Olympus Fluoview FV 300 Laser Scanning Biologic Microscope).

6.3.6 In vitro drug release

Drug-loaded CMS were placed in 1.5 mL of the release media, whose pHs were gradually increased to mimic the fluid through the gastrointestinal tract. The pHs were maintained at 1 for 1 h, 2 for 1 h, 5 for 2 h, 6.8 for 4 h, and 7.4 for 4 h. The release media contained the dispersant (0.5% v/v Tween 80) to prevent CMS agglomeration. The suspensions of drug-loaded CMS were incubated at 37 °C while continuously agitated by inversion (~8 rpm). Absorbance of the sampled supernatant was measured spectrophotometrically. The amount of drug release at each time interval was summed from the amount measured at the previous time interval resulting in cumulative release.

6.4 Results

6.4.1 Differently crosslinked uniform chitosan microspheres

Uniform CMS with different crosslinking densities were fabricated as previously described in this dissertation [105]. The chitosan was cross-linked utilizing glutaraldehyde of different concentrations (Table 6.1) and for each crosslinking density, the CMS with three different sizes were made (Table 6.2). Figure 6.1 shows the resulting CMS. The average diameters were 24 μm , 28 μm , and 35 μm for C0; 23 μm , 29 μm , and 38 μm for C1; and 25 μm , 28 μm , and 38 μm for C2. Regardless of the crosslinking density, all MS exhibited excellent uniformity (std < 1.33 μm). The rough surface of the MS was known to cause initial burst due to the increase in the surface area [40]. Thus, it is important to obtain the smooth surface morphology. Our method proved to be beneficial because it provided the CMS with smooth surfaces regardless of their size and crosslinking density as shown in Figure 6.2.

The CMS after water uptake were examined, from which the drug was

actually released. Figures 6.3 and 6.4 show the CMS swollen at two different buffer solutions of pHs = 7.4 and 1.0, respectively. Due to the water uptake, the diameters of the CMS increased during suspension in the aqueous media. Even after the swell, the CMS retained excellent uniformity (std < ± 1.70) and sphericity, which provided further proof that the particle size control, was accurately maintained throughout the present drug release study. Figure 6.5 and Table 6.2 show the sizes of the CMS in two different states: dry and wet in two different buffer solutions (pHs = 7.4 and 1.0). Regardless of crosslinking density, the diameter of the CMS increased more at pH = 1.0 than at 7.4. Due to the weak crosslinking, the hydrolysis of chitosan seemed to be more incorporated at the lower pH resulting in more swelling. Therefore, the size differences between each batch of the CMS became as large as 18 μm while the dry CMS showed 10 μm at most (Table 6.2).

6.4.2 Drug distribution

The drug distribution in the CMS is one of the most critical factors in drug release. To examine the effect of drug-chitosan ionic interaction, fluorescent dyes with two distinct polarities were employed as the model drugs, which were Rhodamine B (basic) and Eosin Y (acidic). The cross sections of the drug loaded CMS were observed using a confocal fluorescent microscope. Figures 6.6 and 6.7 show the basic and acidic drug distributions in the CMS, respectively. The basic drug was homogeneously distributed throughout the CMS while the acidic drug was more concentrated near the surface regardless of the size and cross-linking density of the CMS. In this study, to encapsulate the drug, the drug solution was absorbed into the dry CMS. Thus, the drug loading was determined by two competing factors, the diffusion of the drug solution into CMS and the ionic interaction between the drug and chitosan. The basic drug, which has the same polarity with chitosan, seemed to be freely mobile resulting in homogenous distribution mainly caused by

in-diffusion of the drug solution. However, for the acidic drug, due to the attractive force between the drug and chitosan, the drug molecule appeared to complex with chitosan at the same time when the drug solution diffused into the CMS. The drug complexed at the CMS surface seemed to be unable to diffuse into the center resulting in high drug concentration near the surface of the CMS.

6.4.3 In vitro drug release study

An in vitro drug release study was carried out to examine the effect of the ionic interaction by employing model drugs with three different polarities (TO, TR, and DS). The pHs of the release media were gradually increased to simulate the fluids throughout the gastrointestinal tract. Figure 6.8 shows the release profiles of the basic drug (TO). Regardless of the size and cross-linking density, the release was not sustained possibly due to the electrostatic repulsion between the CMS and the drug. Almost 100% release was obtained in 10 min with all CMS.

However, for the strong acidic drug (TR), the effect of the CMS size and cross-linking density was clearly visible (Figure 6.9). For non-cross-linked CMS (C0), all the release profiles merged into one, possibly due to their high dissolution in the release media. However, as the cross-linking density increased, the size effect became notable (Figures 6.9(B) and (C)). Interestingly, the release was more sustained as the size decreased. Although the small CMS were supposed to exhibit faster release due to their large surface area-to-volume ratio, it seemed that for strong acidic drug, the ionic interaction played a more important role than drug out-diffusion. In this study, the drug was loaded into CMS by absorption of the drug solution prepared at pH = 7.4. The resulting CMS, when suspended in pH = 1.0 media, would be more protonated, resulting in stronger cationic charge. Such change in ionic property seemed to depend on the size of the CMS. Namely, the smaller CMS experienced faster protonation in the media of low pH possibly due to

their large surface area, resulting in more drug complex. Because the acidic drug was more concentrated near the surface as shown in Figure 6.7, such dependency on the surface area would be more dominant with strong acid drug. Thus, as shown in Figures 6.9(A) and (B), as the size decreased (i.e., more susceptibility to pH), the drug was released less. The drug release after 1 h was minimal for all small crosslinked CMS (<10%). The effect of cross-linking density, although weak, was also noticeable. As the crosslinking density increased, the total percent release decreased more, possibly due to the stronger resistance to acid. The total percent release during the first 12 h with large CMS decreased from 45.1% to 34.5%, with medium CMS from 36.4% to 12.5%, and with small CMS from 10.0% to 7.1%.

For the weak acid drug (DS), the release was more sustained than the basic drug and more continuous than the strong acid drug (Figure 6.10). Due to the weaker ionic bonding, the release seemed to depend more on the diffusional release, which could also explain the minimal influence of the crosslinking density. Therefore, although the small CMS might have been protonated more rapidly at low pH, the release was still the fastest due to the drug out-diffusion facilitated by their large surface area-to-volume ratio. The release profiles exhibited biphasic patterns, which consisted of the initial burst and the subsequent continuous release. Importantly, the larger the CMS, the less the burst, possibly due to the small surface area-to-volume ratio. The small CMS exhibited more than 70% release during the first 1 hr while the large CMS showed less than 50% release. After the burst release, the release was almost linear for all CMS (~1.25%/hr). Regardless of the crosslinking density, the small CMS could obtain the total 100% release during 12 h.

To further prove complete release of the basic drug and the remainder of the strong acidic drug, the color of CMS after 24 h drug release was examined using an optical microscope. Figure 6.11 shows that the CMS initially loaded with basic

drug became transparent proving that there was no drug remaining. However, as shown in Figure 6.12, the dark bluish color of strong acidic drug (TR) indicated that there was the drug complexed in the CMS even after 24 h release.

6.5 Discussion

The CMS were widely investigated as oral delivery vehicles due to excellent biocompatibility, bioadhesiveness and especially cationic property, that is, pH-dependent release. Drugs such as antigen, DNA, protein, and/or some anti-inflammatory agents, would be more efficacious if delivered specifically to the colonic site [109, 113, 125]. However, the chitosan alone as the encapsulant was known to be undesirable due to its massive hydrolysis at low pH resulting in burst release near the stomach [123]. Several attempts incorporating other polymers as additives were made to improve the drug release behavior, which, however, could be unfavorable due to possible deterioration of the cationic property of CMS and incorporation of undesirable solvent into CMS [118, 122, 125, 127, 128].

In this study, we suggest, and investigate, uniform CMS of precise size and size distribution as a promising colon-specific delivery vehicle. The CMS were crosslinked to make them tolerant to acidic fluid so that they could bypass the gastric cavity [131]. However, low glutaraldehyde concentrations were utilized to minimize the adverse effect. Instead of introducing other additives, precise control over the size and size distribution of the CMS enabled the drug release to be tailored accurately. Even after 24 h suspension in the media of both pHs = 7.4 and 1.0, the uniformity and sphericity of our CMS were well retained (Figures 6.3 and 6.4). One of the appealing scenarios of colon targeting was that the drug in the carrier could be retained as much as possible in the upper gastrointestinal tract but released near the colon by the degradation of the encapsulant polymer [133, 134]. Therefore, in this study, we examined the remaining drug after 12 h as the potential

drug for colon-specific delivery because the pH near the colon would be constant at 7.4 hence no more effect of the pH changes on drug release.

Drugs of three different polarities were employed and their release profiles investigated to assess the feasibility of using our uniform CMS for colon specific delivery. For the delivery of basic drug (TO), the CMS were shown to be unfavorable. Due to the strong repulsion between the drug and chitosan, the free drug molecules appeared to be released instantaneously regardless of the size and crosslinking density of the CMS (Figure 6.8). However, for strong acid drug, more than 90% of the drug could be retained with the small CMS of weak crosslinking density (C1 and C2) even after 12 h suspension in the release media (Figure 6.9). The model drug utilized in this study, TR, had multiple anionic functional groups ($-\text{SO}_3^-$), which might be able to represent strong anionic proteins, peptides, and DNA. Colon-specific delivery of such therapeutic agents were known to be beneficial for their systematic absorption [109, 113, 134, 135]. However, polydisperse CMS might lower the efficiency because, as shown in Figure 6.9, larger CMS lost almost half the drug in 1 h. In this sense, small CMS (23–25 μm) with C1 and C2 were attractive for colon-specific delivery. Precise control over the size and size distribution of CMS allowed for maximization of the amount of drug that could potentially be released at the colon, through degradation of chitosan.

The release of the weak acid drug exhibited the biphasic profiles: an initial burst and the subsequent continuous release (Figure 6.11). The model drug, DS, was known to cause local side effects if released too much in the stomach, prompting the need for colon-specific delivery [122, 123, 125, 133]. All CMS in this work exhibited a burst, which could be lowered by increasing the CMS size. As shown in Figure 6.10, large CMS (35–38 μm), regardless of the crosslinking density, exhibited less than 50% bursts. Thus, while the small CMS exhibited 100% release in 12 h, more than 40% of the drug still remained in the large CMS, which

was again the potential amount of the drug that could be released by CMS degradation [133, 134]. Unlike with the strong acid drug, the large CMS would be favorable for colon-specific delivery of the weak acid drug.

Additional coating on the CMS was suggested as a means to completely prevent the DS release at the stomach [118, 122, 127]. However, although almost no DS was released at the gastric fluid, the size of CMS was not properly controlled thus exhibiting fast release or lack of control after the coating materials disappeared. Use of our uniform CMS as the core would be the promising design for colon-specific delivery of DS. The polymers with pH-dependent solubility, such as Eudragits, could protect our uniform CMS at the gastric cavity, which would subsequently be exposed to both higher pH and colonic enzyme and release the drug in a controlled manner due to their precise size and size distribution.

6.6 Conclusion

Uniform CMS with different crosslinking densities were fabricated for use as oral delivery vehicles. To study their efficacy for colon-specific delivery, model drugs with three different polarities, which were base, strong acid, and weak acid, were employed and encapsulated in the CMS. The drug distributions in the CMS showed that the basic drug was homogeneously distributed while the acid drug was more concentrated near the surface, which proved the charge interaction between the drug and chitosan. The basic drug appeared to be not a good candidate for colon-specific delivery because of its fast release. However, for strong acid drugs such as anionic proteins or peptides, the small CMS with weak crosslinking could be more favorable due to the increased amounts of the drug complexed with the CMS, which would be released by degradation of the CMS at the colon. Weak acid drug, possibly due to the weak bonding strength, showed continuous release during the first 24 h. However, to minimize the burst at the gastric cavity, use of large

CMS was suggested. The uniform CMS in this study were judged to be promising oral delivery vehicles of anionic drugs due to the accurately controlled release profiles facilitated by their monodispersity.

6.7 Figures and Tables

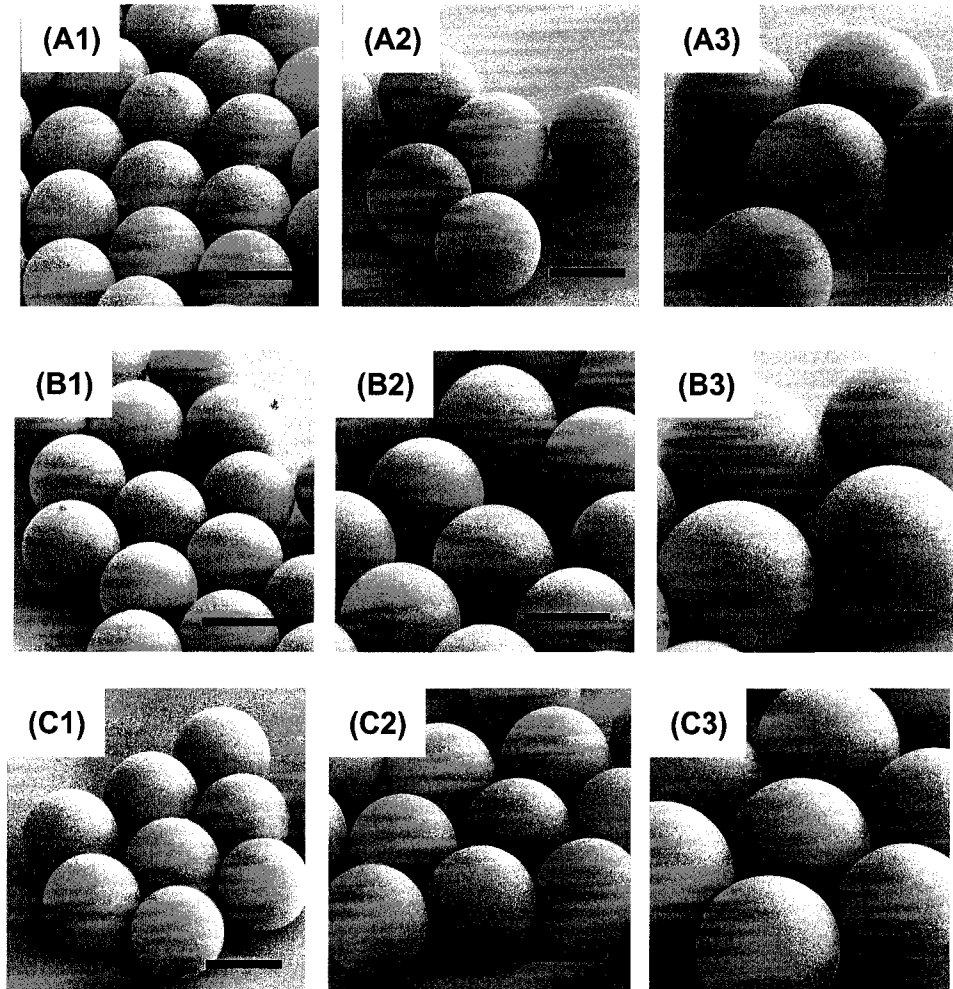


Figure 6.1 SEM micrographs of uniform CMS with different crosslinking densities. CMS with three different sizes were fabricated for each crosslinking condition. The crosslinking conditions utilized were (A1-3) C0, (B1-3) C1, and (C1-3) C2. The diameters were (A1) 24 μm , (A2) 28 μm , (A3) 35 μm , (B1) 23 μm , (B2) 29 μm , (B3) 38 μm , (C1) 25 μm , (C2) 28 μm , and (C3) 38 μm . The scale bars = 20 μm .

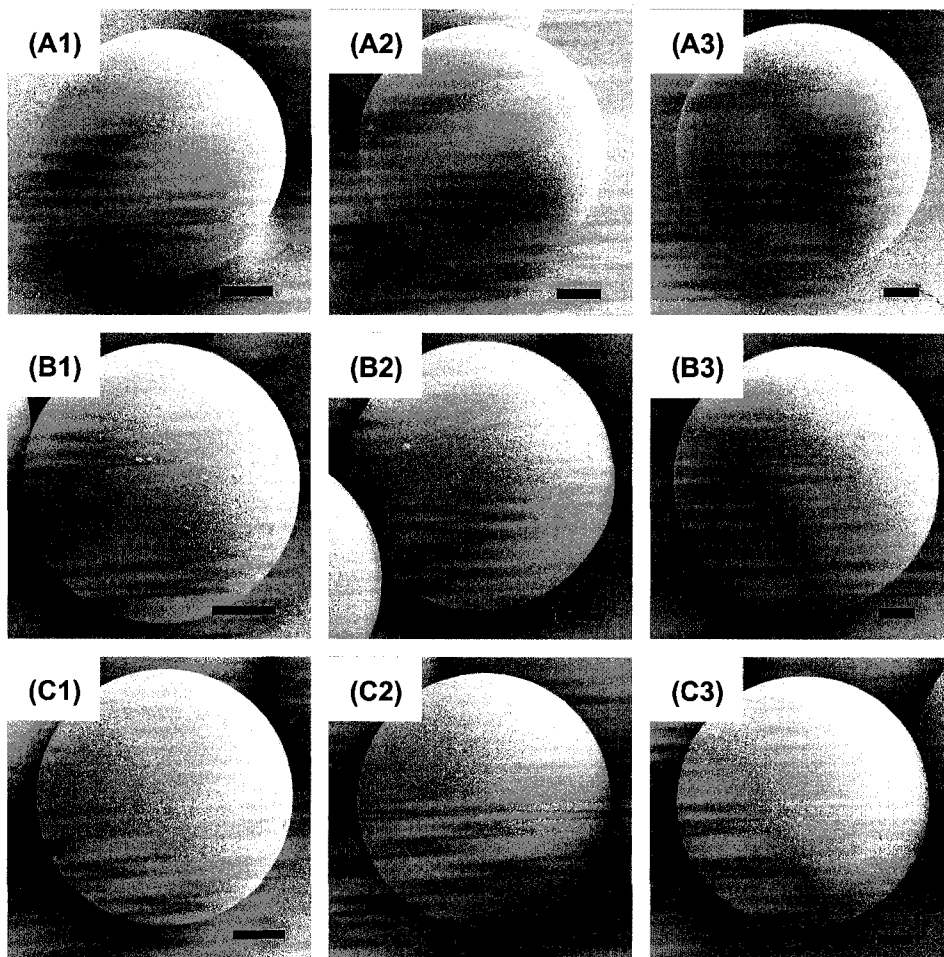


Figure 6.2 Surface morphology of uniform CMS. Regardless of their size and cross-linking density, smooth surfaces were observed. The cross-linking conditions utilized were (A1-3) C0, (B1-3) C1, and (C1-3) C2. The diameters were (A1) 24 μm , (A2) 28 μm , (A3) 35 μm , (B1) 23 μm , (B2) 29 μm , (B3) 38 μm , (C1) 25 μm , (C2) 28 μm , and (C3) 38 μm . The scale bars = 5 μm .

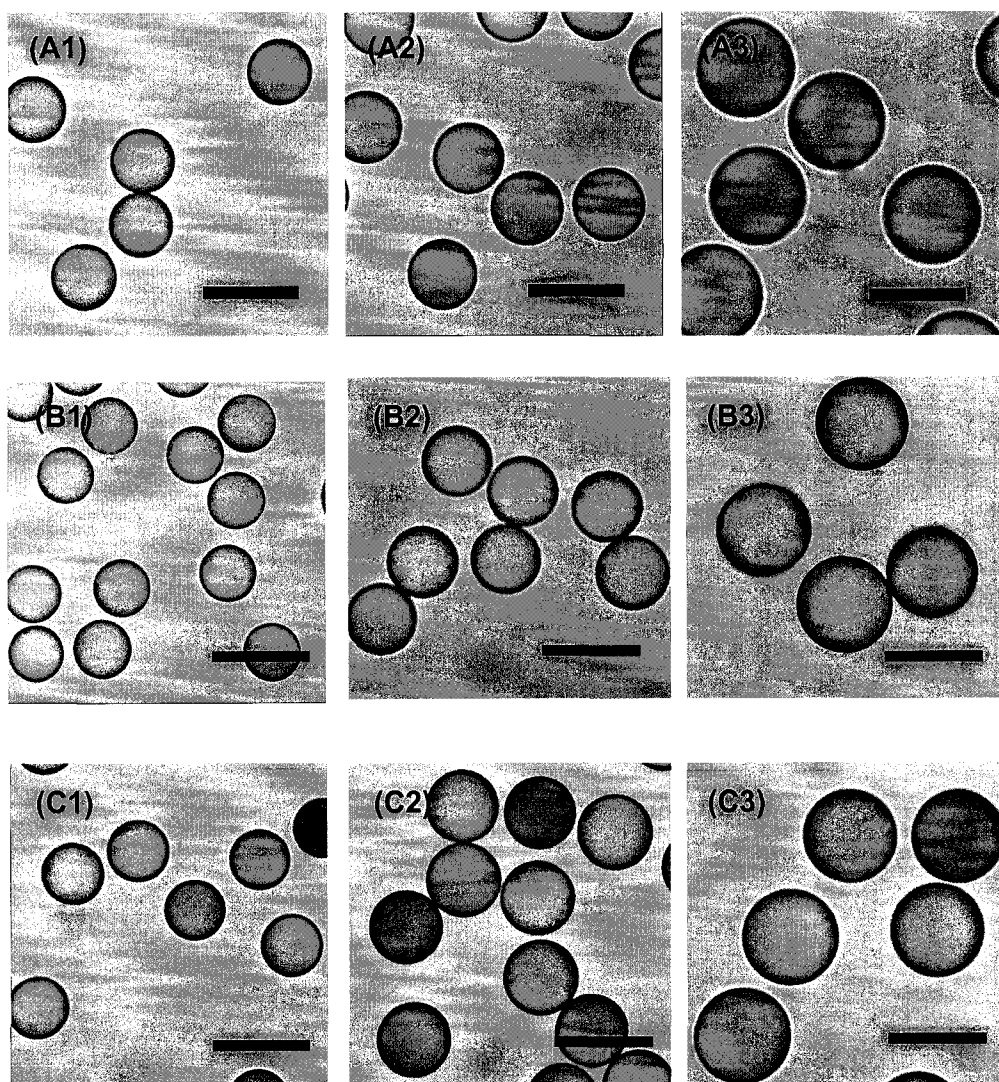


Figure 6.3 Optical micrographs of the wet CMS swollen in pH = 7.4 buffer solution. The cross-linking conditions utilized were (A1-3) C0, (B1-3) C1, and (C1-3) C2. The diameters were shown in Table 6.2. The scale bars = 50 μm .

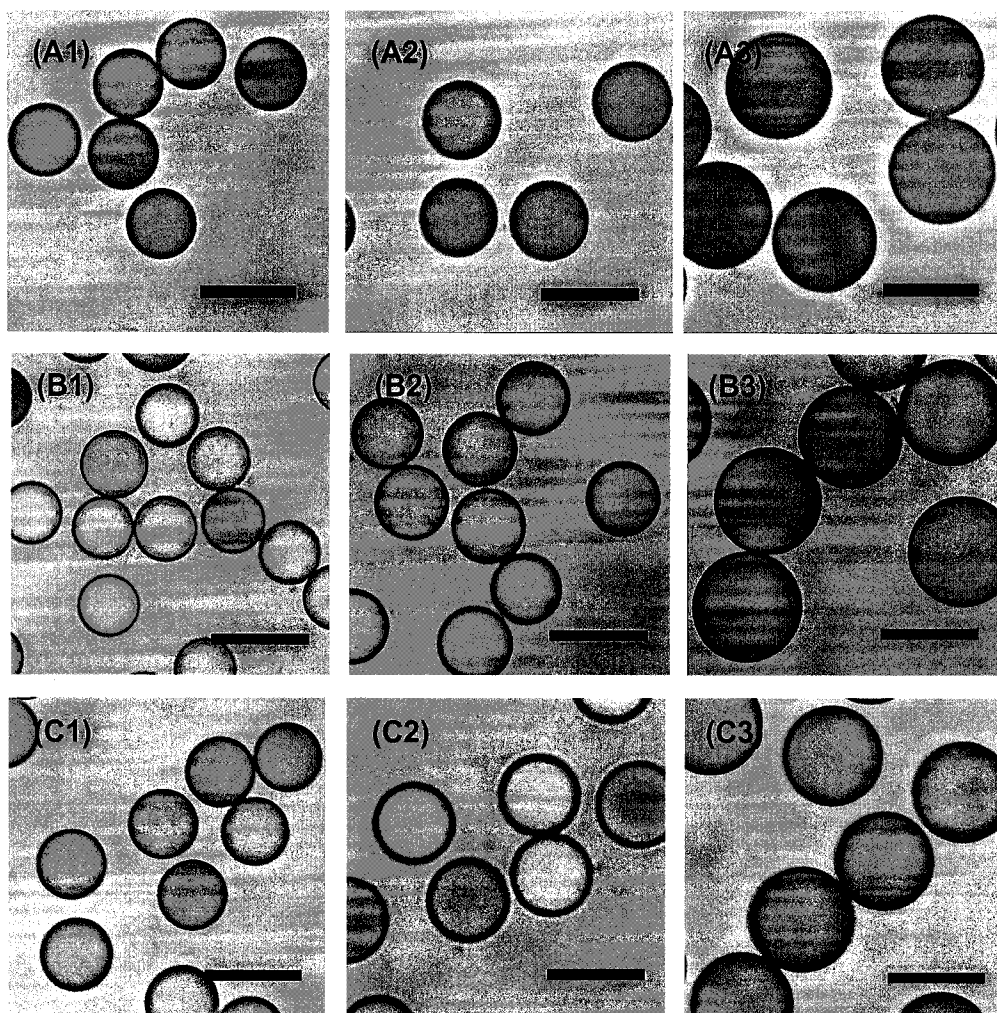


Figure 6.4 Optical micrographs of the wet CMS swollen in pH = 1.0 buffer solution. All CMS swelled more than in pH = 7.4. The cross-linking conditions utilized were (A1-3) C0, (B1-3) C1, and (C1-3) C2. The diameters were shown in Table 6.2. The scale bars = 50 μm .

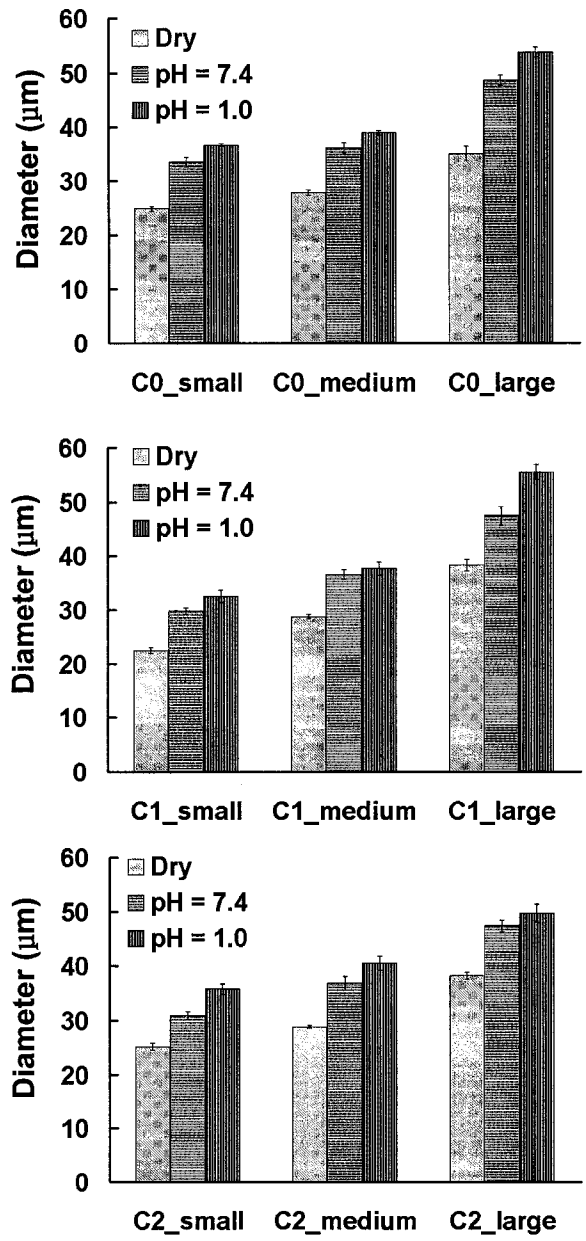


Figure 6.5 The sizes of uniform CMS with different crosslinking densities. The dry CMS were suspended in the media at pHs = 7.4 and 1.0 for 24 h. More than 50 CMS were measured optically.

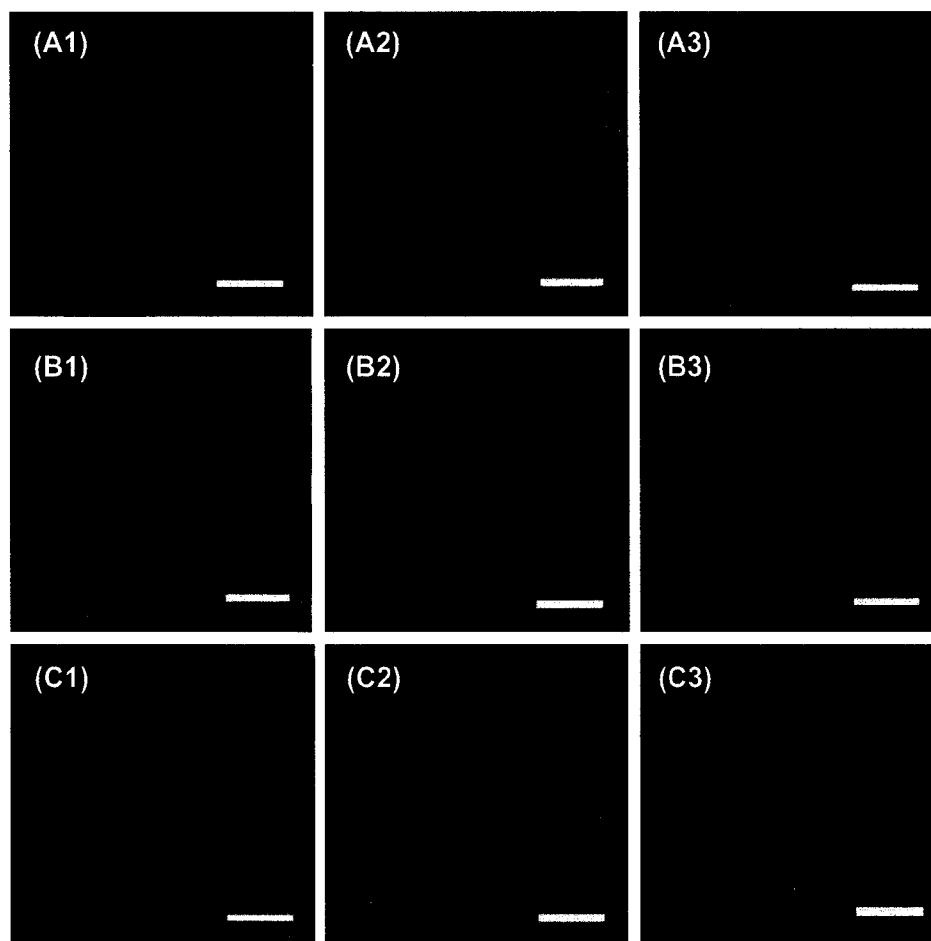


Figure 6.6 Distribution of a basic drug in the CMS as observed by confocal fluorescent microscope. Rhodamine B was employed as the model drug. The crosslinking conditions were (A1-3) C0, (B1-3) C1, and (C1-3) C2. The scale bars were 20 μm .

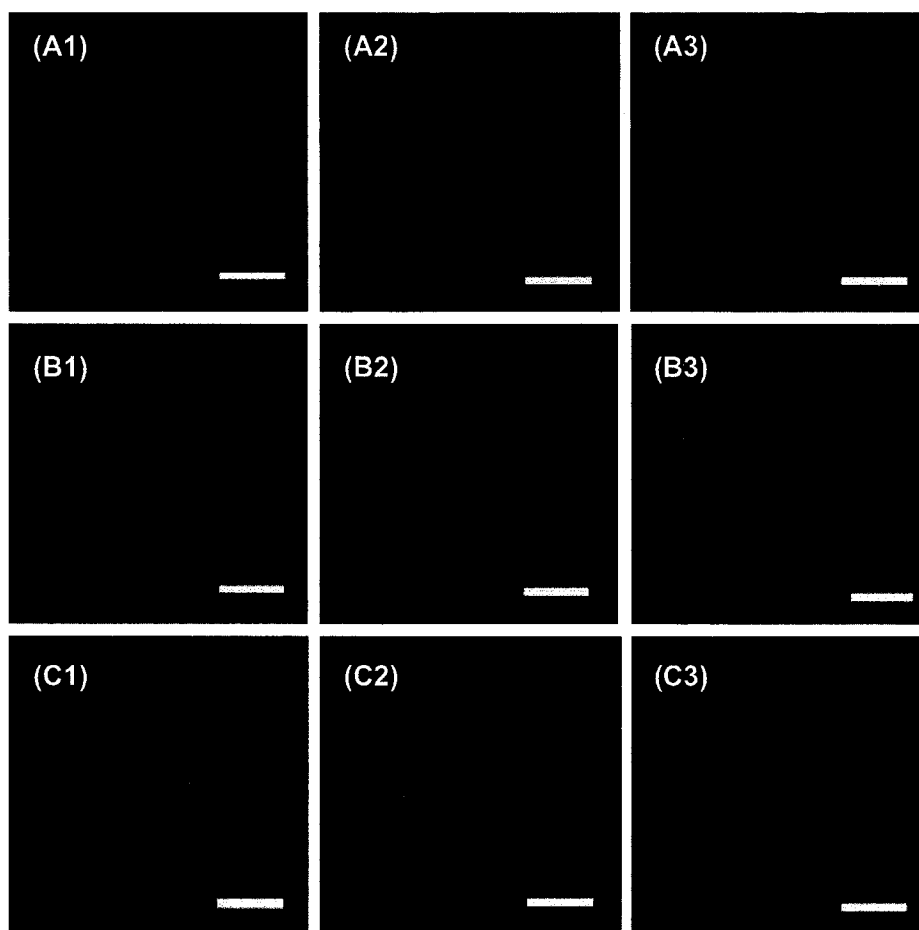


Figure 6.7 Distribution of an acidic drug in the CMS as observed by confocal fluorescent microscope. Eosin Y was employed as the model drug. The cross-linking conditions were (A1-3) C0, (B1-3) C1, and (C1-3) C2. The scale bars were 20 μm .

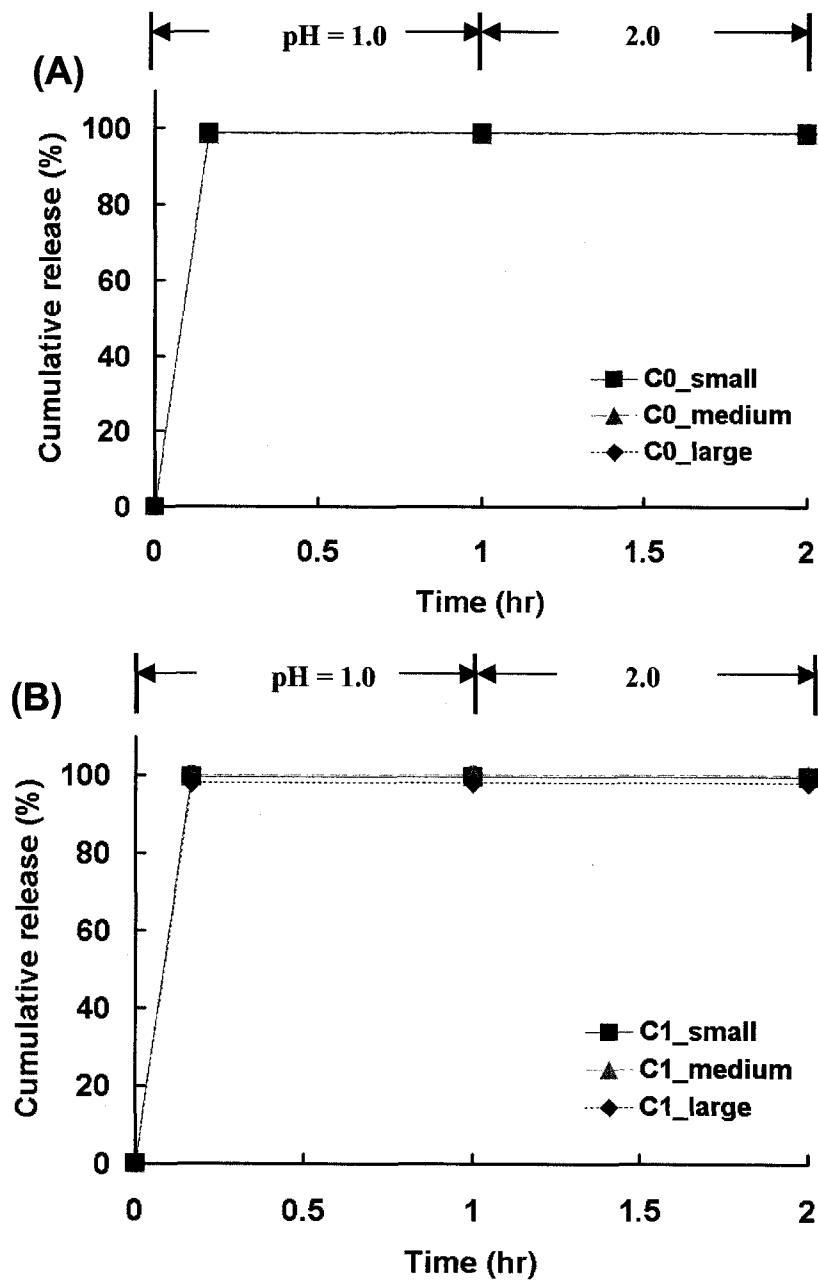


Figure 6.8 Release profiles of a basic drug (toluidine blue) from uniform CMS with different cross-linking densities. The cross-linking densities were: (A) C0, (B) C1, and (C) C2.

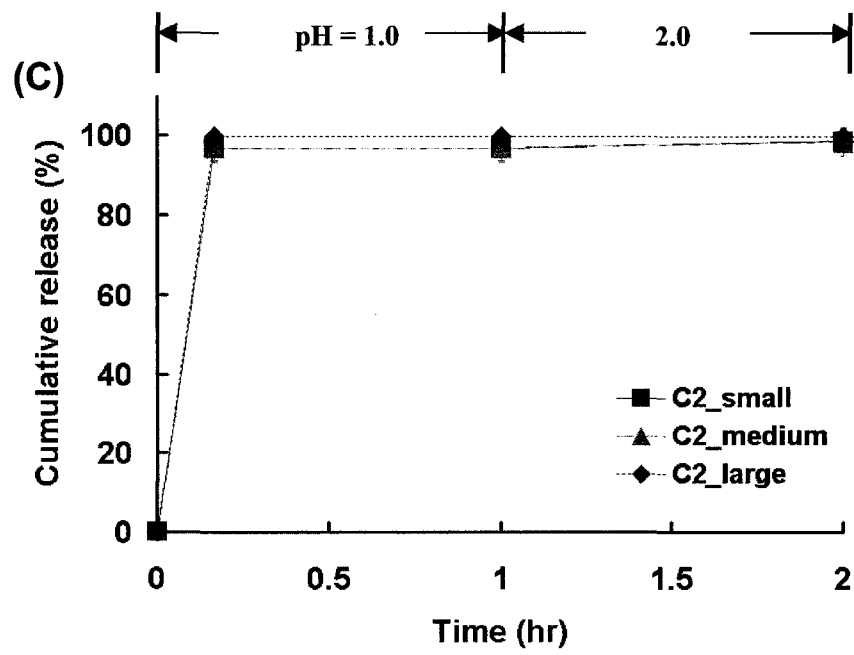


Figure 6.8 Continued

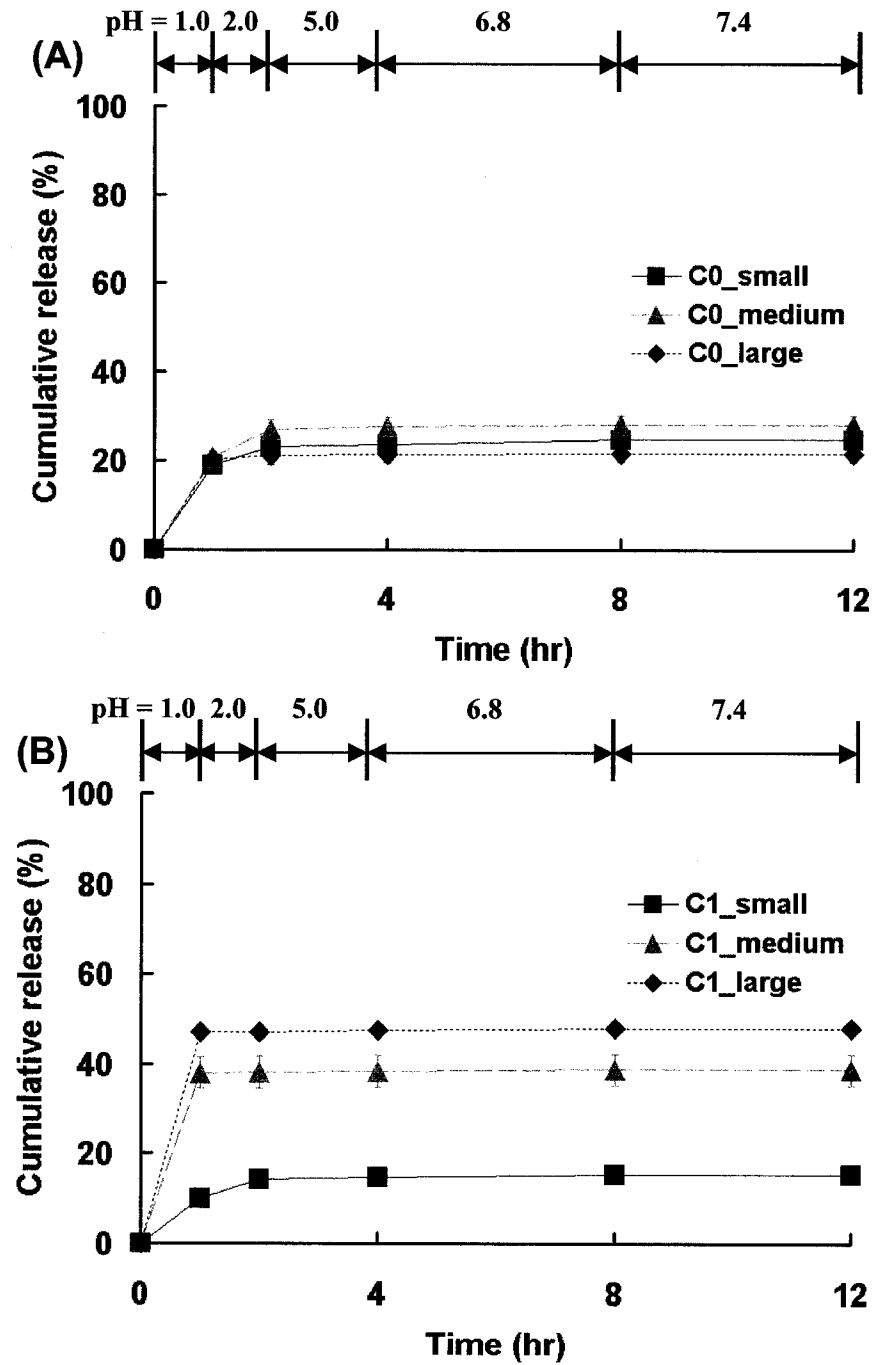


Figure 6.9 Release profiles of a strong acidic drug (trypan blue) from uniform CMS with different cross-linking densities. The cross-linking densities were (A) C0, (B) C1, and (C) C2.

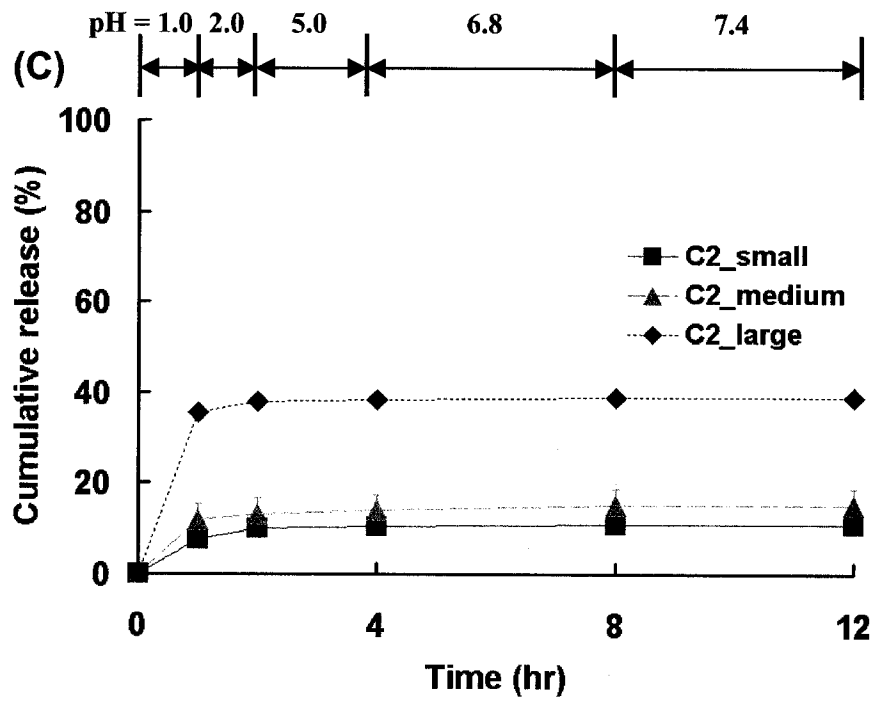


Figure 6.9 Continued

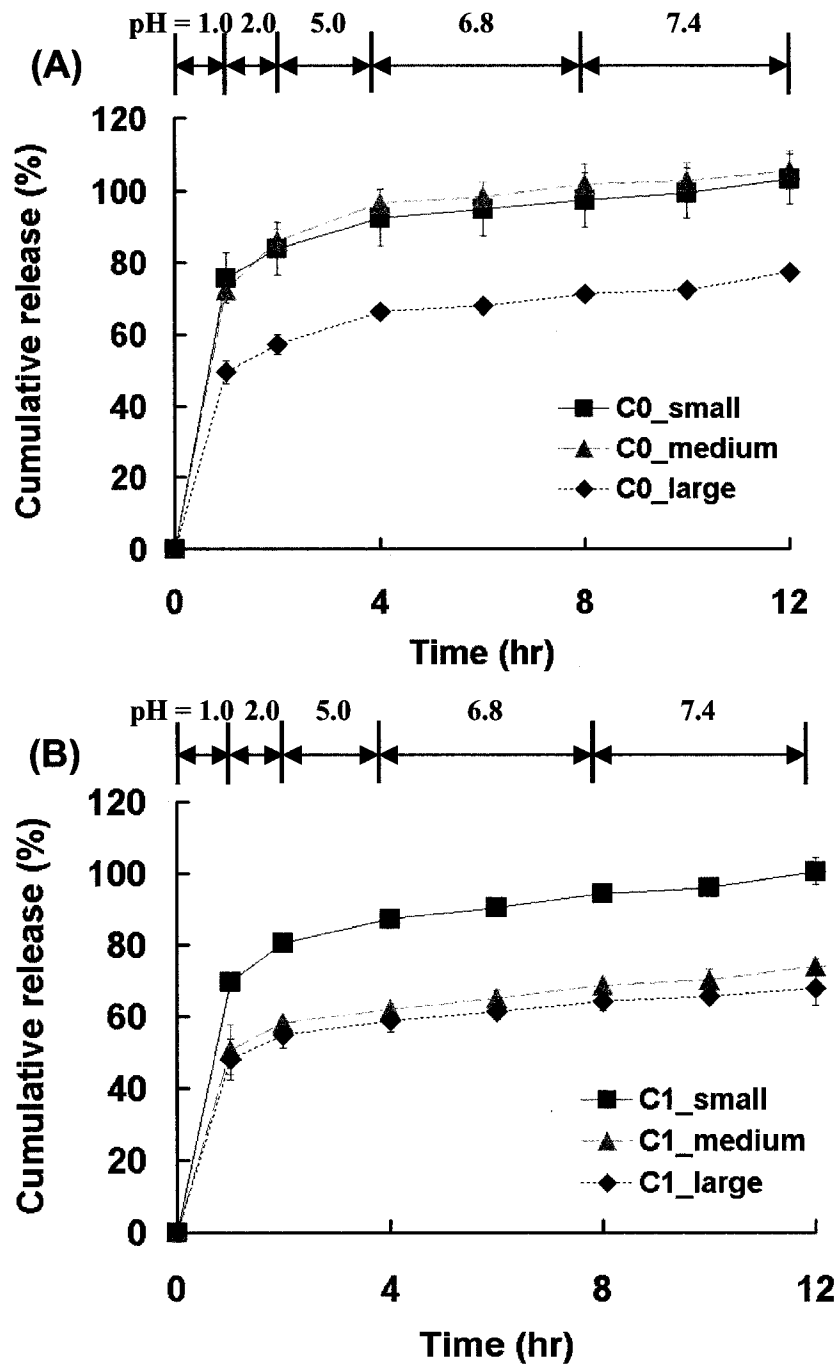


Figure 6.10 Release profiles of a weak acidic drug (diclofenac sodium salt) from uniform CMS with different cross-linking densities. The cross-linking densities were (A) C0, (B) C1, and (C) C2.

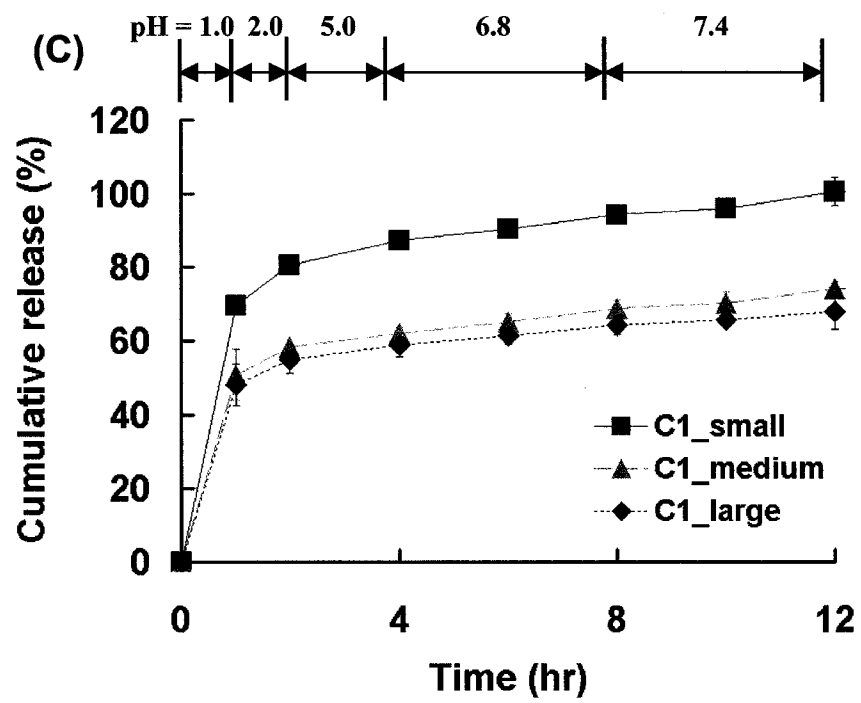


Figure 6.10 Continued

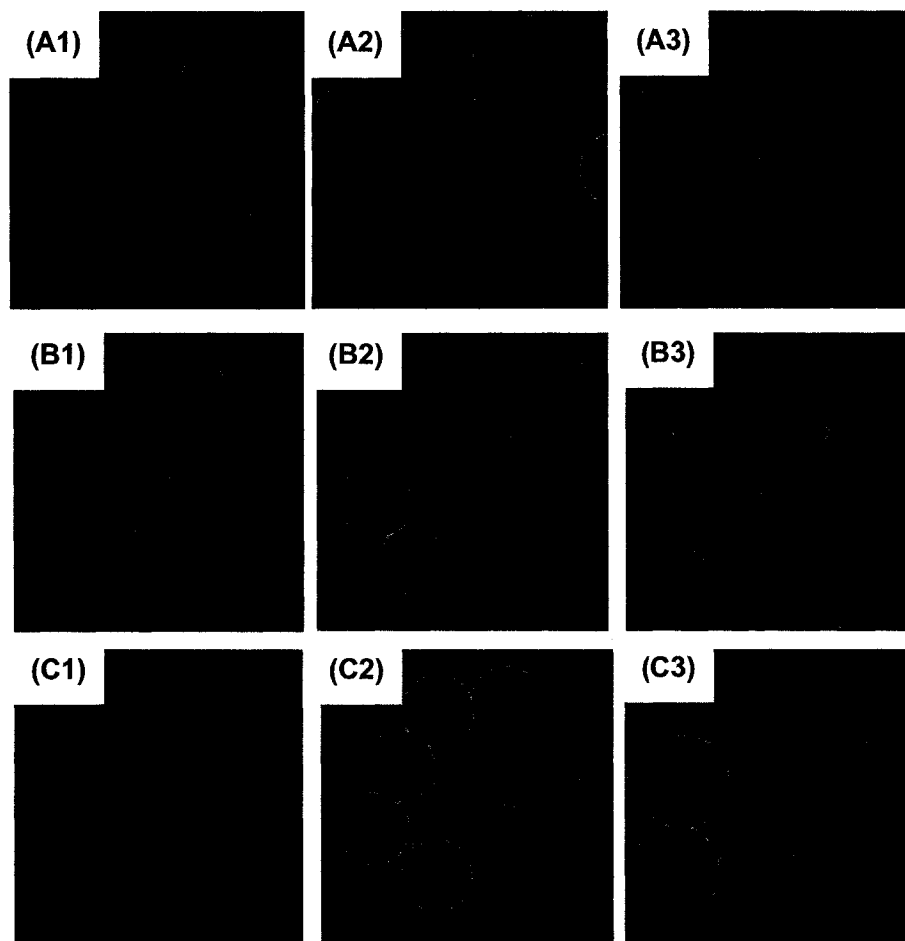


Figure 6.11 Optical micrographs of the CMS after 12 h release of a basic drug (toluidine blue). All exhibited brownish color and transparency, which means a 100% release. The cross-linking conditions utilized were (A) C0, (B) C1, and (C) C2. The scale bars are 50 μm .

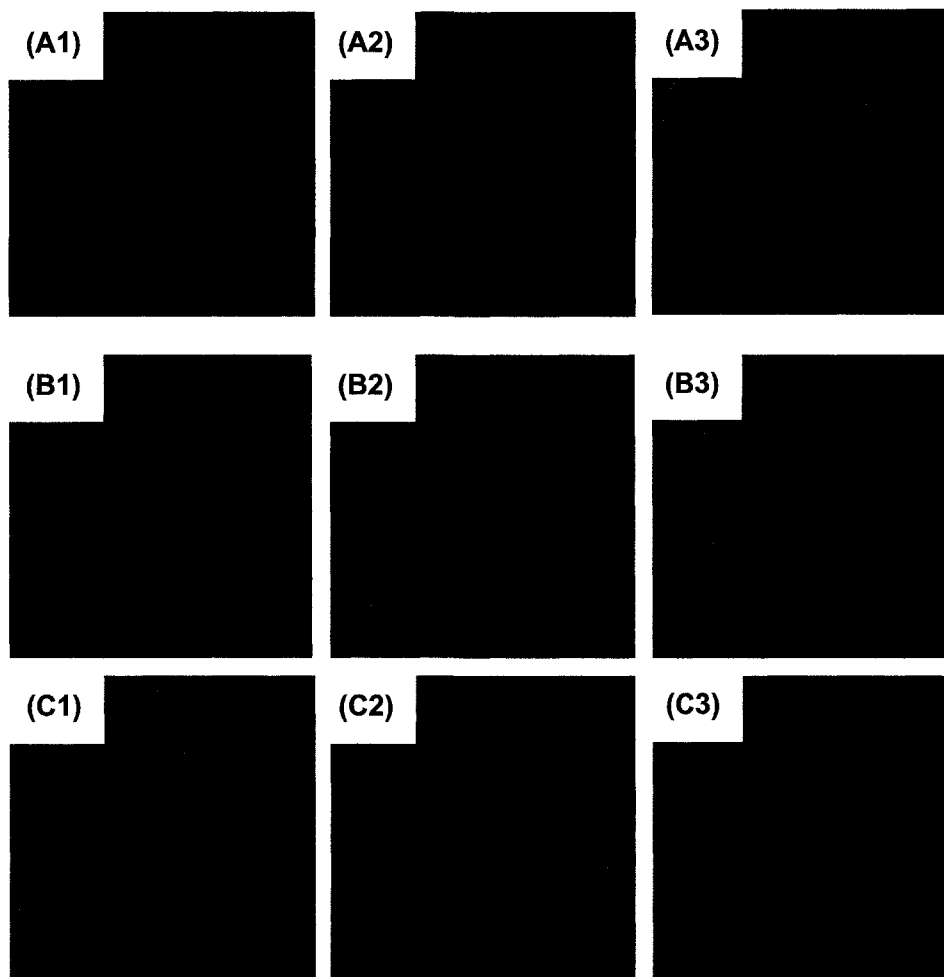


Figure 6.12 Optical micrographs of the CMS after 12 h release of a strong acidic dye (trypan blue). All exhibited dark bluish color indicating that there was drug remaining in the CMS. The cross-linking conditions utilized were (A) C0, (B) C1, and (C) C2. The scale bars are 50 μm .

Table 6.1 The concentrations of glutaraldehyde utilized to cross-link the CMS

Sample name	C0	C1	C2
GA conc. (%)	0	0.0375	0.075

Table 6.2 Average diameters of chitosan microspheres while dry and wet at both pHs = 7.4 and 1.0. More than 50 CMS were measured using an optical microscope

C0 chitosan microspheres

Suspension media	Small	Medium	Large
Dry air	24 (± 0.43)	28 (± 0.49)	35 (± 1.33)
pH = 7.4	34 (± 0.87)	36 (± 0.87)	49 (± 0.95)
pH = 1.0	37 (± 0.27)	39 (± 0.37)	54 (± 0.92)

C1 chitosan microspheres

Suspension media	Small	Medium	Large
Dry air	23 (± 0.51)	29 (± 0.46)	38 (± 1.07)
pH = 7.4	30 (± 0.56)	36 (± 0.87)	47 (± 1.70)
pH = 1.0	33 (± 1.15)	38 (± 1.16)	56 (± 1.39)

C2 chitosan microspheres

Suspension media	Small	Medium	Large
Dry air	25 (± 0.69)	28 (± 0.27)	38 (± 0.58)
pH = 7.4	31 (± 0.73)	37 (± 1.28)	47 (± 1.11)
pH = 1.0	36 (± 0.97)	41 (± 1.24)	50 (± 1.62)

CHAPTER 7

CONCLUSIONS

Drug delivery mediated by biodegradable and/or biocompatible microspheres (MS) have been of great interest because of their versatility, ease of preparation, and simplicity of administration through various routes. However, the conventional methods were only able to produce MS with wide size distributions, giving rise to uncertainties in the data interpretation and poor reproducibility of the results. Due to the surface-area to volume ratio, the size and size distribution of the MS are critical factors in determining the drug diffusion and/or polymer degradation, which in turn, influence the drug release. In this thesis work, we have developed novel, yet very effective and practical, methods of fabricating uniform MS of various biocompatible/biodegradable polymers. These MS were subsequently used to study the in-vitro drug release, in an effort to assess their utility as advanced drug delivery vehicles.

The basic scheme of the present fabrication method, namely the PPF method, originated from the work of my thesis advisor, Professor Kyekyoon (Kevin) Kim, which included fabrication of precision microspheres of frozen hydrogen and microcapsules of silica aerogel. Previously, the PPF method was applied to PLG and polyanhydride in our group and the resulting MS were used for the release study. Due to their excellent uniformity and narrow size distribution the MS exhibited precisely controlled drug release behaviors. In this work we have applied the scheme to different polymers such as ethyl cellulose (EC), chitosan, starch, and gelatin, to examine the effectiveness of the PPF method with other biomaterials.

The PPF method, extensively utilized and further developed in this study for fabrication of uniform MS, employed three different forces: mechanical,

hydrodynamic, and electric. A combined use of the mechanical and hydrodynamic forces enabled the method to be free from usual limitations imposed by the solution viscosity and nozzle dimension. A nonsolvent carrier stream flowing faster than the polymer solution jet allowed the jet thickness to become smaller than the nozzle orifice, while the mechanical force caused break-up of the jet into uniform drops. Because EC dissolves in hydrophobic solvent, water was employed for the carrier stream. However, hydrogels such as chitosan, starch, and gelatin required the use of oil phase as a carrier stream, instead. Upon generation, the uniform drops needed to be separated to avoid agglomeration and retain their uniformity. The drop agglomeration was successfully prevented by employing a surfactant for EC and an electric force for hydrogels. Especially with the use of electric force, the method became truly non-toxic and most suitable for biomedical applications. The separated drops were subjected to hardening to obtain the dry MS. Depending on the kinds of solvent, their evaporation was facilitated either at room temperature or at an elevated temperature. Since gelatin degrades at high temperature, it required use of a low temperature to form gelled drops, followed by solvent extraction afterwards.

Conventional methods, often promoted by others for their effectiveness, could not achieve precise control over the MS size due to the restrictions imposed by the polymer kinds and reactor dimensions. However, the methods developed in this work overcame such limitations due to dynamic applications of various techniques employed that are possible with the PPF method. The concurrent use of three different techniques, which were the generation of uniform solution drops, prevention of agglomeration, and facilitation of particle hardening, allowed us to achieve much more and with more control than any other available methods.

The strategy for selecting a polymer as an encapsulant was determined by the administration routes, kinds of drugs, and desirable release profiles. For

example, EC was a good candidate for oral, buccal, and rectal delivery. Hydrogels could very well be appropriate delivery vehicles for hydrophilic therapeutic agents such as protein, peptide, and DNA. Thus, the ability to use a variety of polymers proved to be the advantage and versatility of the MS-mediated drug delivery systems. In this study, we employed uniform MS of EC, chitosan, and gelatin as such delivery vehicles.

For EC, almost linear release could be obtained with small MS (30- and 35- μm) of low-viscosity EC. The precise control over the size enabled us to obtain more even drug distribution in the MS, by which the initial burst release could be substantially suppressed. We also examined the effect of crosslinking on uniform gelatin microspheres (GMS). Because GMS dissolved rapidly in aqueous solution, cross-linking was often carried out by suspending the non-crosslinked GMS in glutaraldehyde solution. Due to glutaraldehyde concentration gradient, heterogeneous crosslinking took place in the GMS, which provided the MS surface with stronger resistance to degradation but with less drug bonding. As a result, the release was not sustained longer with increased crosslinking although the GA concentrations increased from a certain value. We found that the size control of GMS was essential to optimization of crosslinking conditions, by which the cytotoxicity of glutaraldehyde could be minimized but the efficacy of drug delivery maximized. The chitosan microspheres (CMS) were also examined for colon-specific delivery. Various investigators had previously employed additive polymers to achieve colon-specific delivery. However, due to the complexity of the fabrication method and the resulting incorporation of toxic solvent, the approaches did not appear to be desirable. In this work, because of the uniformity of the MS and the cationic property of chitosan, we were able to demonstrate that the release of an acidic drug could be accurately targeted to colonic site without any other additives.

In conclusion, we have developed a novel method particularly suited to fabricating uniform biomaterial-based MS of precisely controlled size and size distribution. We have demonstrated that the resulting MS were advantageous in achieving precisely controlled drug delivery. Due to its compatibility with a wide range of biomedical materials and applications, the present method should also be applicable to cell encapsulation, bio-imaging, fabrication of biological sensors, and even food engineering. With the proven flexibility and versatility of the PPF method and a number of applications demonstrated in this work, it is hopefully concluded that the present work may have planted a seed, if in a modest way, for the advancement and evolution of biomedical science and technology.

REFERENCES

- [1] M. M. Struck, "Biopharmaceutical R&D success rates and development times. A new analysis provides benchmarks for the future," *Bio/Technology*, vol. 12, pp. 674-677, 1994.
- [2] C. Berkland, K. Kim, and D. W. Pack, "Fabrication of PLG microspheres with precisely controlled and monodisperse size distributions," *J. Control Release*, vol. 73, pp. 59-74, 2001.
- [3] R. S. Langer and N. A. Peppas, "Present and future applications of biomaterials in controlled drug delivery systems," *Biomaterials*, vol. 2, pp. 201-14, 1981.
- [4] N. K. Varde and D. W. Pack, "Microspheres for controlled release drug delivery," *Expert. Opin. Biol. Ther.*, vol. 4, pp. 35-51, 2004.
- [5] M. Dutt and G. K. Khuller, "Sustained release of isoniazid from a single injectable dose of poly (DL-lactide-co-glycolide) microparticles as a therapeutic approach towards tuberculosis," *Int. J. Antimicrob. Agents*, vol. 17, pp. 115-122, 2001.
- [6] I. J. Castellanos, W. O. Cuadrado, and K. Griebenow, "Prevention of structural perturbations and aggregation upon encapsulation of bovine serum albumin into poly(lactide-co-glycolide) microspheres using the solid-in-oil-in water technique," *J. Pharm. Pharmacol.*, vol. 53, pp. 1099-1107, 2001.
- [7] Y. Y. Yang, T. S. Chung, and N. P. Ng, "Morphology, drug distribution, and in vitro release profiles of biodegradable polymeric microspheres containing protein fabricated by double-emulsion solvent extraction/evaporation method," *Biomaterials*, vol. 22, pp. 231-241, 2001.
- [8] K. Abu-Izza, L. Tambrallo, and D. R. Lu, "In vivo evaluation of zidovudine (AZT)-loaded ethylcellulose microspheres after oral administration in beagle dogs," *J. Pharm. Sci.*, vol. 86, pp. 554-559, 1997.
- [9] S. Roy, M. Pal, and B. K. Gupta, "Indomethacin-loaded microspheres: design and preparation by a multiple-emulsification technique and their in vitro evaluation," *Pharm. Res.*, vol. 9, pp. 1132-1136, 1992.
- [10] P. C. Wu, Y. B. Huang, J. I. Chang, M. J. Tsai, and Y. H. Tsai, "Preparation and evaluation of sustained release microspheres of potassium chloride prepared with ethylcellulose," *Int. J. Pharm.*, vol. 260, pp. 115-121, 2003.

- [11] C. Sajeev, G. Vinay, R. Archana, and R. N. Saha, "Oral controlled release formulation of diclofenac sodium by microencapsulation with ethyl cellulose," *J. Microencapsul.*, vol. 19, pp. 753-760, 2002.
- [12] G. Uzunkaya and N. Bergisadi, "In vitro drug liberation and kinetics of sustained release indomethacin suppository," *Farmaco*, vol. 58, pp. 509-512, 2003.
- [13] C. Y. Yang, S. Y. Tsay, and R. C. Tsiang, "Encapsulating aspirin into a surfactant-free ethyl cellulose microsphere using non-toxic solvents by emulsion solvent-evaporation technique," *J. Microencapsul.*, vol. 18, pp. 223-236, 2001.
- [14] S. W. Kim, Y. H. Bae, and T. Okano, "Hydrogels: swelling, drug loading, and release," *Pharm. Res.*, vol. 9, pp. 283-290, 1992.
- [15] J. A. Ko, H. J. Park, S. J. Hwang, J. B. Park, and J. S. Lee, "Preparation and characterization of chitosan microparticles intended for controlled drug delivery," *Int. J. Pharm.*, vol. 249, pp. 165-174, 2002.
- [16] A. Berthold, K. Cremer, and J. Kreuter, "Preparation and characterization of chitosan microspheres as drug carrier for prednisolone sodium phosphate as model for anti-inflammatory drugs," *J. Control Release*, vol. 39, pp. 17-25, 1996.
- [17] S. Ozbas-Turan, C. Aral, L. Kabasakal, M. Keyer-Uysal, and J. Akbuga, "Co-encapsulation of two plasmids in chitosan microspheres as a non-viral gene delivery vehicle," *J. Pharm. Pharmacol. Sci.*, vol. 6, pp. 27-32, 2003.
- [18] J. E. Lee, K. E. Kim, I. C. Kwon, H. J. Ahn, S. H. Lee, H. Cho, H. J. Kim, S. C. Seong, and M. C. Lee, "Effects of the controlled-released TGF-beta 1 from chitosan microspheres on chondrocytes cultured in a collagen/chitosan/glycosaminoglycan scaffold," *Biomaterials*, vol. 25, pp. 4163-4173, 2004.
- [19] L. Illum, P. Watts, A. N. Fisher, M. Hinchcliffe, H. Norbury, I. Jabbal-Gill, R. Nankervis, and S. S. Davis, "Intranasal delivery of morphine," *J. Pharmacol. Exp. Ther.*, vol. 301, pp. 391-400, 2002.
- [20] R. Hejazi and M. Amiji, "Stomach-specific anti-H. pylori therapy; part III: effect of chitosan microspheres crosslinking on the gastric residence and local tetracycline concentrations in fasted gerbils," *Int. J. Pharm.*, vol. 272, pp. 99-108, 2004.

- [21] S. P. Vyas and C. P. Jain, "Bioadhesive polymer-grafted starch microspheres bearing isosorbide dinitrate for buccal administration," *J. Microencapsul.*, vol. 9, pp. 457-464, 1992.
- [22] L. Wikingsson and I. Sjöholm, "Polyacryl starch microparticles as adjuvant in oral immunisation, inducing mucosal and systemic immune responses in mice," *Vaccine*, vol. 20, pp. 3355-3363, 2002.
- [23] N. Rydell and I. Sjöholm, "Oral vaccination against diphtheria using polyacryl starch microparticles as adjuvant," *Vaccine*, vol. 22, pp. 1265-1274, 2004.
- [24] M. A. Vandelli, F. Rivasi, P. Guerra, F. Forni, and R. Arletti, "Gelatin microspheres crosslinked with D,L-glyceraldehyde as a potential drug delivery system: preparation, characterisation, in vitro and in vivo studies," *Int. J. Pharm.*, vol. 215, pp. 175-184, 2001.
- [25] Y. Tabata and Y. Ikada, "Vascularization effect of basic fibroblast growth factor released from gelatin hydrogels with different biodegradabilities," *Biomaterials*, vol. 20, pp. 2169-2175, 1999.
- [26] H. Nakase, K. Okazaki, Y. Tabata, M. Ozeki, N. Watanabe, M. Ohana, S. Uose, K. Uchida, T. Nishi, M. Mastuura, H. Tamaki, T. Itoh, C. Kawanami, and T. Chiba, "New cytokine delivery system using gelatin microspheres containing interleukin-10 for experimental inflammatory bowel disease," *J. Pharmacol. Exp. Ther.*, vol. 301, pp. 59-65, 2002.
- [27] Y. Tabata, Ikada, Y., Morimoto, K., Katsumata, H., Yabuta, T., "Surfactant-free preparation of biodegradable hydrogel microspheres for protein release," *J. Bioactive Compatible Polymers*, vol. 14, pp. 371-384, 1999.
- [28] Y. Ikada and Y. Tabata, "Protein release from gelatin matrices," *Adv. Drug Deliv. Rev.*, vol. 31, pp. 287-301, 1998.
- [29] M. Yamamoto, Y. Takahashi, and Y. Tabata, "Controlled release by biodegradable hydrogels enhances the ectopic bone formation of bone morphogenetic protein," *Biomaterials*, vol. 24, pp. 4375-4383, 2003.
- [30] T. A. Holland, J. K. Tessmar, Y. Tabata, and A. G. Mikos, "Transforming growth factor-beta1 release from oligo(poly(ethylene glycol) fumarate) hydrogels in conditions that model the cartilage wound healing environment," *J. Control Release*, vol. 94, pp. 101-114, 2004.

- [31] I. M. Van Der Lubben, F. A. Konings, G. Borchard, J. C. Verhoef, and H. E. Junginger, "In vivo uptake of chitosan microparticles by murine Peyer's patches: Visualization studies using confocal laser scanning microscopy and immunohistochemistry," *J. Drug Target*, vol. 9, pp. 39-47, 2001.
- [32] C. R. Dass and M. A. Burton, "Microsphere-mediated targeted gene therapy of solid tumors," *Drug Deliv.*, vol. 6, pp. 243-252, 1999.
- [33] A. Lavasanifar, R. Ghalandari, Z. Ataei, M. E. Zolfaghari, and S. A. Mortazavi, "Microencapsulation of theophylline using ethylcellulose: in vitro drug release and kinetic modelling," *J. Microencapsul.*, vol. 14, pp. 91-100, 1997.
- [34] C. Thies, "A survey of microencapsulation processes," in *Microencapsulation: Methods and Industrial Applications*, vol. 73, S. Benita, Ed. New York: Marcel Dekker, Inc., 1996, pp. 1-19.
- [35] R. Hejazi and M. Amiji, "Stomach-specific anti-H. pylori therapy. I: Preparation and characterization of tetracycline-loaded chitosan microspheres," *Int. J. Pharm.*, vol. 235, pp. 87-94, 2002.
- [36] F. L. Mi, S. S. Shyu, C. T. Chen, and J. Y. Schoung, "Porous chitosan microsphere for controlling the antigen release of Newcastle disease vaccine: Preparation of antigen-adsorbed microsphere and in vitro release," *Biomaterials*, vol. 20, pp. 1603-12, 1999.
- [37] H. Chen, J. C. Wu, and H. Y. Chen, "Preparation of ethylcellulose microcapsules containing theophylline by using emulsion non-solvent addition method," *J. Microencapsul.*, vol. 12, pp. 137-147, 1995.
- [38] R. Fernandez-Urrusuno, J. M. Gines, and E. Morillo, "Development of controlled release formulations of alachlor in ethylcellulose," *J. Microencapsul.*, vol. 17, pp. 331-342, 2000.
- [39] Y. Huang, M. Yeh, and C. Chiang, "Formulation factors in preparing BTM-chitosan microspheres by spray drying method," *Int. J. Pharm.*, vol. 242, pp. 239-242, 2002.
- [40] P. He, S. S. Davis, and L. Illum, "Chitosan microspheres prepared by spray drying," *Int. J. Pharm.*, vol. 187, pp. 53-65, 1999.
- [41] N. Grattard, M. Pernin, B. Marty, G. Roudaut, D. Champion, and M. Le Meste, "Study of release kinetics of small and high molecular weight substances dispersed into spray-dried ethylcellulose microspheres," *J. Control Release*, vol. 84, pp. 125-135, 2002.

- [42] C. Amiet-Charpentier, P. Gadille, B. Digat, and J. P. Benoit, "Microencapsulation of rhizobacteria by spray-drying: formulation and survival studies," *J. Microencapsul.*, vol. 15, pp. 639-659, 1998.
- [43] L. S. Mok, K. Kim, and T. P. Bernat, "Equilibrium of a liquid in a spherical shell due to gravity, surface tension, and van der Waals forces," *Phys. Fluids*, vol. 28, pp. 1227-1232, 1985.
- [44] J. E. Kirwan, T. A. Lee, G. N. Schroering, H. Krier, J. E. Peters, J. P. Renie, and K. Kim, "An experimental and theoretical study of a monodisperse spray," *AIAA J. Propulsion and Power*, vol. 4, pp. 299-307, 1988.
- [45] N. K. Kim, K. Kim, D. A. Payne, and R. S. Upadhye, "Fabrication of hollow silica aerogel spheres by a droplet generation method and sol-gel processing," *J. Vac. Sci. Technol. A*, vol. 7, pp. 1181-1184, 1989.
- [46] K. Y. Jang, K. Kim, and R. S. Upadhye, "Study of sol-gel processing for fabrication of hollow silica-aerogel spheres," *J. Vac. Sci. Technol. A*, vol. 8, pp. 1732-1735, 1990.
- [47] C. A. Foster, K. Kim, R. J. Turnbull, and C. D. Hendricks, "Apparatus for producing uniform solid spheres of hydrogen," *Rev. Sci. Instrum.*, vol. 48, pp. 625-631, 1977.
- [48] R. P. Gillard, K. Kim, and R. J. Turnbull, "Spherical hydrogen pellet generator for magnetic confinement fusion research," *Rev. Sci. Instrum.*, vol. 52, pp. 183-190, 1981.
- [49] J. L. Guttman, C. D. Hendricks, K. Kim, and R. J. Turnbull, "An investigation of the effects of system parameters on the production of hollow hydrogen droplets," *J. Appl. Phys.*, vol. 50, pp. 4139-4142, 1979.
- [50] L. Rayleigh, in *Proc. Lond. Math. Soc.*, vol. 10, 1879, p. 4.
- [51] L. Rayleigh, in *Philos. Mag. S. G.*, vol. 14, 1882, p. 184.
- [52] C. Berkland, K. Kim, and D. W. Pack, "PLG microsphere size controls drug release rate through several competing factors," *Pharm. Res.*, vol. 20, pp. 1055-1062, 2003.
- [53] C. Berkland, M. King, A. Cox, K. Kim, and D. W. Pack, "Precise control of PLG microsphere size provides enhanced control of drug release rate," *J. Control Release*, vol. 82, pp. 137-147, 2002.

- [54] C. Berklund, M. J. Kipper, B. Narasimhan, K. K. Kim, and D. W. Pack, "Microsphere size, precipitation kinetics and drug distribution control drug release from biodegradable polyanhydride microspheres," *J. Control Release*, vol. 94, pp. 129-141, 2004.
- [55] E. Esposito, R. Cortesi, and C. Nastruzzi, "Gelatin microspheres: influence of preparation parameters and thermal treatment on chemico-physical and biopharmaceutical properties," *Biomaterials*, vol. 17, pp. 2009-2020, 1996.
- [56] B. Lu, J. Q. Zhang, and H. Yang, "Lung-targeting microspheres of carboplatin," *Int. J. Pharm.*, vol. 265, pp. 1-11, 2003.
- [57] D. K. Cheng, *Field and Wave Electromagnetics*. New York: Addison-Wesley Publishing Company, Inc., 1989.
- [58] M. M. Crowley, B. Schroeder, A. Fredersdorf, S. Obara, M. Talarico, S. Kucera, and J. W. McGinity, "Physicochemical properties and mechanism of drug release from ethyl cellulose matrix tablets prepared by direct compression and hot-melt extrusion," *Int. J. Pharm.*, vol. 269, pp. 509-522, 2004.
- [59] Z. Shen and S. Mitragotri, "Intestinal patches for oral drug delivery," *Pharm. Res.*, vol. 19, pp. 391-395, 2002.
- [60] B. Sa, A. K. Bandyopadhyay, and B. K. Gupta, "Effect of microcapsule size and polyisobutylene concentration on the release of theophylline from ethylcellulose microcapsules," *J. Microencapsul.*, vol. 13, pp. 207-218, 1996.
- [61] C. Y. Yang, S. Y. Tsay, and R. C. Tsiang, "An enhanced process for encapsulating aspirin in ethyl cellulose microcapsules by solvent evaporation in an O/W emulsion," *J. Microencapsul.*, vol. 17, pp. 269-277, 2000.
- [62] S. Roy, S. K. Das, M. Pal, and B. K. Gupta, "Design and in vitro evaluation of dapson-loaded micropellets of ethyl cellulose," *Pharm. Res.*, vol. 6, pp. 945-948, 1989.
- [63] R. Dinarvand, S. Mirfattahi, and F. Atyabi, "Preparation, characterization and in vitro drug release of isosorbide dinitrate microspheres," *J. Microencapsul.*, vol. 19, pp. 73-81, 2002.
- [64] M. Zandi, A. Pourjavadi, S. A. Hashemi, and H. Arabi, "Preparation of ethyl cellulose microcapsules containing perphenazine and polymeric perphenazine based on acryloyl chloride for physical and chemical studies of drug release control," *Polymer International*, vol. 47, pp. 413-418, 1998.

- [65] W. J. Lin and T. L. Wu, "Modification of the initial release of a highly water-soluble drug from ethyl cellulose microspheres," *J. Microencapsul.*, vol. 16, pp. 639-646, 1999.
- [66] C. Dubernet, J. P. Benoit, N. A. Peppas, and F. Puisieux, "Ibuprofen-loaded ethylcellulose microspheres: release studies and analysis of the matrix structure through the Higuchi model," *J. Microencapsul.*, vol. 7, pp. 555-565, 1990.
- [67] H. Arabi, S. A. Hashemi, and M. Fooladi, "Microencapsulation of allopurinol by solvent evaporation and controlled release investigation of drugs," *J. Microencapsul.*, vol. 13, pp. 527-535, 1996.
- [68] J. Wang, B. M. Wang, and S. P. Schwendeman, "Mechanistic evaluation of the glucose-induced reduction in initial burst release of octreotide acetate from poly(D,L-lactide-co-glycolide) microspheres," *Biomaterials*, vol. 25, pp. 1919-1927, 2004.
- [69] T. Yamada, H. Onishi, and Y. Machida, "Sustained release ketoprofen microparticles with ethylcellulose and carboxymethylethylcellulose," *J. Control Release*, vol. 75, pp. 271-282, 2001.
- [70] M. Asada, H. Takahashi, H. Okamoto, H. Tanino, and K. Danjo, "Theophylline particle design using chitosan by the spray drying," *Int. J. Pharm.*, vol. 270, pp. 167-174, 2004.
- [71] E. Dini, S. Alexandridou, and C. Kiparissides, "Synthesis and characterization of cross-linked chitosan microspheres for drug delivery applications," *J. Microencapsul.*, vol. 20, pp. 375-385, 2003.
- [72] I. El-Gibaly, "Development and in vitro evaluation of novel floating chitosan microcapsules for oral use: comparison with non-floating chitosan microspheres," *Int. J. Pharm.*, vol. 249, pp. 7-21, 2002.
- [73] I. El-Gibaly, A. M. Meki, and S. K. Abdel-Ghaffar, "Novel B melatonin-loaded chitosan microcapsules: in vitro characterization and antiapoptosis efficacy for aflatoxin B1-induced apoptosis in rat liver," *Int. J. Pharm.*, vol. 260, pp. 5-22, 2003.
- [74] L. Strindelius, L. Degling Wikingsson, and I. Sjöholm, "Extracellular antigens from *Salmonella enteritidis* induce effective immune response in mice after oral vaccination," *Infect Immun.*, vol. 70, pp. 1434-1442, 2002.

- [75] B. H. Woo, G. Jiang, Y. W. Jo, and P. P. DeLuca, "Preparation and characterization of a composite PLGA and poly(acryloyl hydroxyethyl starch) microsphere system for protein delivery," *Pharm. Res.*, vol. 18, pp. 1600-1606, 2001.
- [76] G. Jiang, W. Qiu, and P. P. DeLuca, "Preparation and in vitro/in vivo evaluation of insulin-loaded poly(acryloyl-hydroxyethyl starch)-PLGA composite microspheres," *Pharm. Res.*, vol. 20, pp. 452-459, 2003.
- [77] C. Sturesson and L. Degling Wikingsson, "Comparison of poly(acryl starch) and poly(lactide-co-glycolide) microspheres as drug delivery system for a rotavirus vaccine," *J. Control Release*, vol. 68, pp. 441-450, 2000.
- [78] B. Brime, M. P. Ballesteros, and P. Frutos, "Preparation and in vitro characterization of gelatin microspheres containing Levodopa for nasal administration," *J. Microencapsul.*, vol. 17, pp. 777-784, 2000.
- [79] S. E. Leucuta, G. Ponchel, and D. Duchene, "Oxprenolol release from bioadhesive gelatin/poly(acrylic acid) microspheres," *J. Microencapsul.*, vol. 14, pp. 511-522, 1997.
- [80] J. Wang, Y. Tabata, D. Bi, and K. Morimoto, "Evaluation of gastric mucoadhesive properties of aminated gelatin microspheres," *J. Control Release*, vol. 73, pp. 223-231, 2001.
- [81] K. Morimoto, H. Katsumata, T. Yabuta, K. Iwanaga, M. Kakemi, Y. Tabata, and Y. Ikada, "Evaluation of gelatin microspheres for nasal and intramuscular administrations of salmon calcitonin," *Eur. J. Pharm. Sci.*, vol. 13, pp. 179-185, 2001.
- [82] M. Yamamoto, Y. Sakakibara, K. Nishimura, M. Komeda, and Y. Tabata, "Improved therapeutic efficacy in cardiomyocyte transplantation for myocardial infarction with release system of basic fibroblast growth factor," *Artif. Organs*, vol. 27, pp. 181-184, 2003.
- [83] T. A. Holland, Y. Tabata, and A. G. Mikos, "In vitro release of transforming growth factor-beta 1 from gelatin microparticles encapsulated in biodegradable, injectable oligo(poly(ethylene glycol) fumarate) hydrogels," *J. Control Release*, vol. 91, pp. 299-313, 2003.
- [84] K. Kawai, S. Suzuki, Y. Tabata, Y. Ikada, and Y. Nishimura, "Accelerated tissue regeneration through incorporation of basic fibroblast growth factor-impregnated gelatin microspheres into artificial dermis," *Biomaterials*, vol. 21, pp. 489-499, 2000.

- [85] Y. Sakakibara, K. Nishimura, K. Tambara, M. Yamamoto, F. Lu, Y. Tabata, and M. Komeda, "Prevascularization with gelatin microspheres containing basic fibroblast growth factor enhances the benefits of cardiomyocyte transplantation," *J. Thorac. Cardiovasc. Surg.*, vol. 124, pp. 50-56, 2002.
- [86] Y. Kimura, M. Ozeki, T. Inamoto, and Y. Tabata, "Time course of de novo adipogenesis in matrigel by gelatin microspheres incorporating basic fibroblast growth factor," *Tissue Eng.*, vol. 8, pp. 603-613, 2002.
- [87] Y. Kimura, M. Ozeki, T. Inamoto, and Y. Tabata, "Adipose tissue engineering based on human preadipocytes combined with gelatin microspheres containing basic fibroblast growth factor," *Biomaterials*, vol. 24, pp. 2513-2521, 2003.
- [88] S. Oe, Y. Fukunaka, T. Hirose, Y. Yamaoka, and Y. Tabata, "A trial on regeneration therapy of rat liver cirrhosis by controlled release of hepatocyte growth factor," *J. Control Release*, vol. 88, pp. 193-200, 2003.
- [89] D. L. Stocum, "Frontiers in medicine: regeneration," *Science*, vol. 276, p. 57, 1997.
- [90] T. Nakahara, T. Nakamura, E. Kobayashi, M. Inoue, K. Shigeno, Y. Tabata, K. Eto, and Y. Shimizu, "Novel approach to regeneration of periodontal tissues based on in situ tissue engineering: effects of controlled release of basic fibroblast growth factor from a sandwich membrane," *Tissue Eng.*, vol. 9, pp. 153-162, 2003.
- [91] Y. C. Huang, C. H. Chiang, and M. K. Yeh, "Optimizing formulation factors in preparing chitosan microparticles by spray-drying method," *J. Microencapsul.*, vol. 20, pp. 247-260, 2003.
- [92] S. A. Agnihotri and T. M. Aminabhavi, "Controlled release of clozapine through chitosan microparticles prepared by a novel method," *J. Control Release*, vol. 96, pp. 245-259, 2004.
- [93] T. Nisisako, T. Torii, and T. Higuchi, "Novel Microreactors for functional polymer beads," *Chem. Eng. J.*, vol. 101, pp. 23-29, 2004.
- [94] S. Iwamoto, K. Nakagawa, S. Sugiura, and M. Nakajima, "Preparation of gelatin microbeads with a narrow size distribution using microchannel emulsification," *AAPS Pharm. Sci. Tech.*, vol. 3, p. E25, 2002.
- [95] Y. Senuma, C. Lowe, Y. Zweifel, J. G. Hilborn, and I. Marison, "Alginate hydrogel microspheres and microcapsules prepared by spinning disk atomization," *Biotechnol. Bioeng.*, vol. 67, pp. 616-622, 2000.

- [96] L. Martin-Banderas, A. Rodriguez-Gil, A. Cebolla, S. Chavez, T. Berdun-Alvarez, J. M. F. Garcia, M. Flores-Mosquera, and A. M. Ganan-Calvo, "Towards high-throughput production of uniformly encoded microparticles," *Adv. Mater.*, vol. 18, pp. 559-564, 2006.
- [97] Y. C. Huang, M. K. Yeh, S. N. Cheng, and C. H. Chiang, "The characteristics of betamethasone-loaded chitosan microparticles by spray-drying method," *J. Microencapsul.*, vol. 20, pp. 459-472, 2003.
- [98] Y. Y. Yang, H. H. Chia, and T. S. Chung, "Effect of preparation temperature on the characteristics and release profiles of PLGA microspheres containing protein fabricated by double-emulsion solvent extraction/evaporation method," *J. Control Release*, vol. 69, pp. 81-96, 2000.
- [99] B. B. Youan, T. L. Jackson, L. Dickens, C. Hernandez, and G. Owusu-Ababio, "Protein release profiles and morphology of biodegradable microcapsules containing an oily core," *J. Control Release*, vol. 76, pp. 313-326, 2001.
- [100] K. Iwanaga, T. Yabuta, M. Kakemi, K. Morimoto, Y. Tabata, and Y. Ikada, "Usefulness of microspheres composed of gelatin with various cross-linking density," *J. Microencapsul.*, vol. 20, pp. 767-776, 2003.
- [101] M. Konishi, Y. Tabata, M. Kariya, H. Hosseinkhani, A. Suzuki, K. Fukuhara, M. Mandai, K. Takakura, and S. Fujii, "In vivo anti-tumor effect of dual release of cisplatin and adriamycin from biodegradable gelatin hydrogel," *J. Control Release*, vol. 103, pp. 7-19, 2005.
- [102] E. Gendler, S. Gendler, and M. E. Nimni, "Toxic reactions evoked by glutaraldehyde-fixed pericardium and cardiac valve tissue bioprosthesis," *J. Biomed. Mater. Res.*, vol. 18, pp. 727-736, 1984.
- [103] E. Zeiger, B. Gollapudi, and P. Spencer, "Genetic toxicity and carcinogenicity studies of glutaraldehyde—A review," *Mutat. Res.*, vol. 589, pp. 136-151, 2005.
- [104] H. C. Liang, W. H. Chang, K. J. Lin, and H. W. Sung, "Genipin-crosslinked gelatin microspheres as a drug carrier for intramuscular administration: in vitro and in vivo studies," *J. Biomed. Mater. Res. A*, vol. 65, pp. 271-282, 2003.
- [105] Y. B. Choy, H. Choi, and K. Kim, "Novel electric-field assisted method for fabrication of uniform biodegradable hydrogel microspheres," *Adv. Mater.*, submitted for publication.

- [106] H. Akin and N. Hasirci, "Preparation and characterization of crosslinked gelatin microspheres," *J. App. Polymer Sci.*, vol. 58, pp. 95-100, 1995.
- [107] S. Matsuda, H. Iwata, N. Se, and Y. Ikada, "Bioadhesion of gelatin films crosslinked with glutaraldehyde," *J. Biomed. Mater. Res.*, vol. 45, pp. 20-27, 1999.
- [108] I. M. van der Lubben, J. C. Verhoef, A. C. van Aelst, G. Borchard, and H. E. Junginger, "Chitosan microparticles for oral vaccination: Preparation, characterization and preliminary in vivo uptake studies in murine Peyer's patches," *Biomaterials*, vol. 22, pp. 687-694, 2001.
- [109] U. Guliyeva, F. Oner, S. Ozsoy, and R. Hazirolu, "Chitosan microparticles containing plasmid DNA as potential oral gene delivery system," *Eur. J. Pharm. Biopharm.*, vol. 62, pp. 17-25, 2006.
- [110] R. Hejazi and M. Amiji, "Stomach-specific anti-H. pylori therapy. II. Gastric residence studies of tetracycline-loaded chitosan microspheres in gerbils," *Pharm. Dev. Technol.*, vol. 8, pp. 253-262, 2003.
- [111] S. Kockisch, G. D. Rees, S. A. Young, J. Tsibouklis, and J. D. Smart, "Polymeric microspheres for drug delivery to the oral cavity: an in vitro evaluation of mucoadhesive potential," *J. Pharm. Sci.*, vol. 92, pp. 1614-1623, 2003.
- [112] S. Kockisch, G. D. Rees, S. A. Young, J. Tsibouklis, and J. D. Smart, "In situ evaluation of drug-loaded microspheres on a mucosal surface under dynamic test conditions," *Int. J. Pharm.*, vol. 276, pp. 51-58, 2004.
- [113] L. Y. Wang, Y. H. Gu, Z. G. Su, and G. H. Ma, "Preparation and improvement of release behavior of chitosan microspheres containing insulin," *Int. J. Pharm.*, vol. 311, pp. 187-195, 2006.
- [114] K. G. Desai and H. J. Park, "Encapsulation of vitamin C in tripolyphosphate cross-linked chitosan microspheres by spray drying," *J. Microencapsul.*, vol. 22, pp. 179-192, 2005.
- [115] B. C. Thanoo, M. C. Sunny, and A. Jayakrishnan, "Cross-linked chitosan microspheres: preparation and evaluation as a matrix for the controlled release of pharmaceuticals," *J. Pharm. Pharmacol.*, vol. 44, pp. 283-286, 1992.
- [116] I. M. van der Lubben, G. Kersten, M. M. Fretz, C. Beuvery, J. Coos Verhoef, and H. E. Junginger, "Chitosan microparticles for mucosal vaccination against diphtheria: oral and nasal efficacy studies in mice," *Vaccine*, vol. 21, pp. 1400-1408, 2003.

- [117] I. M. van der Lubben, F. A. van Opdorp, M. R. Hengeveld, J. J. Onderwater, H. K. Koerten, J. C. Verhoef, G. Borchard, and H. E. Junginger, "Transport of chitosan microparticles for mucosal vaccine delivery in a human intestinal M-cell model," *J. Drug Target*, vol. 10, pp. 449-456, 2002.
- [118] M. Hori, H. Onishi, and Y. Machida, "Evaluation of Eudragit-coated chitosan microparticles as an oral immune delivery system," *Int. J. Pharm.*, vol. 297, pp. 223-234, 2005.
- [119] P. Calvo, C. Remunan-Ropez, J. L. Vila-Jato, and M. J. Alonso, "Novel hydrophilic chitosan-polyethylene oxide nanoparticles as protein carriers," *J. Appl. Polym. Sci.*, vol. 63, pp. 125-132, 1997.
- [120] R. F. Urrusuno, P. Calvo, C. R. Lopez, J. L. V. Jato, and M. J. Alonso, "Enhancement of nasal absorption of insulin using chitosan nanoparticles," *Pharm. Res.*, vol. 16, pp. 1576-1581, 1999.
- [121] K. C. Gupta and M. N. Ravi Kumar, "pH dependent hydrolysis and drug release behavior of chitosan/poly(ethylene glycol) polymer network microspheres," *J. Mater. Sci. Mater. Med.*, vol. 12, pp. 753-759, 2001.
- [122] M. L. Lorenzo-Lamosa, C. Remunan-Lopez, J. L. Vila-Jato, and M. J. Alonso, "Design of microencapsulated chitosan microspheres for colonic drug delivery," *J. Control Release*, vol. 52, pp. 109-118, 1998.
- [123] K. C. Gupta and M. N. Ravi Kumar, "Drug release behavior of beads and microgranules of chitosan," *Biomaterials*, vol. 21, pp. 1115-1119, 2000.
- [124] A. J. Ribeiro, R. J. Neufeld, P. Arnaud, and J. C. Chaumeil, "Microencapsulation of lipophilic drugs in chitosan-coated alginate microspheres," *Int. J. Pharm.*, vol. 187, pp. 115-123, 1999.
- [125] M. L. Gonzalez-Rodriguez, M. A. Holgado, C. Sanchez-Lafuente, A. M. Rabasco, and A. Fini, "Alginate/chitosan particulate systems for sodium diclofenac release," *Int. J. Pharm.*, vol. 232, pp. 225-234, 2002.
- [126] C. Remunan-Lopez, M. L. Lorenzo-Lamosa, J. L. Vila-Jato, and M. J. Alonso, "Development of new chitosan-cellulose multicore microparticles for controlled drug delivery," *Eur. J. Pharm. Biopharm.*, vol. 45, pp. 49-56, 1998.
- [127] N. Shimono, T. Takatori, M. Ueda, M. Mori, Y. Higashi, and Y. Nakamura, "Chitosan dispersed system for colon-specific drug delivery," *Int. J. Pharm.*, vol. 245, pp. 45-54, 2002.

- [128] R. M. Lucinda-Silva and R. C. Evangelista, "Microspheres of alginate-chitosan containing isoniazid," *J. Microencapsul.*, vol. 20, pp. 145-152, 2003.
- [129] D. O. Corrigan, A. M. Healy, and O. I. Corrigan, "Preparation and release of salbutamol from chitosan and chitosan co-spray dried compacts and multiparticulates," *Eur. J. Pharm. Biopharm.*, vol. 62, pp. 295-305, 2006.
- [130] L. Y. Wang, G. H. Ma, and Z. G. Su, "Preparation of uniform sized chitosan microspheres by membrane emulsification technique and application as a carrier of protein drug," *J. Control Release*, vol. 106, pp. 62-75, 2005.
- [131] S. R. Jameela and A. Jayakrishnan, "Glutaraldehyde cross-linked chitosan microspheres as a long acting biodegradable drug delivery vehicle: studies on the in vitro release of mitoxantrone and in vivo degradation of microspheres in rat muscle," *Biomaterials*, vol. 16, pp. 769-775, 1995.
- [132] K. Aiedeh and M. O. Taha, "Synthesis of chitosan succinate and chitosan phthalate and their evaluation as suggested matrices in orally administered, colon-specific drug delivery systems," *Arch. Pharm. Pharm. Med. Chem.*, vol. 332, pp. 103-107, 1999.
- [133] I. Orienti, T. Cerchiara, B. Luppi, F. Bigucci, G. Zuccari, and V. Zecchi, "Influence of different chitosan salts on the release of sodium diclofenac in colon-specific delivery," *Int. J. Pharm.*, vol. 238, pp. 51-59, 2002.
- [134] H. Zhang, I. A. Alsarra, and S. H. Neau, "An in vitro evaluation of a chitosan-containing multiparticulate system for macromolecule delivery to the colon," *Int. J. Pharm.*, vol. 239, pp. 197-205, 2002.
- [135] S. Onal and F. Zihnioglu, "Encapsulation of insulin in chitosan-coated alginate beads: oral therapeutic peptide delivery," *Artif. Cells Blood Substit. Immobil. Biotechnol.*, vol. 30, pp. 229-237, 2002.

AUTHOR'S BIOGRAPHY

Young Bin Choy was born in Seoul, Korea, on August 17, 1976. He received the BS degree from the School of Electrical Engineering (Seoul, 1999) at Seoul National University. He received the MS degree in electrical and computer engineering at the University of Wisconsin–Madison in 2000 and the PhD degree at the University of Illinois at Urbana-Champaign in 2006.

He worked as an intern at LG Corporate Institute of Technology from January 1999 to June 1999. He was a teaching assistant in the Medical Instrumentation Laboratory at the University of Wisconsin–Madison, in fall 2000 and spring 2001. His research at the University of Wisconsin–Madison was on radio frequency mediated ablation of biological tissues. After graduation, he conducted research on fabrication of uniform biomaterial-based microspheres for advanced drug delivery systems at the University of Illinois at Urbana-Champaign.

Young Bin Choy was a member of the Institute of Electrical and Electronics Engineers from 2000 to 2001 and is now a member of the Controlled Release Society.